NASA Contractor Report 178227

CONSOLIDATION PROCESSING PARAMETERS AND ALTERNATIVE PROCESSING METHODS FOR POWDER METALLURGY Al - Cu - Mg - X - X ALLOYS

K. K. SANKARAN

MCDONNELL DOUGLAS ASTRONAUTICS COMPANY - ST. LOUIS DIVISION
MCDONNELL DOUGLAS CORPORATION
ST. LOUIS, MISSOURI 63166

Contract NAS1 - 16967
February 1987

National Aeronautics and
Space Administration

Langley Research Center
Hampton, Virginia 23665-5225

NASA Contractor Report 178227

CONSOLIDATION PROCESSING PARAMETERS AND ALTERNATIVE PROCESSING METHODS FOR POWDER METALLURGY Al - Cu - Mg - X - X ALLOYS

K. K. SANKARAN

MCDONNELL DOUGLAS ASTRONAUTICS COMPANY - ST. LOUIS DIVISION
MCDONNELL DOUGLAS CORPORATION
ST. LOUIS, MISSOURI 63166

Contract NAS1 - 16967
February 1987

National Aeronautics and
Space Administration

Langley Research Center
Hampton, Virginia 23665-5225

PREFACE

This report presents the results of research performed from 27 September 1982 through 29 August 1986 by the McDonnell Douglas Astronautics Company - St. Louis Division under the National Aeronautics and Space Administration Contract NAS1-16967 entitled "Consolidation Processing Parameters and Alternative Processing Methods for Powder Metallurgy Al-Cu-Mg-X-X Alloys." The intent of the study was to systematically investigate the relationships between the powder consolidation processing parameters and the microstructure and properties of the fully processed alloys, and to evaluate alternative alloying and consolidation methods which have the potential to reduce material and processing cost and enhance product quality.

The research was performed in the Product and Materials Engineering Department, with Dr. K. K. Sankaran as the Principal Investigator. Novamet, a unit of INCO Alloy Products Company, was the principal sub-contractor, with Dr. S. J. Donachie and Dr. P. S. Gilman supervising all of the powder processing. Mr. D. L. Dicus of the NASA-Langley Research Center was the Technical Manager for the contract.

CONTENTS

CONTENTS (continued)

LIST OF FIGURES

LIST OF FIGURES (continued)

LIST OF TABLES

LIST OF TABLES (continued)

1. INTRODUCTION

Vacuum degassing is an important step in the consolidation processing of aluminum alloy powder into billets for hot working. Insufficient degassing may cause defects such as hydrogen-induced porosity and blistering which degrade the properties of the wrought alloys. While innovative processing techniques are being developed to improve the quality and reduce the cost of powder-processed aluminum alloys (1, 2), the successful near-term use of these alloys will depend upon improving the efficiency of vacuum degassing through a metallurgical understanding of the changes occurring during consolidation. To this end, the present effort is aimed at determining the influence of varying the vacuum degassing parameters on the microstructure and properties of powder-processed aluminum alloys. In addition, using alloys prepared by consolidating prealloyed rapidly solidified powder in sealed aluminum containers as the baseline, the study also attempts to determine the effectiveness of alternative processing techniques such as mechanical alloying for powder production, and containerless vacuum hot pressing for powder consolidation. The intent is to systematically investigate the relationships between the powder consolidation processing parameters and the microstructure and properties of the fully processed alloys, and to evaluate alternative alloying and consolidation methods which have the potential to reduce material cost and enhance product quality.

2. BACKGROUND

Wrought aluminum alloys prepared from rapidly solidified powder have demonstrated a potential for developing superior combinations of properties compared with ingot metallurgy (IM) alloys (3). Such improvements are due to the microstructural refinements and the increased solid solubilities resulting from the rapid solidification. Examples of property enhancement include the better strength and stress corrosion resistance of alloys 7090 and 7091 compared with that of IM 7XXX-series alloys (4), the improved strength and toughness of powder metallurgy (PM) 2XXX-series alloys over that of equivalent IM alloys (5), and the elevated-temperature stability of Al-Fe-X (X=Ce, Cr, Mo, or V+Si) alloys not achievable in IM alloys (6-9). However, the use of such alloys has generally been limited by a lack of complete understanding of the relationships between processing and properties. Additionally, the manufacturing technology for the rolling of plate and sheet products from large billets is still under development, and the alloys are available principally only as forgings and extrusions.

In the conventional consolidation processing of powder-processed aluminum alloys, the alloy powder is pressed into a porous compact, vacuum degassed, consolidated into a fully dense billet, and formed into a wrought product (10). The purpose of vacuum degassing is to dehydrate the hydrated oxide film on the powder surface and to liberate the moisture prior to full densification. During the diffusion of the liberated water through the porous compact, additional reaction with the powder surface may result in thicker oxide films and the evolution of hydrogen. Since the minimum temperature at which the alloy must be heated for complete dehydration is not known, degassing is commonly performed above the highest temperature to which the alloy will be subsequently exposed (the solution heat treatment temperature for precipitation-hardened alloys) (10). This approach eliminates potential problems such as porosity and surface blistering by avoiding the evolution of hydrogen subsequent to full densification. However, high degassing temperatures irreversibly coarsen the refined microstructures and degrade the properties, particularly of the dispersion-strengthened alloys.

A recent study (11) conducted on alloy 7091 and an Al-Fe-Ce alloy observed the break-up and distribution of the oxide film during the hot pressing and subsequent hot working of the degassed billet. This study reported that the amorphous oxide film remaining on the surface of 7091 alloy powder was fully dehydrated following vacuum degassing. While these and other studies have recognized the importance of the consolidation processing steps in the total PM processing of aluminum alloys, information on the effects of varying the vacuum degassing parameters on the microstructure and properties is not generally available. Also, important systems such as the aluminum-lithium alloys which possess more complex and reactive surface oxides have not received attention.

Recently, approaches such as mechanical alloying (12) and containerless vacuum hot pressing (13) have been developed as alternatives to powder preparation by the rapid solidification of a prealloyed melt and conventional

powder consolidation using sealed aluminum containers, respectively. The advantages of mechanical alloying include the incorporation of strengthening by oxides, carbides, and a high density of sub-structural defects. Containerless vacuum hot pressing avoids the disadvantages of conventional processing such as leakage into the container and the need to cool and reheat the degassed billet, and has the potential to reduce production costs and enhance material quality. However, the influence of vacuum degassing parameters on the stability of the sub-structures and the resultant properties of the mechanically alloyed materials, and on the microstructures and properties of alloys processed by containerless vacuum hot pressing has not been studied. The potential effectiveness of employing these alternative approaches to improve the properties of PM aluminum alloys has also not been determined systematically.

3. RESEARCH OBJECTIVES AND APPROACH

This study is a systematic investigation of the relationships between the consolidation processing parameters and the microstructure and properties of powder metallurgy (PM) Al-Cu-Mg-X-X alloys. The study also investigates the consolidation processing of alloys prepared by alternative powder preparation and consolidation techniques, and compares their characteristics with those prepared from atomized, rapidly solidified powder and consolidated by conventional means using sealed aluminum containers. The overall goal is to develop an understanding of the sensitivity of PM alloys to processing variations, and to explore simplified processing methods which can reduce production costs and enhance material quality.

3.1 Objectives

The objectives of this investigation are to (1) identify the critical parameters associated with the conventional consolidation processing of prealloyed Al-Cu-Mg-X-X alloy powder, and evaluate the effects of varying these parameters on the microstructure and properties of the fully processed alloys (Conventional consolidation processing is defined as the cold compaction of prealloyed powder followed by vacuum degassing and hot pressing in a sealed aluminum canister.), (2) investigate alternative means that do not employ fully prealloyed powder for producing Al-Cu-Mg-X-X alloy compositions, and evaluate the effects of these alternative means on the consolidation processing, and the homogeneity, microstructure, and properties of the fully processed alloys, and (3) investigate alternative consolidation processing methods for Al-Cu-Mg-X-X alloys, identify the critical parameters associated with these methods, and evaluate the effects of varying these parameters on the microstructure and properties of the fully processed alloys.

3.2 Approach

Alloys prepared by the conventional consolidation of atomized, rapidly solidified powder were used as the baseline for this study. Mechanical alloying was chosen as the alternative powder production method, and containerless vacuum hot pressing was chosen as the alternative consolidation method. Because complete dehydration of the surface oxides and the removal of moisture are critical to achieving the full potential of PM alloys, vacuum degassing parameters were chosen as being critical for both conventional and containerless consolidation. Consolidated billets were hot extruded and heat treated for evaluation. To achieve the program objectives, the effort was divided into the following three tasks:

Task I: Conventional Consolidation of Prealloyed (PA) Powder

Task II: Conventional Consolidation of Mechanically Alloyed (MA) Powder

Task III: Consolidation by Containerless Vacuum Hot Pressing (CVHP) of PA and MA powder.

3.2.1 Selection of Alloy Compositions - Two alloys with nominal compositions of Al-4Cu-1Mg-1.5Li-0.2Zr and Al-4Cu-1Mg-1.5Fe-0.75Ce, respectively, were selected for this study. The program approach was to study these alloys prepared from both PA and MA powder under Tasks I and II, and the PA Li-containing alloy and the MA Fe- and Ce-containing alloy under Task III.

The Al-4Cu-1Mg-1.5Li-0.2Zr composition was selected on the basis of the beneficial effects of Li additions and the current emphasis on Al-Li alloys (14). In addition, Li-containing alloys are expected to possess complex and more reactive surface oxides compared with the other aluminum alloys. Among the various Al-Li alloys being developed, Al-Cu-Mg-Li alloys possess superior combinations of strength and toughness. The amounts of Cu, Mg, and Li in the alloy are such that their full dissolution is expected at the selected solution heat treatment temperature of 773K (932°F). The addition of Zr is based on the beneficial effects of Al_3Zr in controlling recrystallization and enhancing properties. Because of the availability of oxides and carbides for sub-structural refinement, Zr was not included in the Li-containing alloy prepared by mechanical alloying.

The Al-4Cu-1Mg-1.5Fe-0.75Ce composition was selected on the basis of the known beneficial effects of adding Fe and Ce on the elevated temperature properties. Similar to the amounts of Fe and Ni in the 2618 aluminum alloy, the amounts of Fe and Ce were selected to provide strength enhancement at moderately elevated temperatures near 422K (300°F). The ratio of the amounts of Fe and Ce was based on the superior elevated temperature properties reported for an Al-8Fe-4Ce alloy (6). Elemental additions of Fe and Ce may not be feasible by mechanical alloying, since the aluminum may coat these elements during processing and prevent their homogeneous distribution. To achieve homogeneous alloying, the Fe- and Ce-containing alloys were to be mechanically alloyed using elemental Al, Cu and, Mg powder, and prealloyed, rapidly solidified Al-1.6Fe-0.8Ce powder prepared by atomization.

3.2.2 Selection of Consolidation Processing Parameters - For each of the alloys under the three tasks, the vacuum degassing temperatures were chosen both above and below the solution heat treatment temperature of 773K (932°F). The intent was to determine the need for vacuum degassing above the highest post-consolidation processing temperature. For conventional consolidation (Tasks I and II), the approach was to cold isostatically press the powder, encapsulate and seal in an aluminum alloy container, vacuum degas, hot press at 675K (756°F) to full density, and remove the container prior to extrusion. For CVHP (Task III), the approach was to degas the loose powder in a vacuum chamber which is itself part of the pressing die, and hot press at the same temperature to full density. A nominal billet diameter of 150 mm (6 in.) was chosen for both conventional and CVHP consolidation. A reduction ratio of 16:1 was chosen for extruding the billets at 600K (621°F) into bars of rectangular cross-section with an aspect ratio of 5:1. The 5:1 aspect ratio is expected to prevent strengthening from axisymmetric deformation texture. Additionally, due to the influence of dispersoids in stabilizing the hot-worked sub-structure, an extrusion ratio of 8:1 with a 5:1 aspect ratio was also planned for the Fe- and Ce-containing alloy under Tasks I and II. The consolidation processing parameters targeted for this study are presented in Table 1.

TABLE 1. CONSOLIDATION PROCESSING PARAMETERS INITIALLY SELECTED FOR STUDY

TASK	ALLOY	VACUUM DEGASSING TEMPERATURE		VACUUM DEGASSING TIME	EXTRUSION RATIO
		K	°F	h	
I	PA Al-4Cu-1Mg-1.5Li-0.2Zr	750	891	6	16
		750	891	12	16
		790	963	6	16
	PA Al-4Cu-1Mg-1.5Fe-0.75Ce	750	891	12	8
		750	891	12	16
		790	963	6	16
II	MA Al-4Cu-1Mg-1.5Li	750	891	6	16
		750	891	12	16
		790	963	6	16
	MA Al-4Cu-1Mg-1.5Fe-0.75Ce	750	891	12	8
		750	891	12	16
		790	963	6	16
III	PA Al-4Cu-1Mg-1.5Li-0.2Zr	750	891	6	16
		790	963	6	16
	MA Al-4Cu-1Mg-1.5Fe-0.75Ce	750	891	6	16
		790	963	6	16

4. EXPERIMENTAL PROCEDURES

4.1 Powder Production

4.1.1 Li-Containing Alloys - PA Al-4Cu-1Mg-1.5Li-0.2Zr powder was produced by helium gas atomization at Valimet, Inc., Stockton, CA. During the collection of the atomized powder, a flash occurred in the system which filters the very fine fractions for disposal. The recovered powder, which was not affected by the flash, was screened through an 80 mesh (170 μm) sieve for further processing.

MA Al-4Cu-1Mg-1.5Li powder was produced by Novamet (a unit of INCO Alloy Products Company), Wyckoff, NJ at its Haskell, NY facilities. The powder was produced by a process which is proprietary to Novamet. After attrition, the MA powder was heated at 700K (800°F) under a vacuum to remove the residual stearic acid. The stearic acid is used as a process control agent to balance the welding and fracturing of the powder particles during attrition. This organic agent also supplies the carbon necessary for the formation of aluminum carbides in the alloy.

4.1.2 Fe- and Ce-Containing Alloys - PA Al-4Cu-1Mg-1.5Fe-0.75Ce and Al-1.6Fe-0.8Ce powder were produced by flue gas atomization at the Alcoa Technical Center, Alcoa Center, PA. The atomized powder was screened through an 100 mesh (149 μm) sieve for further processing.

MA Al-4Cu-1Mg-1.5Fe-0.75Ce powder was produced by Novamet using PA Al-1.6Fe-0.8Ce powder and elemental Al, Cu, and Mg powder. As discussed in the following paragraphs, problems during powder consolidation also necessitated the mechanical alloying of this powder from the respective elemental powders.

4.2 Billet Consolidation Processing

4.2.1 Conventional Consolidation of Li-Containing Alloys (Tasks I and II) - Cold isostatic pressing (CIP) of PA Al-4Cu-1Mg-1.5Li-0.2Zr powder was believed to present potential safety hazards, because in addition to the flash that had occurred during powder collection, it was also reported by Valimet that 52.5 pct. of the atomized powder was smaller than 44 μm (-325 mesh size). Should leaks develop in the bag during the CIP of such powder, reaction of the powder with the pressurizing fluid may cause a hazardous situation. Therefore, it was decided to cold compact the PA powder and, for consistency, the MA powder uniaxially using mechanical means. However, the first attempt to uniaxially press the PA powder in an extrusion press at Reactive Metals Inc., Ashtabula, OH, resulted in an explosion and a fire. Although the extrusion press liner was maintained at 644K (700°F), uniaxial pressing is accomplished in one minute or less and the powder itself is not heated while pressing. It is believed that under the pressure of the cold compaction, the reaction between the reactive powder surface and the entrapped air built up a large internal pressure that eventually blew off the welded container and exposed the powder. Possible ignition sources include the residual lubricant in the extrusion chamber, or the flame heating the extrusion press liner.

The problems discussed in the preceding paragraph necessitated the pressing of the Li-containing alloy powder under controlled laboratory conditions so as to prevent further hazardous incidents. Since laboratory facilities for the cold pressing of 150 mm (6 in.) diameter compacts were not readily available, it was decided to cold press both the PA and MA Li-containing powder into 114 mm (4.5 in.) diameter compacts at the Novamet facilities.

Three batches each of appropriate amounts of the PA and MA powder were uniaxially cold compacted in 114 mm (4.5 in.) diameter mild steel containers to about 75 pct. of the theoretical density. Following this step, the mild steel containers were machined off and the compacts were loaded into 114 mm (4.5 in.) diameter 6061-Al alloy containers fitted with evacuation tubes. The compacts were heated in a fluidized bed furnace and vacuum degassed using the parameters shown in Table 1. Following vacuum degassing, the billets were cooled, the evacuation tubes were crimped and cut, and the compacts were sealed by welding. The degassed and sealed compacts were then heated at 675K (756°F) for three hours and hot upset to full density at the same temperature in an extrusion press. The 6061-Al containers were then machined off and the billets were ready for extrusion.

4.2.2 Conventional Consolidation of Fe- and Ce-Containing Alloys (Tasks I and II) - To expedite powder processing, it was initially decided to uniaxially cold press both the PA and MA Al-4Cu-1Mg-1.5Fe-0.75Ce powder using procedures similar to that attempted at Reactive Metals, Inc. for the Li-containing alloys. While three batches each of the PA and MA Fe- and Ce-containing powder were pressed without incident, the densities of these cold-pressed compacts were about 90 pct. of the theoretical rather than the intended 70-80 pct. The pores are not inter-connected at 90 pct. density, and the vacuum degassing of these compacts was not considered feasible. Since the Fe- and Ce-containing powder is safer to handle than the Li-containing powder, it was again decided to CIP this powder into 150 mm (6 in.) diameter compacts for Tasks I and II. A new batch of powder was prepared by mechanically alloying elemental Al, Cu, and Mg powder and PA Al-1.6Fe-0.8Ce powder. However, during the heating of this MA powder for removing the process control agent, failure of the vacuum system resulted in its contamination and caused its rejection. Since all of the PA Al-1.6Fe-0.8Ce powder had been consumed, the alloy was made by mechanically alloying elemental Al, Cu, Mg, Fe, and Ce powder for further processing.

Three batches each of PA and MA powder (prepared from elemental powder) were cold isostatically pressed under a pressure of 207 MPa (30 ksi) at Dynamet Technology, Burlington, MA. The compacts, which were 140 mm (5.5 in.) in diameter and about 80 pct. dense, were loaded into 6061-Al alloy containers fitted with evacuation tubes. Using procedures similar to that used for the Li-containing alloys, the compacts were vacuum degassed in accordance with the parameters shown in Table 1, hot upset, and the 6061-Al containers were machined off.

4.2.3 Containerless Vacuum Hot Pressing of Li-Containing and Fe- and Ce-Containing Alloys (Task III) - During the period in which problems were being experienced in the consolidation processing of alloys under Tasks I and II,

two Al-4Cu-1Mg-1.5Li-0.2Zr billets (using prealloyed powder) and two Al-4Cu-1Mg-1.5Fe-0.75Ce billets (using mechanically alloyed powder) were prepared under Task III by containerless vacuum hot pressing. The two Al-4Cu-1Mg-1.5Fe-0.75Ce billets were consolidated from powder mechanically alloyed using elemental Al, Cu, and Mg powder and prealloyed Al-1.6Fe-0.8Ce powder.

The only die available at Novamet for containerless vacuum hot pressing was designed for pressing 280 mm (11 in.) diameter billets. To press the four 150 mm (6 in.) diameter billets, an aluminum tube was placed inside and concentric with the 280 mm (11 in.) die. The tube, whose inner diameter was such as to yield a billet of the desired diameter, was filled with the alloy powder to be consolidated. The remainder of the die was filled with commercial grade aluminum powder with appropriate demarcation using copper powder. The tube was withdrawn, and the entire assembly was heated in the CVHP chamber. After the interface between the commercial aluminum powder and the alloy powder reached the vacuum degassing temperature (determined by prior calibration), the powder was degassed for the desired time and pressed. The 280 mm (11 in.) composite billets were then machined to produce the alloy billets of the appropriate diameter. The vacuum degassing parameters for these four billets were in accordance with that shown in Table 1.

In addition to the above four billets, five other billets were also processed by CVHP. These five billets included one 114 mm (4.5 in.) diameter billet made from the PA Al-4Cu-1Mg-1.5Li-0.2Zr powder, one 114 mm (4.5 in.) and one 150 mm (6 in.) diameter billet each made from the MA Al-4Cu-1Mg-1.5Li powder, and two 150 mm (6 in.) diameter billets made from the MA Al-4Cu-1Mg-1.5Fe-0.75Ce powder prepared from fully elemental powder that had been used for billet pressing under Task II. The first three of these five billets were added to provide a comparison between billets of different diameters, and between the PA and MA Li-containing materials consolidated using both conventional and containerless processing. The last two billets were added to provide a comparison with the alloys prepared earlier under this task using elemental Al, Cu, and Mg powder and prealloyed Al-1.6Fe-0.8Ce powder. These five billets were again prepared as composite billets using the 280 mm (11 in.) die and an inner aluminum tube of the appropriate diameter, followed by machining the 280 mm (11 in.) composite billets to produce the alloy billets of the appropriate diameter. The vacuum degassing parameters for the five additional billets were selected to provide relevant comparisons with the sixteen billets originally planned for the program.

The consolidation processing parameters for the billets of the twenty-one alloys, numbered 1 through 21, are presented in Table 2.

TABLE 2. BILLET CONSOLIDATION PROCESSING PARAMETERS

TASK	ALLOY	ALLOY NUMBER	VACUUM DEGASSING TEMPERATURE		TIME	HOT PRESSING TEMPERATURE		BILLET DIAMETER	
			K	°F	h	K	°F	mm	in.
I	PA Al-4Cu-1Mg-1.5Li-0.2Zr	1	750	891	6	675	756	114	4.5
		2	750	891	12	675	756	114	4.5
		3	790	963	6	675	756	114	4.5
	PA Al-4Cu-1Mg-1.5Fe-0.75Ce	4	750	891	12	675	756	150	6.0
		5	750	891	12	675	756	150	6.0
		6	790	963	6	675	756	150	6.0
II	MA Al-4Cu-1Mg-1.5Li	7	750	891	6	675	756	114	4.5
		8	750	891	12	675	756	114	4.5
		9	790	963	6	675	756	114	4.5
	MA Al-4Cu-1Mg-1.5Fe-0.75Ce	10	750	891	12	675	756	150	6.0
		11	750	891	12	675	756	150	6.0
		12	790	963	6	675	756	150	6.0
III	PA Al-4Cu-1Mg-1.5Li-0.2Zr	13	750	891	6	750	891	114	4.5
		14	750	891	6	750	891	150	6.0
		15	790	963	6	790	963	150	6.0
	MA Al-4Cu-1Mg-1.5Li	16	750	891	6	750	891	114	4.5
		17	750	891	6	750	891	150	6.0
	MA Al-4Cu-1Mg-1.5Fe-0.75Ce	18	750	891	6	750	891	150	6.0
	(Using PA Al-1.6Fe-0.8Ce)	19	790	963	6	790	963	150	6.0
	MA Al-4Cu-1Mg-1.5Fe-0.75Ce	20	750	891	6	750	891	150	6.0
	(Using Elemental Powder)	21	790	963	6	790	963	150	6.0

4.3 Extrusion

Based upon Novamet's experience with similar alloys, the extrusion temperature was increased from the planned 600K (621°F) to 644K (700°F). The billets were coated with Fel-Pro C 300 lubricant and preheated for three hours at 644K (700°F). The 114 mm (4.5 in.) diameter billets were extruded through a rectangular die with a nominal cross section of 51 mm (2 in.) by 13 mm (0.5 in.) at a speed of 91 mm/s (3.6 in./s) and a pressure of 483 MPa (70 ksi).The 150 mm (6 in.) diameter billets, except those of alloys 4 and 10, were extruded through a rectangular die with a nominal cross section of 63 mm (2.5 in.) by 15 mm (0.6 in.). Billets of alloys 4 and 10 were extruded through a rectangular die with a nominal cross section of 102 mm (4 in.) by 25 mm (1 in.).

The extrusion speed and pressure were not recorded for the 150 mm (6 in.) diameter billets. The dimensions of the twenty-one extrusions are presented in Table 3.

TABLE 3. EXTRUSION DIMENSIONS

TASK	ALLOY	ALLOY NUMBER	REDUCTION RATIO	ASPECT RATIO	CROSS SECTION mm (in.)
I	PA Al-4Cu-1Mg-1.5Li-0.2Zr	1, 2 and 3	16	4	51 x 13 (2.0 x 0.5)
	PA Al-4Cu-1Mg-1.5Fe-0.75Ce	4	7	4	102 x 25 (4.0 x 1.0)
		5 and 6	19	4	63 x 15 (2.5 x 0.6)
II	MA Al-4Cu-1Mg-1.5Li	7, 8 and 9	16	4	51 x 13 (2.0 x 0.5)
	MA Al-4Cu-1Mg-1.5Fe-0.75Ce	10	7	4	102 x 25 (4.0 x 1.0)
		11 and 12	19	4	63 x 15 (2.5 x 0.6)
III	PA Al-4Cu-1Mg-1.5Li-0.2Zr	13	16	4	51 x 13 (2.0 x 0.5)
		14 and 15	19	4	63 x 15 (2.5 x 0.6)
	MA Al-4Cu-1Mg-1.5Li	16	16	4	51 x 13 (2.0 x 0.5)
		17	19	4	63 x 15 (2.5 x 0.6)
	MA Al-4Cu-1Mg-1.5Fe-0.75Ce (Using PA Al-1.6Fe-0.8Ce)	18 and 19	19	4	63 x 15 (2.5 x 0.6)
	MA Al-4Cu-1Mg-1.5Fe-0.75Ce (Using Elemental Powder)	20 and 21	19	4	63 x 15 (2.5 x 0.6)

4.4 Post-Extrusion Processing

All of the alloys were solution heat treated at 773K (932°F) for one hour, quenched in water at room temperature, and age-hardened. To determine

the aging conditions for the alloys for evaluating their mechanical properties, attempts were made to determine the age-hardening behavior of one alloy each of the PA and MA Li-containing alloys processed by both conventional consolidation and containerless vacuum hot pressing (alloys 3, 9, 13, and 16) at room temperature, 433K (320°F), 463K (374°F), and 493K (428°F). Because of a defect in the extrusion of alloy 16, the age-hardening study of this alloy was not completed. Based on the observed age-hardening behavior of alloys 3, 9, and 13, all of the Li-containing alloys were aged both at room temperature for a minimum of seven days to stable hardness, and at 463K (374°F) for 16 hours to peak hardness. Also, since these aging conditions are similar to those used for the conventional 2XXX-series alloys, and the aging temperatures are not expected to influence the precipitation/coarsening of the Fe- and Ce-containing dispersoids, the same aging conditions were chosen for all of the PA and MA Al-4Cu-1Mg-1.5Fe-0.75Ce alloys as chosen for the Li-containing alloys.

To enhance the kinetics of precipitation and to increase the strength of the alloys, precipitation-hardened 2XXX-series aluminum alloys are commonly cold worked following solution heat treatment and prior to aging. Additionally, powder-processed aluminum alloy extrusions are also cold worked by stretching prior to aging so that the stresses induced during quenching from the solution heat treatment temperature can be relieved. The influence of cold working prior to aging on the age-hardening response of these alloys is determined by the respective precipitation mechanisms responsible for strengthening. Based upon the alloy composition and the alloying method, the alloys can be grouped, as shown in Table 4, into four different classes with each class representing a certain combination of strengthening mechanisms. To determine the need for cold working the alloys prior to aging, attempts were made to stretch one representative alloy from each of the four different classes. While alloys 3 and 6 were successfully stretched, the high strength of the MA alloys precluded the stretching of alloys 9 and 12. Based upon these results, except for stretching a few selected alloys to determine the influence on tensile properties, the mechanical properties of all of the alloys were determined without stretching. Additionally, to determine the influence of the solution heat treatment temperature, alloys 5 and 6 were solution heat treated at 753K (896°F) and 788K (959°F) and naturally aged. The aging time at 463K (374°F) was also varied for alloys 2, 5, 8, and 11.

TABLE 4. STRENGTHENING MECHANISMS FOR THE ALLOYS

ALLOYS	STRENGTHENING MECHANISMS
1, 2, 3, 13, 14, and 15	Precipitation Hardening (PH)
7, 8, 9, 16, and 17	PH + Oxide/Carbide Dispersion Strengthening (O/C-DS)
4, 5, and 6	PH + Intermetallic Dispersion Strengthening (IM-DS)
10, 11, 12, 18, 19, 20, and 21	PH + O/C-DS + IM-DS

4.5 Characterization of the Microstructure and Properties

The chemical composition of the PA Al-4Cu-1Mg-1.5Li-0.2Zr and Al-4Cu-1Mg-1.5Fe-0.75Ce powder, and all of the twenty-one extrusions were determined from triplicate samples at the McDonnell Douglas Corporation. The chemical composition of the PA Al-4Cu-1Mg-1.5Li-0.2Zr powder was also determined by Valimet and from duplicate samples by Homogeneous Metals, Inc., Clayville, NY, and that of the PA Al-4Cu-1Mg-1.5Fe-0.75Ce powder was also determined by Alcoa. The chemical composition was determined by atomic absorption spectrometric analysis of solutions of the alloys in a mixture of nitric and hydrochloric acids. The hydrogen contents of the PA powder and all of the hot-pressed billets and extrusions were determined from duplicate samples by a fusion method at Leco, Inc., St. Joseph, MI. Since all of the MA powder had been consumed in billet processing, it was not available for characterization. The PA Al-4Cu-1Mg-1.5Li-0.2Zr and Al-4Cu-1Mg-1.5Fe-0.75Ce powder were also examined by optical and scanning electron microscopy.

The densities of all of the extrusions were determined, and samples of selected alloys were examined by optical microscopy. The sub-structures of selected alloys were characterized at Lambda Research, Cincinnati, OH by determining the (111) pole figures by the back-reflection technique using the Schultz apparatus, and the back-reflection pin-hole patterns.

The tensile properties at room temperature of all of the alloys in the longitudinal orientation and of selected alloys in the transverse orientation were determined in accordance with the ASTM Standard E8. Unless indicated otherwise, the tensile properties are based on the results of duplicate tests. Round sub-size specimens with threaded ends and a nominal reduced-section of 4 mm (0.160 in.) were used to determine the tensile properties in the longitudinal direction of all of the alloys, except alloys 4 and 10, following solution heat treatment at 773K (932°F) for one hour and natural aging to stable hardness or artificial aging at 463K (374°F) for 16 hours to peak hardness. Such specimens were also used to determine the tensile properties of alloys 3 and 6 which were stretched prior to aging, and the transverse tensile properties of alloys 3, 7, 14, 17, 18, and 19 following natural aging. However, the longitudinal properties of alloys 7, 14, 15, 16, and 17, and the transverse properties of alloys 3 and 7 could not be determined owing to failure in the threaded ends of the specimens. Round specimens with unthreaded ends and a nominal reduced-section diameter of 6 mm (0.25 in.) were then used to determine the longitudinal tensile properties of (i) alloys 4, 7, 10, 14, 15, 16, and 17 following solution heat treatment at 773K (932°F) for one hour and either natural aging or artificial aging at 463K (374°F) for 16 hours, (ii) alloys 2, 5, 8, and 11 following a similar solution heat treatment and aging at 463K (374°F) for six and 33 hours, (iii) alloy 2 following a similar solution heat treatment and aging at 463K (374°F) for 12 hours, and (iv) alloys 5 and 6 following solution heat treatment at either 753K (896°F) or 788K (959°F) for one hour and natural aging.

To obtain a measure of the plane strain fracture toughness of the alloys, notched tension tests were conducted on selected alloys in both the longitudinal and transverse orientations. The tests were conducted in accordance with the ASTM Standard E602 using 12.7 mm (0.5 in.) diameter specimens.

5. RESULTS AND DISCUSSION

As described in the preceding sections, a total of twenty-one extrusions representing varying combinations of alloy compositions, alloying approach, and consolidation parameters were prepared under the three tasks of the program. In this section, the composition, microstructure, and the age-hardening behavior of the alloys are discussed first. Following this, the effects of varying the vacuum degassing parameters on the properties of the alloys are discussed separately for each of the three tasks and are also compared with each other.

5.1 Powder Characteristics

The chemical compositions of the PA powder alloys are presented in Table 5. The copper content measured by all of the sources of analysis is lower than the nominal in the PA powder samples of both the Al-4Cu-1Mg-1.5Li-0.2Zr and Al-4Cu-1Mg-1.5Fe-0.75Ce alloys, although, as reported later, it is closer to the nominal in all of the extrusions prepared from the PA powder. The reason for this observation is not clear. The amount of Li is higher than the nominal, but the amounts of the other elements are close to the nominal composition. As expected, the hydrogen concentration of the Li-containing alloy powder is also significantly higher than that of the Fe- and Ce- containing alloy powder.

TABLE 5. CHEMICAL COMPOSITION OF THE PREALLOYED POWDER

ALLOY	SOURCE OF ANALYSIS	CHEMICAL COMPOSITION (WT.%)						
		Cu	Mg	Li	Zr	Fe	Ce	H (ppm)
Al-4Cu-1Mg-1.5Li-0.2Zr	Valimet	3.87	1.08	1.85	0.22	--	--	--
	Homogeneous Metals	3.64	1.00	1.74	0.25	--	--	--
	McDonnell Douglas	3.76	0.86	1.73	0.19	0.02	--	--
	Leco	--	--	--	--	--	--	397.6
Al-4Cu-1Mg-1.5Fe-0.75Ce	Alcoa	3.8	1.0	--	--	1.3	0.7	--
	McDonnell Douglas	3.59	0.91	--	--	1.51	0.74	--
	Leco	--	--	--	--	--	--	30.4
Al-1.6Fe-0.8Ce	Alcoa	--	--	--	--	1.6	0.9	--

The particle size distribution of the as-atomized Al-4Cu-1Mg-1.5Li-0.2Zr powder, which was determined by Valimet, is plotted in Figure 1. The size distribution follows log-normal behavior, as is expected for metal powders gas-atomized under constant pressure (15). From the linear, least-squares fit, a geometric mean particle diameter of 40 μm was determined. As reported by Alcoa, about 85 pct. of the PA Al-4Cu-1Mg-1.5Fe-0.75Ce and Al-1.6Fe-0.8Ce powder particles were finer than 325 mesh (44 μm) size.

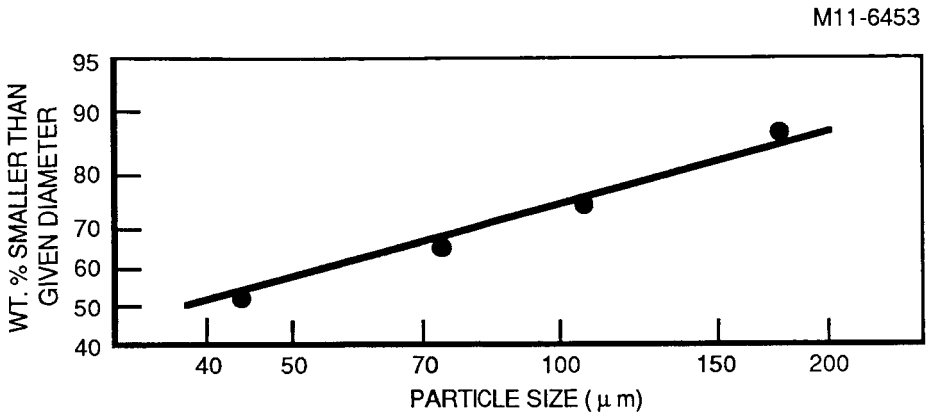

FIGURE 1. PARTICLE SIZE DISTRIBUTION OF ATOMIZED Al - 4Cu - 1Mg - 1.5 Li - 0.2 Zr POWDER

Scanning electron photomicrographs of the PA Al-4Cu-1Mg-1.5Li-0.2Zr and Al-4Cu-1Mg-1.5Fe-0.75Ce powder samples are presented in Figure 2. Powder particles are predominantly spherical, which is typical of inert gas atomized powder. The larger size powder particles of the Al-4Cu-1Mg-1.5Fe-0.75Ce alloy are somewhat elongated and irregular in shape. The surface of the powder particles of the Li-containing alloy is generally also rougher than that of the surface of the Al-4Cu-1Mg-1.5Fe-0.75Ce alloy. The surface characteristics and the morphology of the powder particles of these alloys are determined by the atomization parameters which are proprietary to the powder producers. It is also observed that the size of a significant fraction of the powder particles of both the alloys is less than about 20 μm.

Optical micrographs of samples of the PA Al-4Cu-1Mg-1.5Li-0.2Zr and Al-4Cu-1Mg-1.5Fe-0.75Ce powder particles are presented in Figure 3. The alloys exhibit a cellular-dendritic solidification microstructure with dendrite arm spacings on the order of 1 μm. Based on the correlation developed by Matyja et al. (16), a solidification rate of about 10^5K/s is indicated for these alloys.

Results of analytical characterization of powder by thermogravimetric analysis, mass spectrometry, and x-ray photoelectron spectroscopy suggested the absence of chemically bound water on the surface of PA Al-4Cu-1Mg-1.5Li-0.2Zr powder sample. These studies, which were conducted independently, are summarized in the appendix.

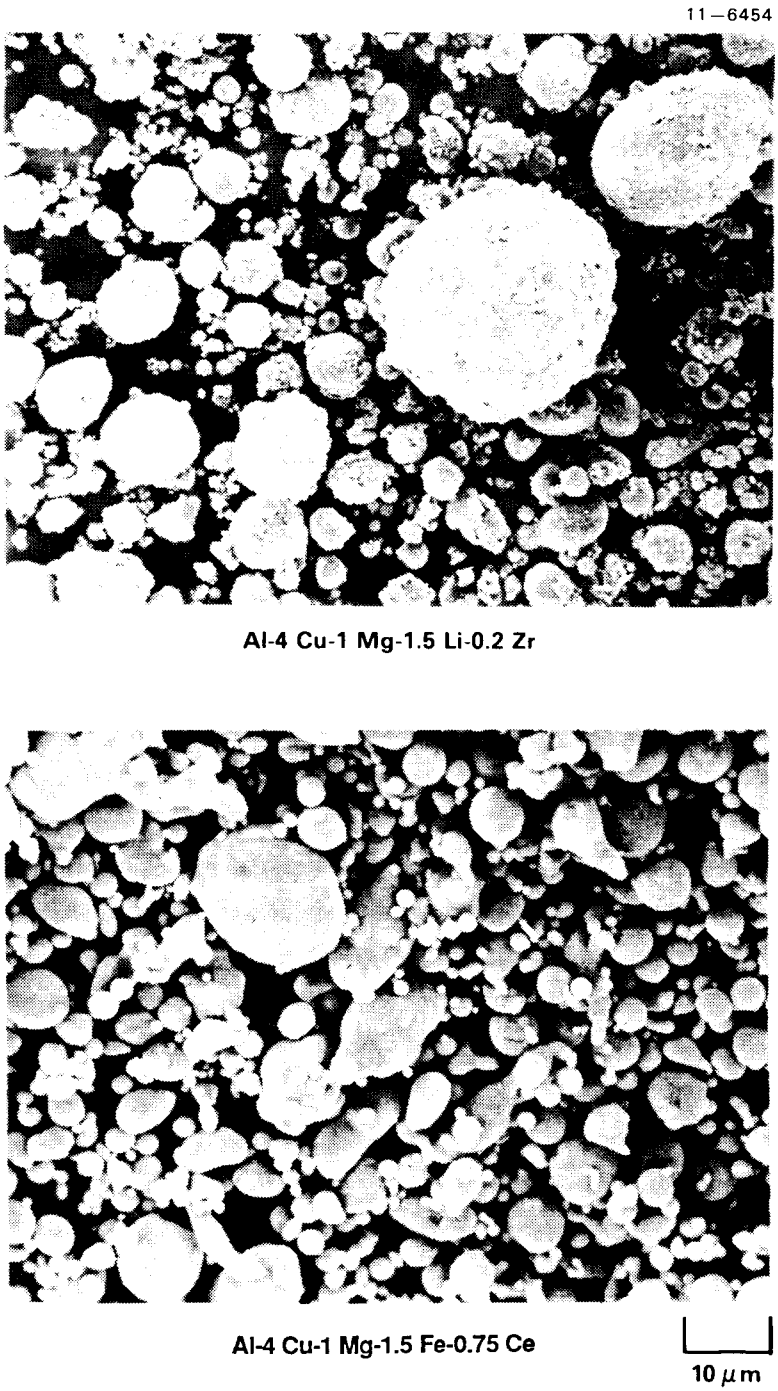

FIGURE 2. APPEARANCE OF THE PREALLOYED POWDER

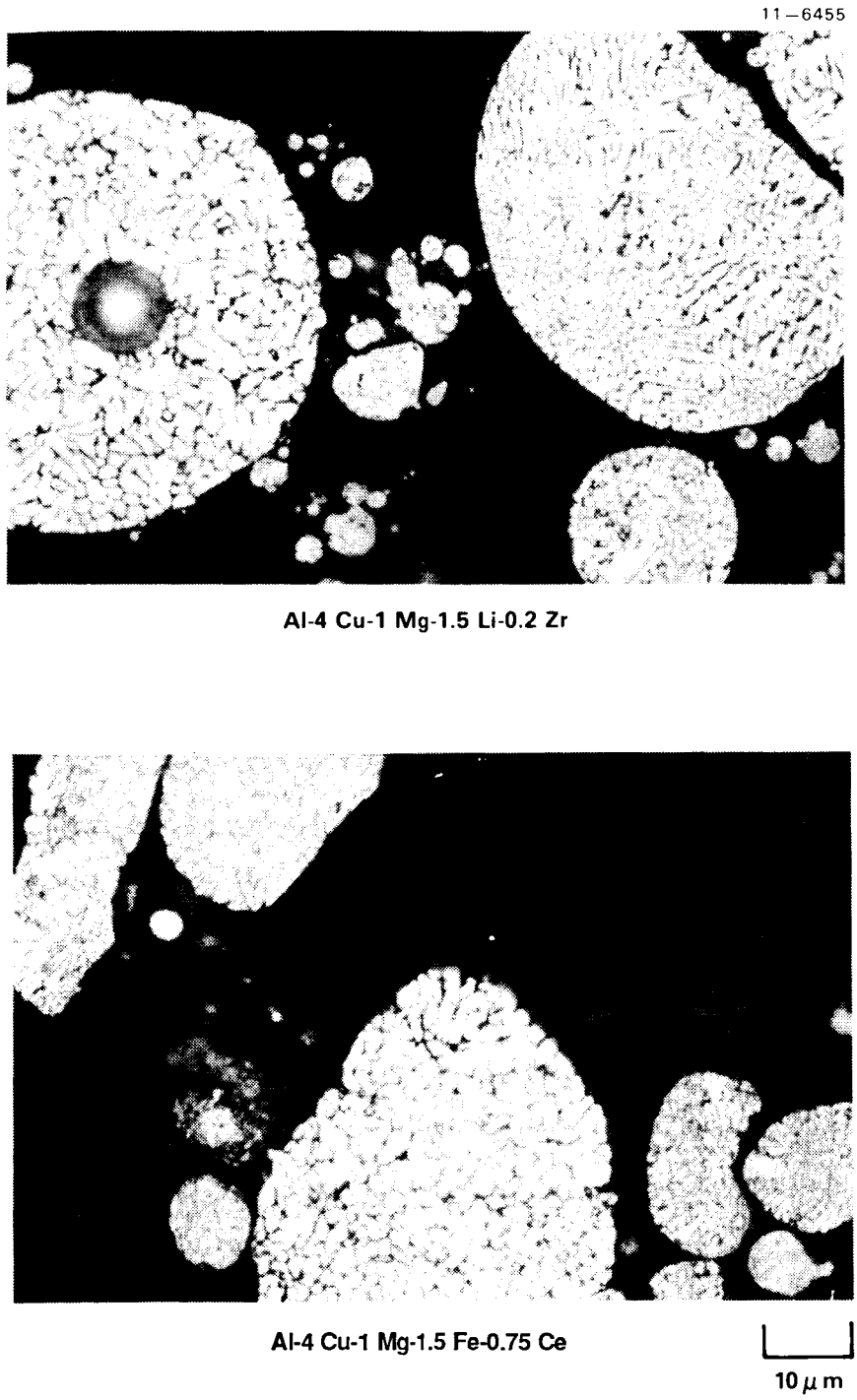

FIGURE 3. AS-SOLIDIFIED MICROSTRUCTURE OF THE PREALLOYED POWDER

5.2 Billet and Extrusion Characteristics

5.2.1 Hydrogen Contents of the Hot-Pressed Billets and Extrusions - The hydrogen contents of the billets and extrusions are presented in Table 6. The hydrogen contents of the hot-pressed billets of the Al-4Cu-1Mg-1.5Li-0.2Zr

TABLE 6. HYDROGEN CONTENT OF THE ALLOYS

TASK	ALLOY	ALLOY NUMBER	VACUUM DEGASSING TEMPERATURE		VACUUM DEGASSING TIME	HOT PRESSING TEMPERATURE		HYDROGEN CONTENT	
			K	°F	h	K	°F	PPM	
								BILLET	EXTRUSION
I	PA Al-4Cu-1Mg-1.5Li-0.2Zr	1	750	891	6	675	756	38.40	34.41
		2	750	891	12	675	756	29.56	25.69
		3	790	963	6	675	756	20.65	34.19
	PA Al-4Cu-1Mg-1.5Fe-0.75Ce	4	750	891	12	675	756	0.96	2.44
		5	750	891	12	675	756	0.97	1.05
		6	790	963	6	675	756	1.92	3.18
II	MA Al-4Cu-1Mg-1.5Li	7	750	891	6	675	756	29.42	33.92
		8	750	891	12	675	756	26.83	31.48
		9	790	963	6	675	756	23.80	24.11
	MA Al-4Cu-1Mg-1.5Fe-0.75Ce	10	750	891	12	675	756	5.65	6.15
		11	750	891	12	675	756	1.88	2.52
		12	790	963	6	675	756	2.60	3.30
III	PA Al-4Cu-1Mg-1.5Li-0.2Zr	13	750	891	6	750	891	176.71	72.74
		14	750	891	6	750	891	91.93	29.75
		15	790	963	6	790	963	45.57	49.81
	MA Al-4Cu-1Mg-1.5Li	16	750	891	6	750	891	62.29	140.00
		17	750	891	6	750	891	349.23	193.32
	MA Al-4Cu-1Mg-1.5Fe-0.75Ce	18	750	891	6	750	891	183.17	58.81
	(Using PA Al-1.6Fe-0.8Ce)	19	790	963	6	790	963	22.50	22.52
	MA Al-4Cu-1Mg-1.5Fe-0.75Ce	20	750	891	6	750	891	7.29	11.96
	(Using Elemental Powder)	21	790	963	6	790	963	18.55	8.59

(alloys 1, 2, and 3) and Al-4Cu-1Mg-1.5Fe-0.75Ce (alloys 4, 5, and 6) alloys prepared by the conventional consolidation of PA powder are about an order of magnitude lower than that of the powder used in preparing these alloys. The hydrogen contents of the MA Li-containing alloys prepared by conventional consolidation (alloys 7, 8, and 9) are similar to those of the corresponding PA alloys (alloys 1, 2, and 3). Although mechanical alloying can be expected to

increase the hydrogen content of aluminum alloys, the effect is not observed in the Li-containing alloys due to their inherently higher hydrogen content. However, such an effect is observed in the Fe- and Ce-containing alloys (compare alloys 10, 11, and 12 with alloys 4, 5, and 6).

For both the PA and MA Li-containing alloys prepared by conventional consolidation, the hydrogen content is lowered by increasing either the degassing time or the temperature (compare alloys 1 and 2, 1 and 3, 7 and 8, and 7 and 9). It has been reported in a previous investigation (17) that the hydrogen concentration of vacuum degassed Li-containing alloy powder passes through a minimum with increasing degassing temperature. Above the degassing temperature corresponding to the minimum in the hydrogen concentration, more of the liberated hydrogen-bearing species is chemically fixed by Li than is physically removed. Such an observation was made in an Al-3Li-1.5Cu-1Mg-0.5Co-0.2Zr alloy for which a degassing temperature of 723K (842°F) resulted in the lowest level of residual hydrogen. However, the lower concentration of Li in the present alloys is probably not sufficient for the chemical fixing of hydrogen, and the efficiency of hydrogen removal increases, although not significantly, with increasing degassing time or temperature. Such an effect is also observed in the PA Li-containing alloys prepared by containerless vacuum hot pressing (compare alloys 13 and 14 with 15). The reason for the increasing hydrogen content with increasing diameter of the MA Al-4Cu-1Mg-1.5Li alloy billet (alloys 16 and 17) is not clear.

The hydrogen contents of the Fe- and Ce-containing alloys are generally lower than those of the Li-containing alloys, and a systematic variation of the hydrogen content with varying degassing parameters is not observed for these alloys prepared by conventional consolidation (alloys 4, 5, 6, 10, 11, and 12). The MA Fe- and Ce-containing alloy powder prepared from partially prealloyed powder appears to have a large initial hydrogen, and a significantly higher amount is removed by degassing at the higher temperature (compare alloys 18 and 19).

Except for the Li-containing alloy billets prepared by the conventional consolidation of the PA or MA powder (alloys 1, 2, 3, 7, 8, and 9), the lack of a systematic variation of the hydrogen contents of the billets with varying degassing parameters is probably because these parameters were not varied over a wide enough range of values. While the two degassing temperatures were chosen to lie above and below the subsequent solution heat treatment temperature, respectively, their proximity precludes wide variations in the degassing efficiency. Nevertheless, for those alloys for which a systematic variation is observed, the degassing efficiency, as measured by the hydrogen content, increases with increasing degassing temperature or time. Additionally, the higher hydrogen content of the billets of both Li-containing and Fe- and Ce-containing alloys processed by CVHP compared with that of the corresponding billets processed by conventional consolidation could be due to the composite billet approach used in containerless consolidation.

The hydrogen contents of the extrusions of the alloys prepared by conventional consolidation (alloys 1 through 12) are generally similar to those of the corresponding hot-pressed billets. For the extrusions of the alloys prepared by containerless consolidation, the hydrogen content, except for alloy 16, is either similar to or lower than that of the corresponding billet.

5.2.2 Chemical Composition of the Extrusions - The chemical compositions of the twenty-one extrusions are presented in Table 7. The overall compositions of the alloys are close to the target. Except for the Cu content of alloy 8 and the Zr content of alloy 1, specific deviations from the nominal composition are systematic. The deviations are the higher Li content (0.25 - 0.35 pct.) of all of the alloys made from the PA powder (alloys 1, 2, 3, 13, 14, and 15), the higher Fe content (0.20 - 0.35 pct.) of all of the alloys made from the MA powder (alloys 10, 11, 12, 18, 19, 20, and 21), and the higher Ce content (0.13 - 0.14 pct.) of the alloys made from the MA powder that used the PA Al-1.6Fe-0.8Ce powder for alloying (alloys 18 and 19).

TABLE 7. CHEMICAL COMPOSITION OF THE EXTRUSIONS

ALLOY	ALLOY NUMBER	CHEMICAL COMPOSITION (WT.%)					
		Cu	Mg	Li	Zr	Fe	Ce
PA Al-4Cu-1Mg-1.5Li-0.2Zr	1	3.90	1.02	1.85	0.40	0.028	--
	2	4.00	1.03	1.83	0.19	0.034	--
	3	3.92	1.01	1.79	0.19	0.060	--
PA Al-4Cu-1Mg-1.5Fe-0.75Ce	4	3.94	0.94	--	--	1.61	0.78
	5	3.90	0.93	--	--	1.61	0.80
	6	3.82	0.92	--	--	1.59	0.78
MA Al-4Cu-1Mg-1.5Li	7	4.08	1.02	1.49	--	0.049	--
	8	4.56	1.15	1.62	--	0.022	--
	9	4.10	1.04	1.44	--	0.022	--
MA Al-4Cu-1Mg-1.5Fe-0.75Ce	10	4.03	1.02	--	--	1.81	0.77
	11	4.13	0.99	--	--	1.78	0.76
	12	3.97	0.99	--	--	1.71	0.74
PA Al-4Cu-1Mg-1.5Li-0.2Zr	13	3.92	1.02	1.77	0.20	0.052	--
	14	3.94	1.03	1.78	0.19	0.020	--
	15	4.03	1.06	1.83	0.20	0.017	--
MA Al-4Cu-1Mg-1.5Li	16	3.98	1.01	1.40	--	0.027	--
	17	4.08	1.03	1.45	--	0.020	--
MA Al-4Cu-1Mg-1.5Fe-0.75Ce	18	4.02	0.97	--	--	1.70	0.88
(Using PA Al-1.6Fe-0.8Ce)	19	4.06	0.97	--	--	1.72	0.89
MA Al-4Cu-1Mg-1.5Fe-0.75Ce	20	3.93	0.99	--	--	1.73	0.73
(Using Elemental Powder)	21	4.11	1.04	--	--	1.83	0.78

5.2.3 Density of the Extrusions - The measured density of the alloys are presented in Table 8. The density values of the alloys are consistent with the corresponding alloy compositions. The density of the Li-containing alloys is about 3.5 - 4.5 pct. lower than that of 2024-Al, while that of the Fe- and Ce-containing alloys is about 1.5 - 3.0 pct. higher. Except for the density of alloy 13, the measured values are also consistent with the deviations in the chemical compositions of the respective alloys.

TABLE 8. DENSITY OF THE EXTRUSIONS

ALLOY	ALLOY NUMBER	DENSITY		PCT. CHANGE RELATIVE TO ALLOY 2024-Al
		g/cm^3	$lb/in.^3$	
PA Al-4Cu-1Mg-1.5Li-0.2Zr	1	2.644	0.0955	- 4.55
	2	2.651	0.0957	- 4.30
	3	2.653	0.0958	- 4.22
PA Al-4Cu-1Mg-1.5Fe-0.75Ce	4	2.818	0.1018	+ 1.73
	5	2.824	0.1020	+ 1.95
	6	2.812	0.1016	+ 1.52
MA Al-4Cu-1Mg-1.5Li	7	2.673	0.0966	- 3.50
	8	2.667	0.0964	- 3.72
	9	2.676	0.0967	- 3.39
MA Al-4Cu-1Mg-1.5Fe-0.75Ce	10	2.847	0.1029	+ 2.78
	11	2.838	0.1025	+ 2.45
	12	2.845	0.1028	+ 2.71
PA Al-4Cu-1Mg-1.5Li-0.2Zr	13	2.670	0.0965	- 3.61
	14	2.646	0.0956	- 4.48
	15	2.640	0.0954	- 4.69
MA Al-4Cu-1Mg-1.5Li	16	2.668	0.0964	- 3.68
	17	2.669	0.0964	- 3.65
MA Al-4Cu-1Mg-1.5Fe-0.75Ce	18	2.844	0.1027	+ 2.67
(Using PA Al-1.6Fe-0.8Ce)	19	2.853	0.1031	+ 3.00
MA Al-4Cu-1Mg-1.5Fe-0.75Ce	20	2.835	0.1024	+ 2.35
(Using Elemental Powder)	21	2.845	0.1028	+ 2.71

5.2.4 Appearance, Microstructure, and Deformation Sub-Structure of the Extrusions - All of the extrusions exhibited hot tearing on the surface with the degree of hot tearing varying from slight to severe. Residual container feed was also observed in some of the alloys prepared by conventional consolidation. Blisters were observed in only one of the alloys (alloy 15). These were present only in the region near the end of push. Extrusions of the alloys 18, 19, 20, and 21 had a rough surface finish. A crack was also present over the entire length of the extrusion of alloy 16.

Optical micrographs of selected alloys in the as-extruded condition are presented in Figure 4. The microstructures are typical of that of powder-processed aluminum alloys in the hot-worked and highly overaged condition. Considerable microstructural refinement is observed. In all of the alloys, the size of the second-phase particles is no larger than about 10 μm. The microstructures of the Li-containing alloys (alloys 3, 7, and 15) exhibit a high volume fraction of 3 - 10 μm particles. The particles in the alloy made from the PA powder (alloys 3 and 15)) are etched to varying degrees by the Keller's etch. The smaller (<2 μm) particles that are not strongly etched are believed to be Al_2Cu, while the larger particles that are attacked strongly are probably ternary compounds containing Li (18). In the alloy made from the MA powder (alloy 7), all of the second-phase particles are strongly attacked suggesting that these are Li-containing phases.

The microstructures of the extrusions of the Al-4Cu-1Mg-1.5Fe-0.75Ce alloy made from both the PA powder (alloy 6), and the MA powder that was made using the PA Al-1.6Fe-0.8Ce powder (alloy 19) show extremely fine and uniformly distributed second-phase particles. The volume fraction of these particles is higher in the latter alloy. In contrast, the presence of coarse particles in the alloy made by the mechanical alloying of elemental powder (alloy 12) suggests that complete and homogeneous alloying of the elemental Fe and Ce particles has not occurred.

The (111) pole figures of the extrusions of alloys 2, 5, 8, and 11 showed similar deformation texture. The difference among these alloys was in the degree of preferred orientation, with alloys 2 and 5 (made from the PA powder) showing a higher degree of texture than alloys 8 and 11 (made from the MA powder). The pole figures of alloys 2 and 5, shown in Figure 5, are representative of hot-worked and fully recovered sub-structures. The maximum x-ray intensities for alloys 8 and 11 were also considerably lower than that for alloys 2 and 5, suggesting that, as expected, the carbides and oxides result in a finer sub-structure in the mechanically alloyed materials.

Attempts to determine the degree of recrystallization of the extrusions of alloys 2, 5, 8, and 11 from pin-hole, back-reflection patterns were rendered difficult by the fluorescence of the alloys, and the relatively low diffracted x-ray intensity. Patterns of moderate quality that were obtained by using special x-ray films and extended exposure times revealed that these alloys possessed unrecrystallized microstructures. These results are also consistent with the microstructural observations and texture measurements.

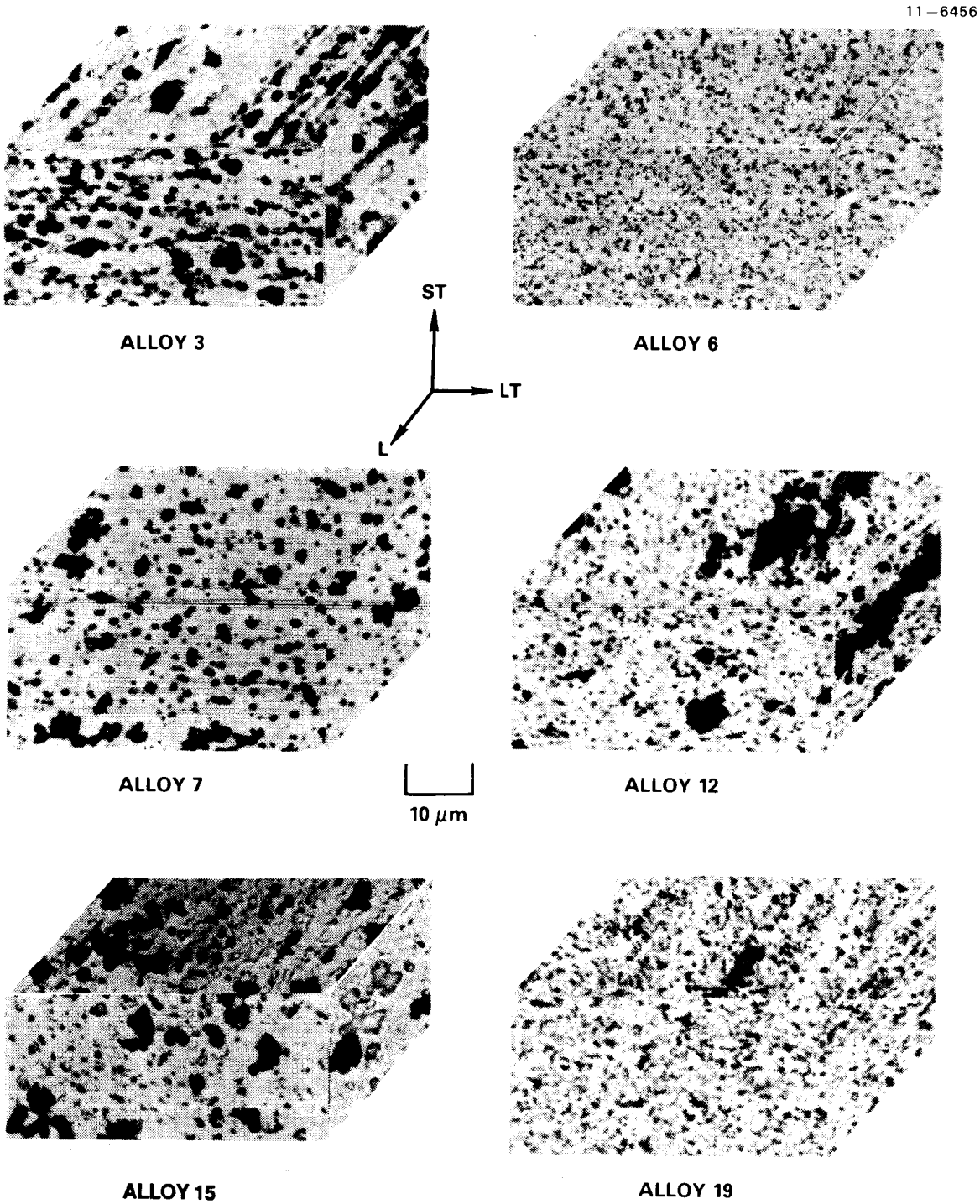

FIGURE 4. MICROSTRUCTURE OF THE AS-EXTRUDED ALLOYS

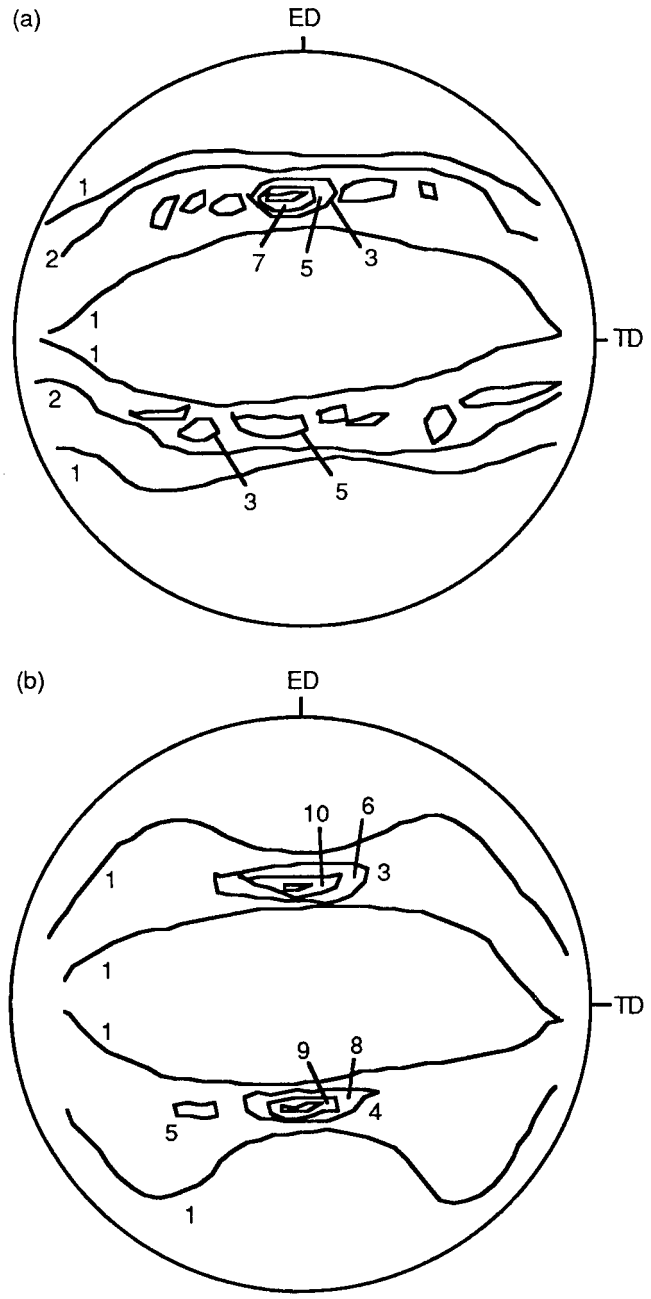

FIGURE 5. (111) POLE FIGURE OF THE AS-EXTRUDED ALLOYS: (a) ALLOY 2 AND (b) ALLOY 5. CONTOUR VALUES ARE RELATIVE TO THE RANDOM INTENSITY.

5.2.5 Microstructure and Sub-Structure of the Solution Heat Treated Alloys - Optical micrographs of the extrusions of the alloys which were solution heat treated at 773K (932°F) for 1 hour are presented in Figure 6. Solution heat treatment did not result in observable recrystallization of these alloys. Several observations can be made by comparing these microstructures with those of the same alloys in the as-extruded condition (Figure 4).

In the PA Al-4Cu-1Mg-1.5Li-0.2Zr alloy (alloys 3 and 15), full dissolution of the excess solute-rich phases is not achieved at 773K (932°F). The Li-content of all of the PA Al-4Cu-1Mg-1.5Li-0.2Zr alloys is higher than the nominal which probably results in a total solute content exceeding the limit of solubility at the solution heat treatment temperature. Except for alloy 8, all of the MA Li-containing alloys have compositions that are close to the nominal, and, as observed in Figure 6, complete dissolution of the coarser, solute-rich phases is achieved in the MA Al-4Cu-1Mg-1.5Li alloy (alloy 7).

The microstructures of alloys 6 and 19 in the solution heat treated condition suggest that full dissolution of the second phases is not achieved at the selected solution heat treatment temperature. In the alloys made from the PA powder, the undissolved second phase particles in the Fe- and Ce-containing alloy (alloy 6) are finer than those in the Li-containing alloys (alloys 3 and 15) and are also uniformly distributed. The size and distribution of the coarse, unalloyed elemental Fe and Ce particles in the Al-4Cu-1Mg-1.5Fe-0.75Ce alloy made by the mechanical alloying of elemental powder (alloy 12) are also unaffected by the solution heat treatment.

The (111) pole figures of the extrusions of alloys 2, 5, 8, and 11 in the solution heat treated condition were similar to those in the as-extruded condition. The difference among the alloys was again in the degree of preferred orientation, with the alloys made from the PA powder exhibiting a higher degree of texture. The pole figures of alloys 2 and 5 in the solution heat treated condition, shown in Figure 7, are representative of hot-worked and recovered alloys. As with the alloys in the as-extruded condition, the maximum x-ray intensities from the alloys made from the MA powder (alloys 8 and 11) were also considerably lower than for the alloys made from the PA powder (alloys 2 and 5). Consistent with the microstructural observations and texture measurements, the pin-hole, back-reflection patterns of alloys 2, 5, 8, and 11 in the solution heat treated condition revealed unrecrystallized microstructures. However, recrystallization of the alloys made from the MA powder cannot be ruled out, since the extremely fine grains typical of these alloys will not be identified by these techniques.

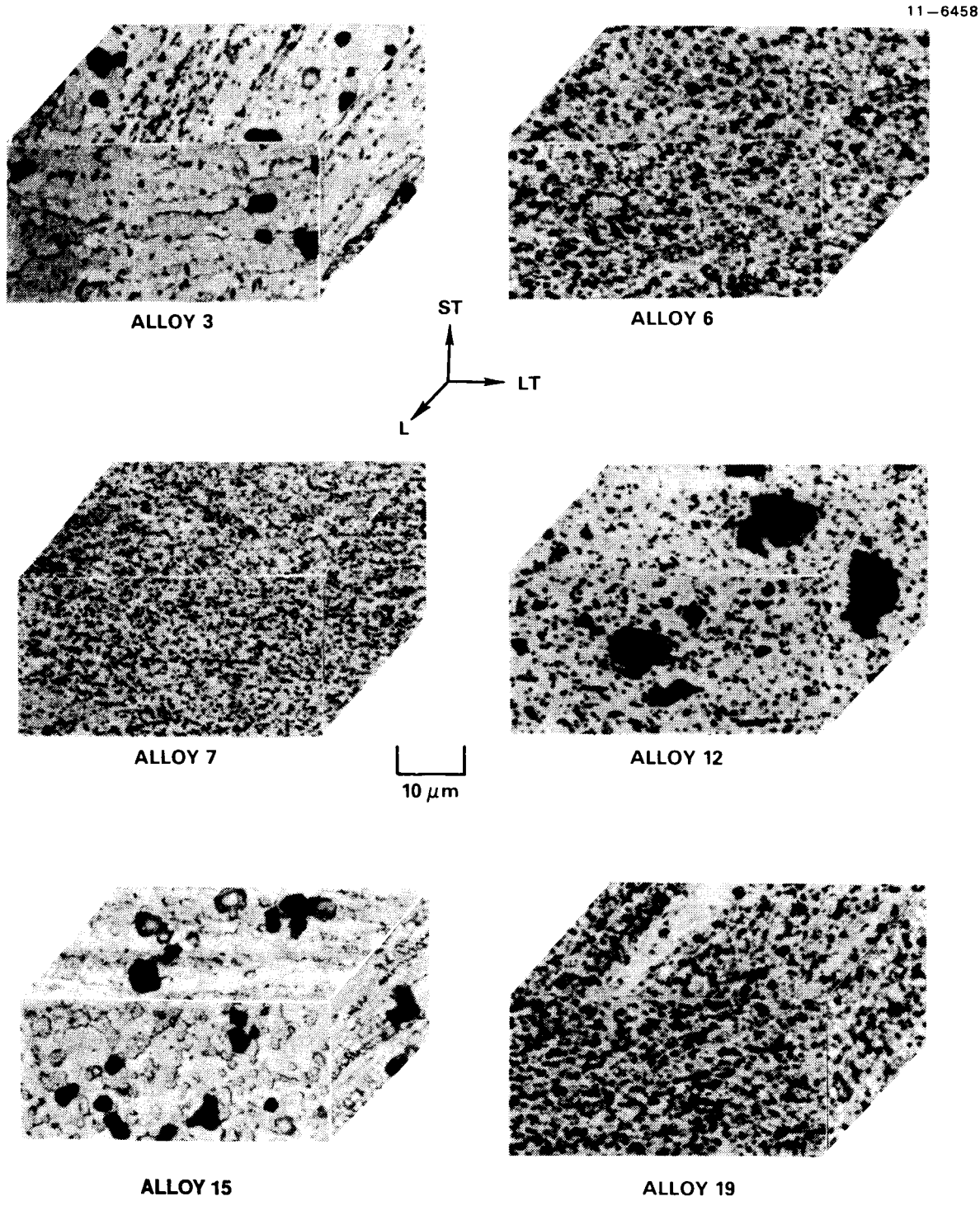

FIGURE 6. MICROSTRUCTURE OF THE SOLUTION HEAT TREATED ALLOYS

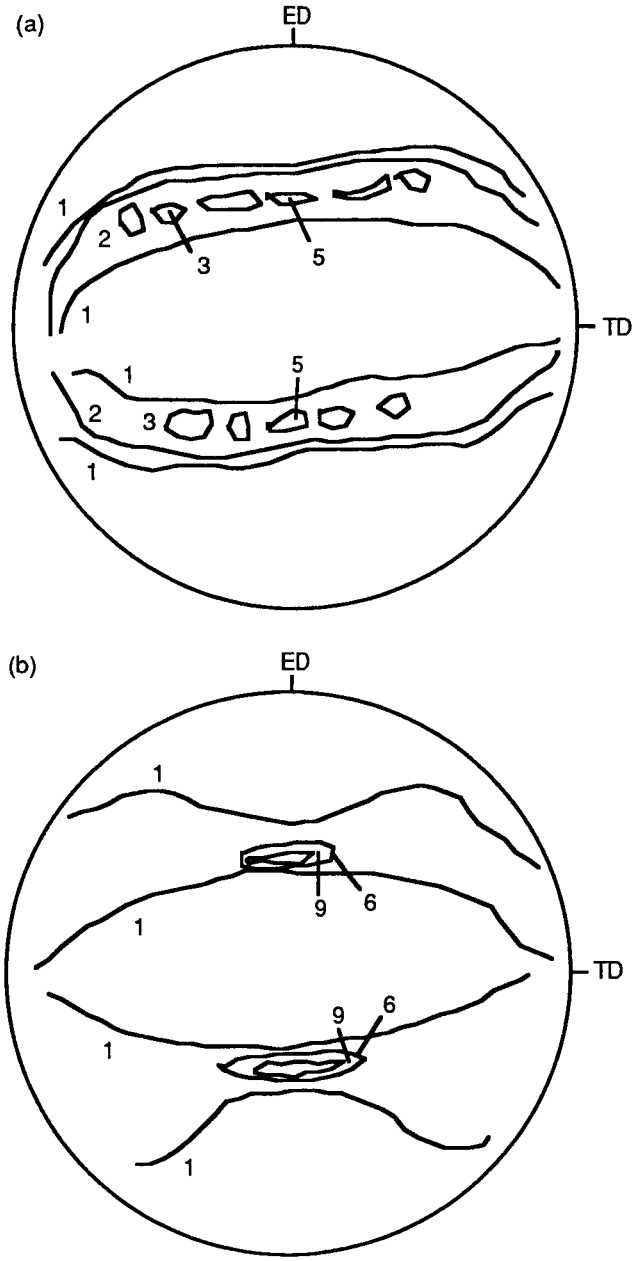

FIGURE 7. (111) POLE FIGURE OF THE SOLUTION HEAT TREATED ALLOYS: (a) ALLOY 2 AND (b) ALLOY 5. CONTOUR VALUES ARE RELATIVE TO THE RANDOM INTENSITY.

5.3 Influence of Post-Extrusion Processing on the Properties

The primary purpose of this study is to investigate the influence of varying the critical consolidation processing parameters on the properties. However, selecting the proper post-consolidation processing parameters is also

essential to obtaining meaningful mechanical properties. Thus, prior to investigating the influence of varying the vacuum degassing parameters on the mechanical properties of the alloys, their age-hardening characteristics were determined for selecting the appropriate aging conditions. Additionally, the influence of cold working by stretching prior to aging, and of varying the solution heat treatment temperature and the aging times at the selected peak aging temperature was also determined for a limited number of representative alloys.

5.3.1 Age-Hardening Behavior - The age-hardening curves of alloys 3, 9, and 13 at room temperature, 433K (320°F), 463K (374°F), and 493K (428°F) following solution heat treatment at 773K (932°F) for 1 hour and water quenching are presented in Figure 8.

M11-6460

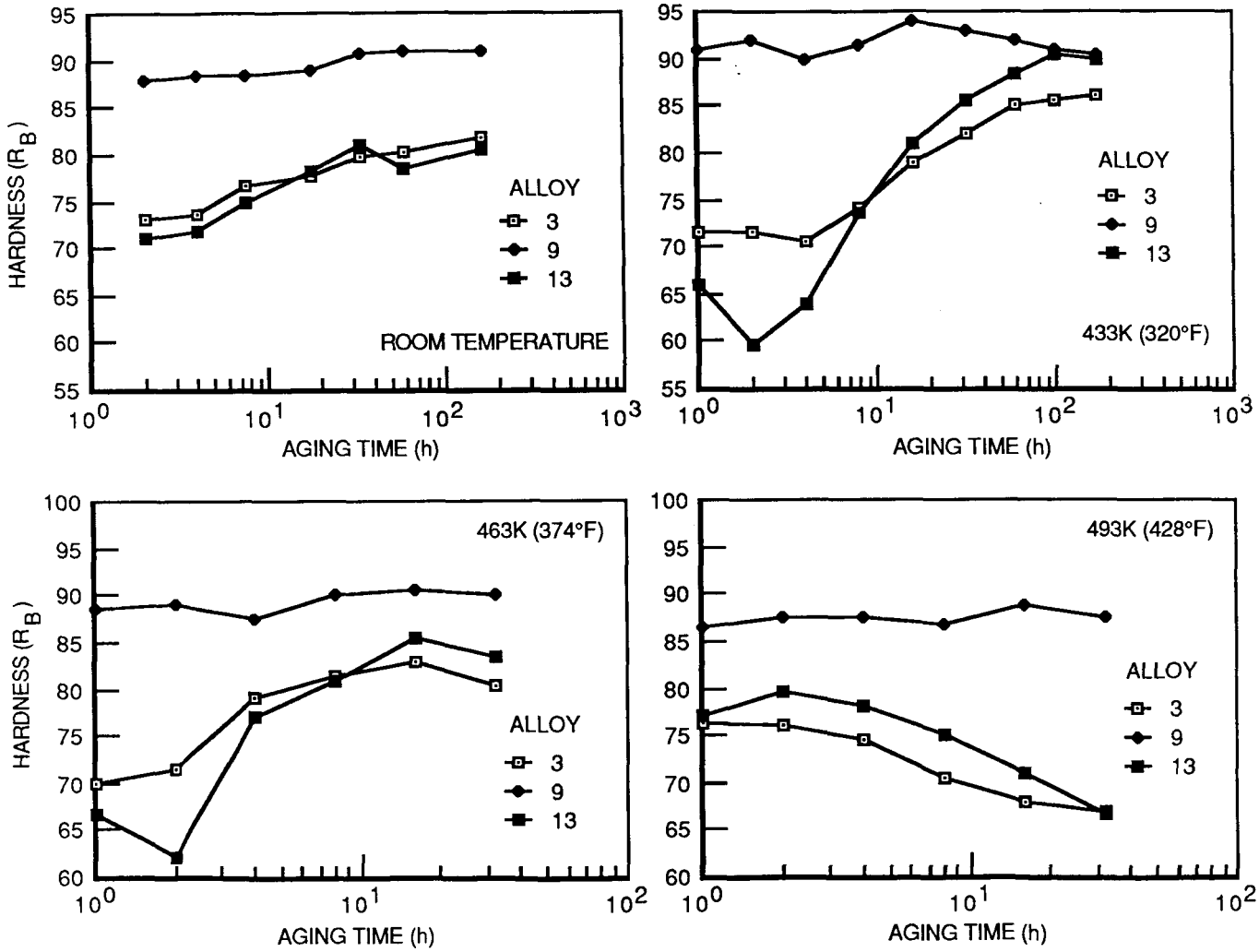

FIGURE 8. AGE-HARDENING CURVES FOR ALLOYS 3, 9, AND 13

The hardening behavior of these alloys indicates that the Li-containing alloys made from the PA powder (alloys 3 and 13) exhibit aging kinetics similar to those of conventional alloys such as 2024-Al. Maximum hardness at 463K (374°F) is achieved after 16 hours, and stable hardness at room temperature is achieved after seven days. Also, longer aging times are required at 433K (320°F) than at 463K (374°F) to achieve peak hardness, although the value of the maximum hardness itself is higher at the lower aging temperature. The hardness of the Li-containing alloy made from the MA powder (alloy 9) is rather insensitive to aging.

Extensive analytical transmission electron microscopic (TEM) studies are required to identify the precipitating phases that are responsible for the observed age-hardening in these alloys. The TEM studies (summarized in the appendix) that were independently conducted were limited to observing the sub-structural features such as the sub-grain and grain structure and the dispersoids. Nevertheless, despite the uncertainties arising from the lack of TEM data, the known precipitation-hardening behavior of the component binary and ternary systems was used to explain the age-hardening behavior of the more complex alloys of this investigation.

It is observed that both of the Li-containing alloys made from the PA powder (alloys 3 and 13) exhibit similar behavior. The dual kinetics exhibited by these alloys, especially at the lower temperatures, may be attributed to a combination of the solid-solution hardening by Li, and the co-precipitation of GP zones/θ"/θ' and δ'(Al_3Li) which occur independently of each other. The solubility of Li decreases with increasing Mg, and an initial increase in the rate of Al_3Li precipitation may result from the Mg in the solid solution. With the onset of the precipitation of Al_2CuMg, the supersaturation of Li and hence the driving force for the precipitation of Al_3Li decreases. The initial drop in the hardness of alloy 13 at 433K (320°F) and 463K (374°F) results from reversion which is a partial breakdown of the GP zones that may have formed upon exposure to room temperature during sample preparation following solution treatment and quenching. Possible precipitation reactions in the Li-containing alloys made from the PA powder are:

$$\text{GP I} \longrightarrow \theta'' \longrightarrow \theta' \longrightarrow Al_2Cu$$

$$\text{Solid Solution} \longrightarrow \delta' \longrightarrow Al_2MgLi\ (Al_2CuLi)$$

$$\text{GP I} \longrightarrow S'' \longrightarrow S' \longrightarrow Al_2CuMg$$

Al_2Cu, Al_2CuLi, and Al_2CuMg are non-coherent precipitates, and their formation on prolonged exposures at elevated temperatures causes overaging and decreases the hardness.

In the Al-4Cu-1Mg-1.5Li alloy made from the MA powder (alloy 9), dispersion strengthening by the oxides and carbides is expected to superimpose on to the mechanisms discussed for the alloys made from the PA powder. The age-hardening kinetics of alloy 9 indicates that the oxides and carbides impart considerable strengthening. The stability of these phases also results in a lower sensitivity of the hardness to the aging conditions. The dispersoids in the alloys made from MA powder are initially amorphous. At temperatures approaching 673K (752°F), the oxides and carbides crystallize to provide γ-Al_2O_3 and Al_4C_3, respectively (19). The solution heat treatment

temperature is sufficiently high to crystallize these phases, and the relatively low aging temperatures have little influence on dispersion strengthening. The rise and fall of the aging curve for alloy 9 is a result of the interaction between hardening by the oxides, carbides, and the solute-rich precipitates. While the variations are repeated in the same sequence at each aging temperature, the exact nature of the superposition of the strengthening mechanisms is uncertain.

The strengthening mechanisms of the Al-4Cu-1Mg-1.5Fe-0.75Ce alloys made from the PA powder are expected to be similar to those of the equivalent 2XXX-series alloys. The intermetallic Fe- and Ce-containing dispersoids are not expected to coarsen at the low aging temperatures. In these alloys made from the MA powder, the dispersion strengthening by the oxides and carbides are also expected to be similar to those in the Li-containing alloys.

Based upon the above observations, unless otherwise indicated, the mechanical properties of all of the alloys were determined after solution heat treatment at 773K (932°F) for 1 hour followed by water quenching and aging either at room temperature for a minimum of 7 days (natural aging, NA) or at 463K (374°F) for 16 hours (artificial aging, AA). While higher peak hardness values were achieved for alloys 3 and 13 after aging for over 100 hours at 433K (320°F), based on the commercial practice for 2024-Al and the practicality to achieve maximum hardness within a reasonably short time, aging for 16 hours at 463K (374°F) was chosen as representative of peak aging.

5.3.2 Effect of Cold-Work on Tensile Properties - As reported in Section 4.4, only alloys made from the PA powder could be stretched successfully. The influence of cold working by a nominal stretch of 1.5 pct., following solution heat treatment at 773K (932°F) for one hour and water quenching and prior to aging, on the mechanical properties of a representative Li-containing alloy (alloy 3, stretched to a permanent set of 1.5 pct.) and an Fe- and Ce-containing alloy (alloy 6, stretched to a permanent set of 1.75 pct.) is presented in Table 9. During the interval between quenching and stretching, the alloys were held at a temperature lower than 248K (-13°F).

TABLE 9. INFLUENCE OF COLD WORKING BY STRETCHING PRIOR TO AGING ON THE LONGITUDINAL TENSILE PROPERTIES

ALLOY	AGING TREATMENT	0.2% OFFSET YIELD STRENGTH		ULTIMATE TENSILE STRENGTH		ELONGATION
		MPa	ksi	MPa	ksi	%
3	NA	441	64	545	79	6
3(S)	NA	448	65	510	74	5
3	AA	393	57	462	67	4
3(S)	AA	469	68	538	78	5
6	NA	193	28	352	51	15
6(S)	NA	248	36	352	51	10
6	AA	179	26	290	42	16
6(S)	AA	269	39	331	48	13

S - Stretched. Properties of alloy 3(S) in the AA condition are from one test.

The influence of plastic deformation prior to age-hardening on the mechanical properties of aluminum alloys depends on the effects of the defects on precipitate nucleation. In Al-Cu-Mg alloys, the precipitation kinetics of GP zones is significantly enhanced by the defects. However, in Al-Cu-Li alloys, the response to cold work is dependent on the relative levels of Cu and Li which determine the type of the strengthening precipitates (20). The addition of Li to Al-Cu alloys is also known to modify the GP zones present in the binary alloy (21). Thus, in contrast with conventional alloys such as 2024-Al, the lack of response to stretching in alloy 3 in the NA condition is perhaps due to the presence of Li-modified GP zones whose kinetics of precipitation is not enhanced by defects. However, in the AA condition, precipitation of the $Al_2Cu(Mg, Li)$ phase is enhanced by cold working with a resultant increase of strength. For alloy 6 in both the NA and AA conditions, the influence of stretch is similar to that observed in alloys such as 2024-Al. The increase in the yield strength is more pronounced than the increase in the tensile strength. The strength enhancement is also accompanied by a decrease in the ductility.

5.3.3 Effect of Solution Heat Treatment Temperature on Tensile Properties - As described earlier, all of the alloys were vacuum degassed both above and below the selected solution heat treatment temperature (773K, 932°F). This temperature was chosen so as to result in the full dissolution of the solute elements in the alloys of the nominal compositions. However, the very low strength of the Fe- and Ce-containing alloys made from the PA Al-4Cu-1Mg-1.5Fe-0.75Ce powder indicated that the solute elements did not fully dissolve at 773K (932°F). To investigate the influence of the solution heat treatment temperature, the tensile properties of alloys 5 and 6 were determined in the longitudinal direction following solution heat treatment at both 753K (896°F) and 788K (959°F), and natural aging. The results of these tests, which are presented in Table 10, clearly show increasing strength with increasing solution heat treatment temperature. Increasing the solution heat treatment temperature increases the solubility of the solute elements thereby increasing the amount of solute available for precipitation hardening. Despite these results, all of the alloys were still solution heat treated at 773K (932°F) since this temperature lies between the two vacuum degassing temperatures and its choice was dictated once the billets were consolidated.

TABLE 10. INFLUENCE OF SOLUTION HEAT TREATMENT (SHT) TEMPERATURE ON THE LONGITUDINAL TENSILE PROPERTIES

ALLOY AND AGING CONDITION	SHT TEMPERATURE		0.2% OFFSET YIELD STRENGTH		ULTIMATE TENSILE STRENGTH		ELONGATION
	K	°F	MPa	ksi	MPa	ksi	%
5 NA	753	896	172	25	331	48	16
5 NA	773	932	207	30	365	53	16
5 NA	788	959	234	34	400	58	15
6 NA	753	896	165	24	324	47	16
6 NA	773	932	193	28	352	51	15
6 NA	788	959	234	34	393	57	13

5.3.4 Effect of Aging Conditions on Tensile Properties - To determine the influence of aging conditions on the mechanical properties, representative alloys (alloys 2, 5, 8, and 11) were aged for varying times at 463K (374°F) following solution heat treatment at 773K (932°F) and water quenching. The longitudinal tensile properties of these alloys, which are presented in Table 11, indicate that the peak strength is achieved after aging for a period of time that is lower than that at which peak hardness is achieved. The effect is particularly pronounced in alloy 2, since the PA Li-containing alloys are strengthened solely by precipitation hardening. In the other alloys, which are additionally strengthened by the dispersoids, the effect is less pronounced due to the relative insensitivity of the dispersion strengthening to exposure at the aging temperature. Overaging by aging for 33 hours does not significantly affect the strength.

TABLE 11. INFLUENCE OF AGING TIME AT 463K (374°F) ON THE LONGITUDINAL TENSILE PROPERTIES

ALLOY	AGING TIME	0.2% OFFSET YIELD STRENGTH		ULTIMATE TENSILE STRENGTH		ELONGATION
	h	MPa	ksi	MPa	ksi	%
2	6	455	66	524	76	4
2	12	462	67	524	76	3
2	16	407	59	469	68	3
2	33	421	61	483	70	3
5	6	200	29	324	47	14
5	16	186	27	296	43	15
5	33	193	28	290	42	15
8	6	531	77	600	87	2
8	16	496	72	593	86	3
8	33	496	72	593	86	2
11	6	379	55	434	63	6
11	16	352	51	421	61	6
11	33	372	54	421	61	6

5.4 Influence of Vacuum Degassing Parameters on the Properties

5.4.1 Task I: Alloys Prepared by the Conventional Consolidation of Prealloyed Powder -

Al-4Cu-1Mg-1.5Li-0.2Zr: The tensile properties of the Al-4Cu-1Mg-1.5Li-0.2Zr alloy made by the conventional consolidation of PA powder are presented in Table 12. Increasing the vacuum degassing temperature results in a moderate increase in the strength of the naturally aged (NA) alloys, as observed by comparing the properties of alloys 1 and 3. However, a similar effect is not observed in the artificially aged (AA) alloys. Additionally, increasing the vacuum degassing time results in a very small increase in the yield stress of both the NA and AA alloys.

TABLE 12. LONGITUDINAL TENSILE PROPERTIES OF THE Al-4Cu-1Mg-1.5Li-0.2Zr ALLOY PREPARED BY THE CONVENTIONAL CONSOLIDATION OF PREALLOYED POWDER

ALLOY AND AGING CONDITION	VACUUM DEGASSING TEMPERATURE		TIME	0.2% OFFSET YIELD STRENGTH		ULTIMATE TENSILE STRENGTH		ELONGATION
	K	°F	h	MPa	ksi	MPa	ksi	%
1 NA	750	891	6	400	58	503	73	5
2 NA	750	891	12	414	60	510	74	3
3 NA	790	963	6	441	64	545	79	6
1 AA	750	891	6	393	57	469	68	3
2 AA	750	891	12	407	59	469	68	3
3 AA	790	963	6	393	57	462	67	4

Also, the ductility of neither the NA nor the AA alloy changes systematically with the variations in the vacuum degassing conditions. These observations suggest that the possible influence of varying the vacuum degassing parameters on the extent of powder degassing is not responsible for the observed changes in the mechanical properties. Additionally, although increasing the vacuum degassing temperature and/or the time decreased the hydrogen content of the billets of this alloy, the relatively low magnitude of this reduction indicates that, as mentioned earlier, these parameters were not varied over a wide enough range of values. The measured values of the tensile properties also suggest that the range over which the parameters were varied is above the minimum necessary for achieving reasonable properties. The increase in the strength of the NA alloy with increasing degassing temperature must then be due to a change in the sub-structure caused by the variation in the extent of elevated temperature exposure during vacuum degassing.

Except for the changes in the vacuum degassing temperature, the processing sequence is identical for alloys 1 and 3. The differences between these alloys could then arise from the changes in the sub-structure due to the varying volume fraction of the Al_3Zr dispersoids. The Zr remains in the supersaturated solid solution in the as-atomized powder. A certain amount of Zr precipitates as Al_3Zr during vacuum degassing, while the remainder precipitates during the thermal exposure prior to hot pressing the billet. Because of the increasing solid solubility of Zr in Al with increasing temperature, the alloy degassed at the higher degassing temperature (alloy 3, degassed at 790K, 963°F) can be expected to have more of this element available in solid solution for the precipitation of Al_3Zr at the hot pressing temperature. Thus, increasing the vacuum degassing temperature will increase the volume fraction of Al_3Zr that is formed during hot pressing at 675K (756°F) with a corresponding reduction of the sub-grain size following extrusion and solution heat treatment. It is also interesting to note that superplastic Al-Cu-Zr alloys are aged at 643K (698°F) for the precipitation of Al_3Zr that restricts the recrystallization and grain growth during elevated temperature forming (22).

The effect of decreasing the sub-grain size on the strength of these alloys can be illustrated by the following approximate and simple calculation. The diameter of the Al_3Zr particles is typically 10 nm and their volume fraction is about 0.005 (22). Using the Zener relation, R = k.r/f, where R is the limiting radius of the growing grain, f is the volume fraction of the particle, and k is close to 1, increasing the f from 0.005 to 0.01 would decrease the sub-grain diameter from 2 μm to 1 μm. By using the Hall-Petch relation,

$$\sigma = \sigma_0 + K.d^{-1/2}$$

where, for aluminum, the frictional stress (σ_0) is 15.6 MPa (2.3 ksi) and the slope (K) is 0.068 MPa(m)$^{1/2}$ (0.062 ksi(in.)$^{1/2}$) (23), it is found that a decrease in the sub-grain diameter (d) from 2 μm to 1 μm increases the Hall-Petch strengthening (σ) from 64 MPa (9.2 ksi) to 84 MPa (12.2 ksi). While the Zener relationship has been derived for calculating the size of the recrystallized grains which grow in the presence of non-shearable particles, the above calculation does serve to illustrate the contribution to the flow stress by the sub-structural refinement due to the Al_3Zr dispersoids.

The volume fraction of Al_3Zr and the size of the sub-grains were not determined in this study. However, the microstructure of alloy 3 (Figure A4 in the appendix) does suggest that the size of the sub-grains in these alloys can be expected to vary over the range that results in the observed variations in the strength of these alloys.

In the alloys strengthened predominantly by shearable precipitates such as GP zones and/or δ' in which deformation tends to concentrate on long and narrow planar slip bands, sub-grain boundaries are effective obstacles to further slip. In contrast, in the alloys strengthened predominantly by precipitates such as T_1, S', or θ', sub-grain boundaries are not as effective. Thus, superposition of the strengthening by the sub-grains on to that from precipitation hardening is effective in the alloys hardened by shearable precipitates such as GP zones and δ', and not in the alloys hardened by the precipitation of phases such as T_1, S'. or θ'. The changes in the tensile properties of the NA alloys (strengthened by shearable precipitates) with varying vacuum degassing temperature, and the lack of similar changes in the properties of the AA alloys (strengthened by phases such as T_1, S'. or θ') can thus be explained on the basis of the variations in the strengthening by the substructure. The relative insensitivity of the properties of the AA alloys is also consistent with the fact that these alloys are highly overaged (aged past the peak yield strength) and the dislocations can by pass the precipitates by the Orowan mechanism. Thus, slip would be more homogeneous and less planar thereby rendering the sub-grains rather ineffective.

The ductility values of the alloys are somewhat lower than to be expected. As discussed earlier, the Li content of these alloys is higher than intended and results in an excess of the solute-rich phases with an accompanying loss of the ductility. The tensile fracture surface of alloy 3, shown in Figure 9, reveals a ductile fracture mode. The 3 - 5 μm undissolved particles are also similar to that revealed by optical metallography. Energy dispersive x-ray analysis identified these particles to be rich in Cu.

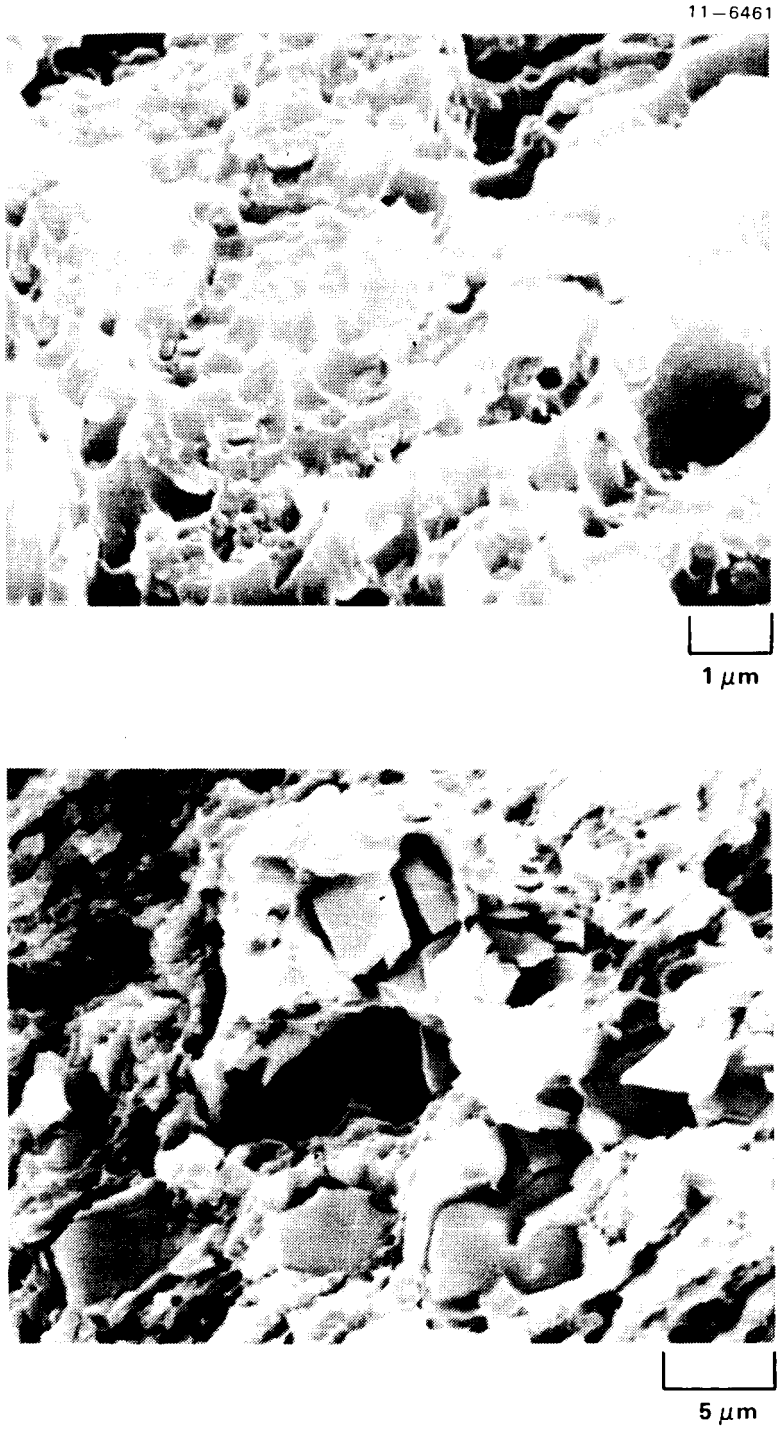

FIGURE 9. TENSILE FRACTURE SURFACE OF ALLOY 3 IN THE ARTIFICIALLY AGED CONDITION

Attempts to determine the tensile properties of these alloys in the transverse direction were not successful due to the low ductility values and the resultant failure in the threaded ends of the specimens. To obtain a measure of the fracture toughness of these alloys, tension tests were conducted on notched specimens of a few selected alloys. The results of these tests are presented in Table 13. Included in the results are the values of the notch tension strength (NTS, the ratio of the maximum load to the initial cross-sectional area in the plane of the notch). For those alloys for which the smooth bar tensile properties were available, the notch yield ratio (NYR, the ratio of the NTS to the smooth bar yield strength), the notch strength ratio (NSR, the ratio of the NTS to the smooth bar tensile strength), and the calculated values of the plane strain fracture toughness (K_{IC}) are also shown.

TABLE 13. NOTCH TENSION PROPERTIES OF THE Al-4Cu-1Mg-1.5Li-0.2Zr ALLOY PREPARED BY THE CONVENTIONAL CONSOLIDATION OF PREALLOYED POWDER

ALLOY AND AGING TREATMENT	ORIENTATION	NTS		NYR	NSR	K_{IC}	
		MPa	ksi			$MPa(m)^{1/2}$	$ksi(in.)^{1/2}$
1 NA	L	365	53	0.91	0.73	18.9	17.2
3 NA	L	352	51	0.80	0.65	18.5	16.8
1 AA	L	269	39	0.68	0.57	13.9	12.6
3 AA	L	262	38	0.67	0.57	13.5	12.3
3 NA	T	165	24	--	-		-
3 AA	T	200	29	-	--	--	--

L - Longitudinal and T - Transverse

K_{IC} values were calculated from the relation:

$$NYR = (4X)\,(1 - (X^2/2))^2$$

where, $X = (K_{IC}/YS)\,(\pi/D)^{-1/2}$, YS is the smooth bar yield strength, and D is the major diameter of the specimen (24). For materials with NYR $\leq$ 1.1, the calculated values of K_{IC} agree to within 10 pct. of the values obtained from more direct measurements. However, because of the approximate nature of the plasticity corrections, agreement is not good for sufficiently ductile alloys.

The notch tension properties and the calculated values of K_{IC} are not affected by the changes in the sub-structure of the alloys caused by the variations in the vacuum degassing parameters. In agreement with the tensile properties, the notch tension properties of the AA alloys are inferior to that of the NA alloys. The poor properties of the alloys in the transverse direction also results in a very low value of the NTS.

Al-4Cu-1Mg-1.5Fe-0.75Ce: The tensile properties of the Al-4Cu-1Mg-1.5Fe-0.75Ce alloy made by the conventional consolidation of the PA powder are presented in Table 14. As discussed in Section 5.3.3, increasing the solution heat treatment temperature increased the strength of this alloy thereby indicating a total solute content in excess of the maximum solid solubility at 773K (932°F). It is possible that the total solute content exceeded the maximum solid solubility even at the higher degassing temperature (790K, 963°F). The excess second-phase particles present in these alloys is nominally composed of three parts - that which would dissolve at 773K (932°F) during solution heat treatment, that which would not dissolve at 773K (932°F) but would dissolve at 790K (963°F), and that which would not dissolve even at 790K (963°F). The extent of coarsening of that part of the second-phase particles attributable to the solute content in excess of the maximum solid solubility at 790K (963°F), is higher in the alloy degassed at this temperature (alloy 6) than in the alloy degassed at the lower temperature (alloy 5). This would explain the small reduction in the strength of alloy 6 compared with that of alloy 5, in either the NA or the AA condition. Additionally, the size of the dispersoids is possibly also not sufficiently small for stabilizing the substructure during hot working, and consequently changing the extrusion ratio does not change the tensile properties. However, while the extent of the dispersion and the sub-structure strengthening may be limited, it is superimposed upon strengthening by shearable precipitates. Consequently, the strength of the NA alloys is higher than that of the corresponding AA alloys.

TABLE 14. LONGITUDINAL TENSILE PROPERTIES OF THE Al-4Cu-1Mg-1.5Fe-0.75Ce ALLOY PREPARED BY THE CONVENTIONAL CONSOLIDATION OF PREALLOYED POWDER

ALLOY AND AGING CONDITION	EXTRUSION RATIO	VACUUM DEGASSING TEMPERATURE		TIME	0.2% OFFSET YIELD STRENGTH		ULTIMATE TENSILE STRENGTH		ELONGATION
		K	°F	h	MPa	ksi	MPa	ksi	%
4 NA	7	750	891	12	207	30	372	54	14
5 NA	19	750	891	12	207	30	365	53	16
6 NA	19	790	963	6	193	28	352	51	15
4 AA	7	750	891	12	193	28	296	43	13
5 AA	19	750	891	12	186	27	296	43	15
6 AA	19	790	963	6	179	26	290	42	16

The tensile fracture surface of alloy 6, shown in Figure 10, reveals a ductile failure mode. The absence of the coarser particles similar to that in the Al-4Cu-1Mg-1.5Li-0.2Zr alloys made from the PA powder results in good values of the ductility. The notch tension properties, presented in Table 15, indicate a high notch tension strength for all of the alloys. Because of the very high plasticity, the K_{IC} values were not calculated.

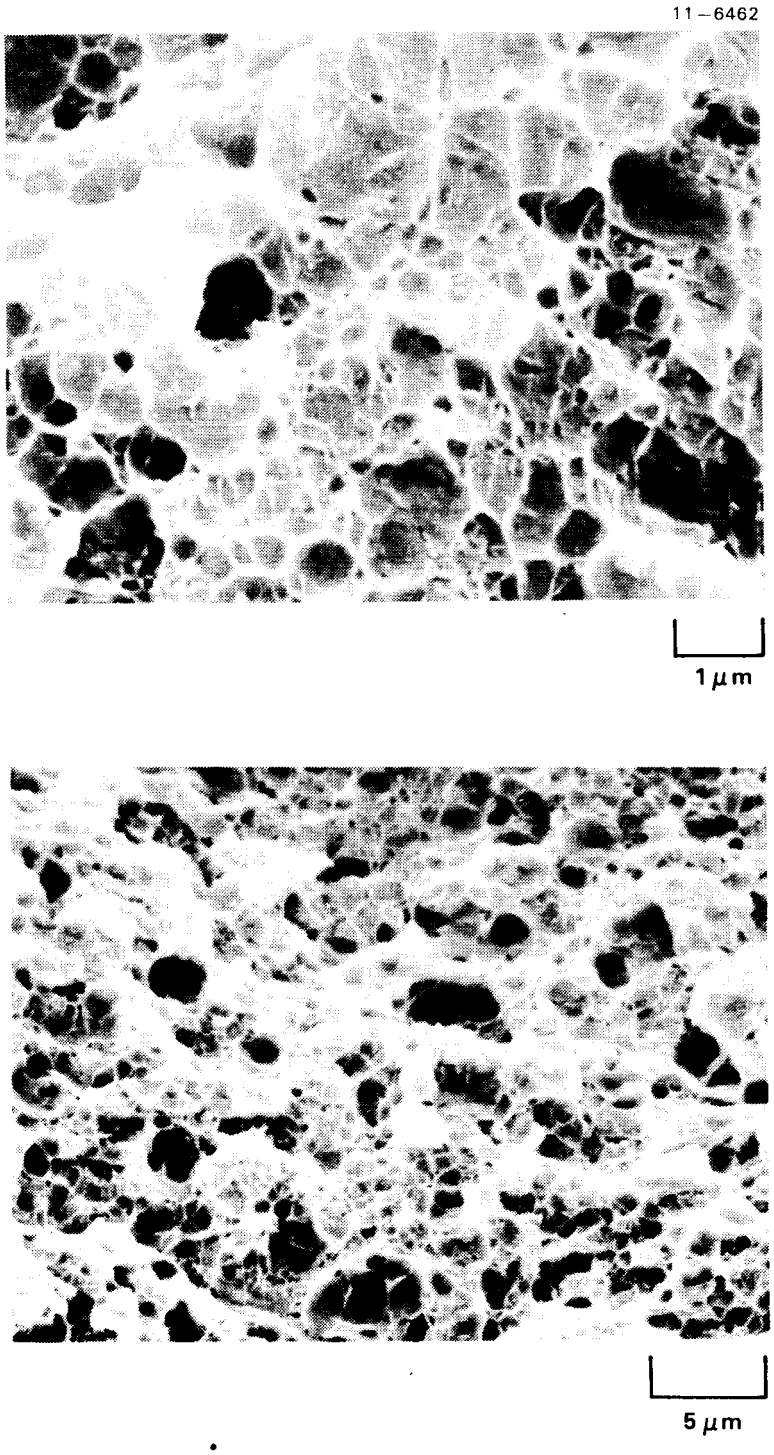

FIGURE 10. TENSILE FRACTURE SURFACE OF ALLOY 6 IN THE ARTIFICIALLY AGED CONDITION

TABLE 15. LONGITUDINAL NOTCH TENSION PROPERTIES OF THE Al-4Cu-1Mg-1.5Fe-0.75Ce ALLOY PREPARED BY THE CONVENTIONAL CONSOLIDATION OF PREALLOYED POWDER

ALLOY AND AGING TREATMENT	NTS		NYR	NSR
	MPa	ksi		
6 NA	434	63	2.21	1.22
6 AA	386	56	2.15	1.33

From the above discussion, it is clear that the only effect of varying the vacuum degassing temperature and/or the time on the properties of Al-4Cu-1Mg-1.5Li-0.2Zr and Al-4Cu-1Mg-1.5Fe-0.75Ce alloys made by the conventional consolidation processing of PA powder appears to be due to the changes in the sub-structure and dispersion strengthening. Together with the success of such techniques as depuretive degassing in achieving good combinations of properties in rapidly solidified 7XXX-series alloys (25), these observations suggest that vacuum degassing above the solution heat treatment temperature may not be necessary, and that once sufficient degassing is achieved, further improvements in the properties of powder-processed aluminum alloys are possible through a proper control of post-consolidation processing.

5.4.2 Task II: Alloys Prepared by the Conventional Consolidation of Mechanically Alloyed Powder -

Al-4Cu-1Mg-1.5Li: The tensile properties of the Al-4Cu-1Mg-1.5Li alloy made by the conventional consolidation of MA powder are presented in Table 16. In contrast with the behavior of the alloys made from PA powder, increasing the vacuum degassing temperature and/or the time decreases the strength of the alloy in both the NA and AA conditions. As with the Al-4Cu-1Mg-1.5Li-0.2Zr alloy made from the PA powder, such behavior can be explained on the basis of the operating strengthening mechanisms.

A significant part of the flow stress of mechanically alloyed materials is due to the dispersion strengthening by the oxides and carbides, and the Hall-Petch strengthening by the very small recrystallized grains. The oxides and carbides are produced during the manufacture of the powder, and any coarsening of these particles during processing will result in a reduction of the strengthening by these particles. The Orowan strengthening by the dispersoids, although not thermally activated, is strongly influenced by the size and spacing of the strengthening particles. The flow stress due to the dispersion strengthening varies inversely with the inter-particle spacing, and an increase of this spacing by the coarsening of the particles will cause a corresponding reduction in the strength. Thus, irrespective of the aging treatment, the strength of the Al-4Cu-1Mg-1.5Li alloy made from the MA powder decreases with increasing vacuum degassing temperature and/or time.

TABLE 16. LONGITUDINAL TENSILE PROPERTIES OF THE Al-4Cu-1Mg-1.5Li ALLOY PREPARED BY THE CONVENTIONAL CONSOLIDATION OF MECHANICALLY ALLOYED POWDER

ALLOY AND AGING CONDITION	VACUUM DEGASSING TEMPERATURE		TIME	0.2% OFFSET YIELD STRENGTH		ULTIMATE TENSILE STRENGTH		ELONGATION
	K	°F	h	MPa	ksi	MPa	ksi	%
7 NA	750	891	6	655	95	676	98	3
8 NA	750	891	12	579	84	641	93	3
9 NA	790	963	6	572	83	614	89	3
7 AA	750	891	6	524	76	621	90	3
8 AA	750	891	12	496	72	593	86	3
9 AA	790	963	6	483	70	565	82	3

Properties of alloy 8 AA are from one test

The strength of the alloys in the AA condition is lower than those of the corresponding alloys in the NA condition. Generally, the strength of unrecrystallized, precipitation-hardened aluminum alloys is higher than that of recrystallized alloys, although grain size itself does not influence the strength. However, in the NA alloys, which are strengthened by shearable precipitates, the small sub-grains (in an unrecrystallized microstructure) such as in the Al-4Cu-1Mg-1.5Li-0.2Zr alloys made from the PA powder (alloys 1, 2, and 3), and the small recrystallized grains such as in the Al-4Cu-1Mg-1.5Li alloys made from the MA powder (alloys 7, 8, and 9) significantly add to the strength of the alloy.

The tensile fracture surface of alloy 9 in the AA condition is shown in Figure 11. While the overall appearance of the fracture surface is oxidized and somewhat unusual, small (0.2 - 0.3 μm) dimples, possibly associated with the oxide and carbide dispersoid particles are observed at the higher magnification. While the failure mode is ductile (fracture results from ductile void nucleation and coalescence), the very high strength of these alloys results in low values of ductility. The notch tension properties and the calculated values of the K_{IC}, shown in Table 17, are lower than the typical values for high-strength aluminum alloys. The properties of the AA alloys are also inferior to those of the NA alloys.

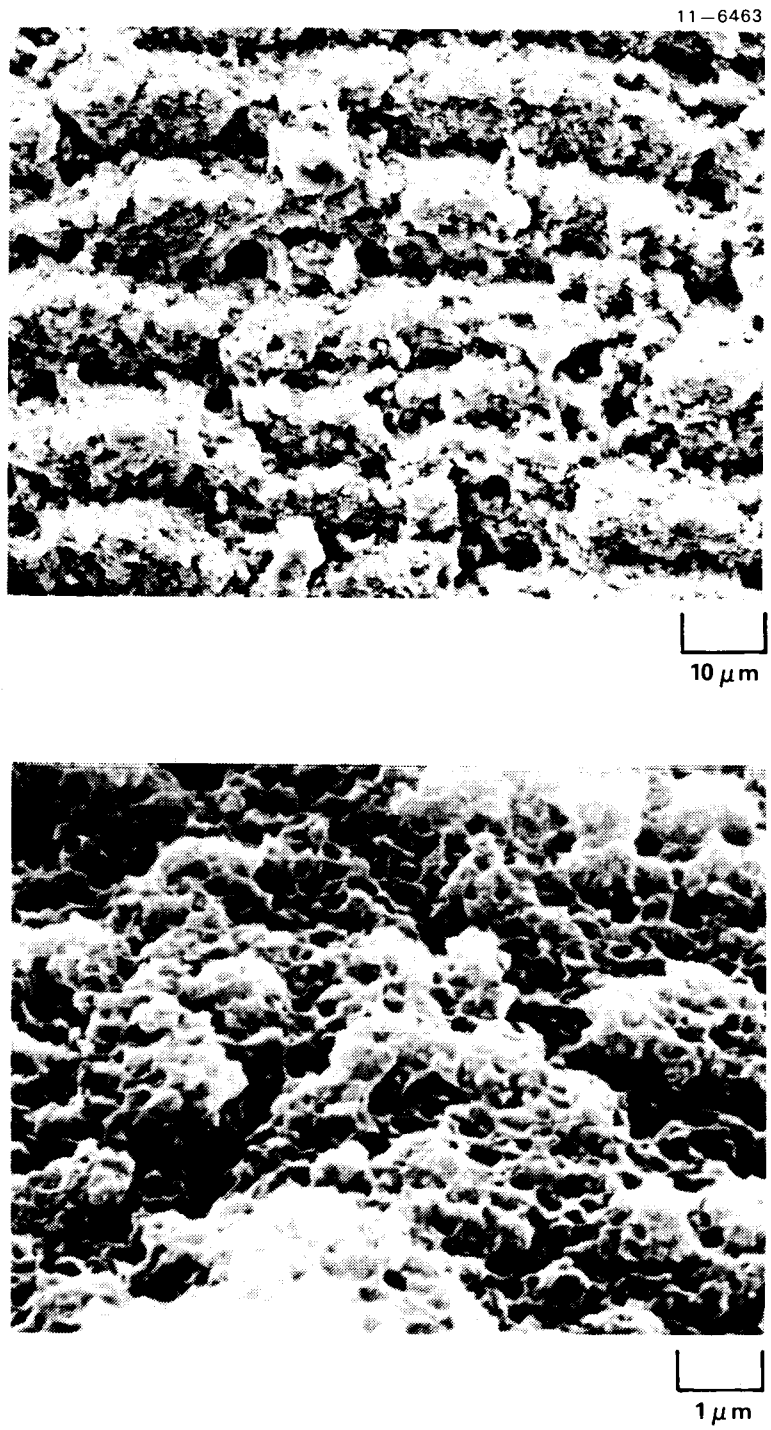

FIGURE 11. TENSILE FRACTURE SURFACE OF ALLOY 9 IN THE ARTIFICIALLY AGED CONDITION

TABLE 17. NOTCH TENSION PROPERTIES OF THE Al-4Cu-1Mg-1.5Li ALLOY PREPARED BY THE CONVENTIONAL CONSOLIDATION OF MECHANICALLY ALLOYED POWDER

ALLOY AND AGING TREATMENT	ORIENTATION	NTS		NYR	NSR	K_{IC}	
		MPa	ksi			$MPa(m)^{1/2}$	$ksi(in.)^{1/2}$
7 NA	L	345	50	0.53	0.51	17.1	15.5
9 NA	L	448	65	0.78	0.73	23.1	21.0
7 AA	L	262	38	0.49	0.41	13.0	11.8
9 AA	L	338	49	0.70	0.60	17.5	15.9
7 NA	T	359	52	--	--	--	--
7 AA	T	248	36	--	--	--	--

L - Longitudinal and T - Transverse

Al-4Cu-1Mg-1.5Fe-0.75Ce: The tensile properties of the Al-4Cu-1Mg-1.5Fe-0.75Ce alloy made by the conventional consolidation of MA powder are presented in Table 18. In contrast with the behavior of the Li-containing alloys, the strength of these alloys extruded using a reduction ratio of 19:1 increases with increasing vacuum degassing temperature, as observed by comparing the properties of alloys 11 and 12. Additionally, increasing the extrusion ratio also reduces the strength significantly, as observed by comparing the properties of alloys 10 and 11. As expected, the strength of the alloy in the AA condition is also lower than that of the corresponding alloy in the NA condition.

TABLE 18. LONGITUDINAL TENSILE PROPERTIES OF THE Al-4Cu-1Mg-1.5Fe-0.75Ce ALLOY PREPARED BY THE CONVENTIONAL CONSOLIDATION OF MECHANICALLY ALLOYED POWDER

ALLOY AND AGING CONDITION	EXTRUSION RATIO	VACUUM DEGASSING TEMPERATURE		TIME	0.2% OFFSET YIELD STRENGTH		ULTIMATE TENSILE STRENGTH		ELONGATION
		K	°F	h	MPa	ksi	MPa	ksi	%
10 NA	7	750	891	12	455	66	496	72	5
11 NA	19	750	891	12	400	58	469	68	9
12 NA	19	790	963	6	455	66	503	73	6
10 AA	7	750	891	12	407	59	455	66	4
11 AA	19	750	891	12	352	51	421	61	6
12 AA	19	790	963	6	414	60	462	67	5

Properties of alloy 11 AA are from one test.

Although the reasons for the observed variation in the mechanical properties of these alloys are not clear, an explanation can be sought in the effect of processing on the homogeneity and the distribution of the alloying elements. As discussed earlier, these alloys, which are made by the mechanical alloying of elemental powder, contain coarse undissolved particles both before and after solution heat treatment (refer to the microstructure of alloy 12 in Figures 4 and 6). Compared with alloy 11 which is degassed at 750K (891°F), degassing of alloy 12 at the higher degassing temperature (790K, 963°F) may result in a better homogenization of the elements and cause additional dispersion strengthening by the precipitation of the intermetallic dispersoids during processing subsequent to vacuum degassing. Thus, the strength of alloy 12 is higher than that of alloy 11 in both the NA and AA conditions. However, the observed effect of the extrusion ratio cannot be explained. These alloys are strengthened by a combination of the fine grain structure, precipitates, and the oxide, carbide, and intermetallic dispersoids. The complexity of the influence of processing on these strengthening features and the interaction among them, renders a prediction and explanation of the deformation and the mechanical properties of these alloys very difficult.

Consistent with the good combination of strength and ductility, the alloys possess reasonable notch tension properties, as shown in Table 19. The tensile fracture surface of alloy 12 in the AA condition is also shown in Figure 12. The fracture surface reveals a significant amount of undissolved particles which together with the very fine oxide and carbide dispersoids results in a bimodal distribution of the dimples.

TABLE 19. NOTCH TENSION PROPERTIES OF THE Al-4Cu-1Mg-1.5Fe-0.75Ce ALLOY PREPARED BY THE CONVENTIONAL CONSOLIDATION OF MECHANICALLY ALLOYED POWDER

ALLOY AND AGING TREATMENT	ORIENTATION	NTS		NYR	NSR	K_{IC}	
		MPa	ksi			$MPa(m)^{1/2}$	$ksi(in.)^{1/2}$
12 NA	L	524	76	1.15	1.04	29.2	26.5
12 AA	L	510	74	1.23	1.10	28.9	26.3
12 NA	T	414	60	--	--	--	--
12 AA	T	414	60	--	--	--	--

L - Longitudinal and T - Transverse

From the above discussion, it is clear that, as with the alloys made from PA powder, the effect of varying the vacuum degassing parameters on the pro-

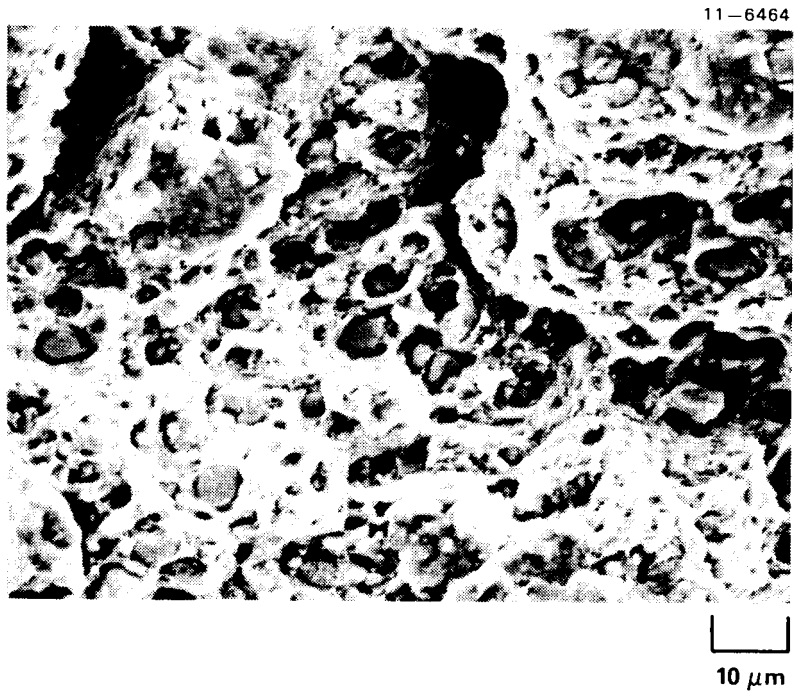

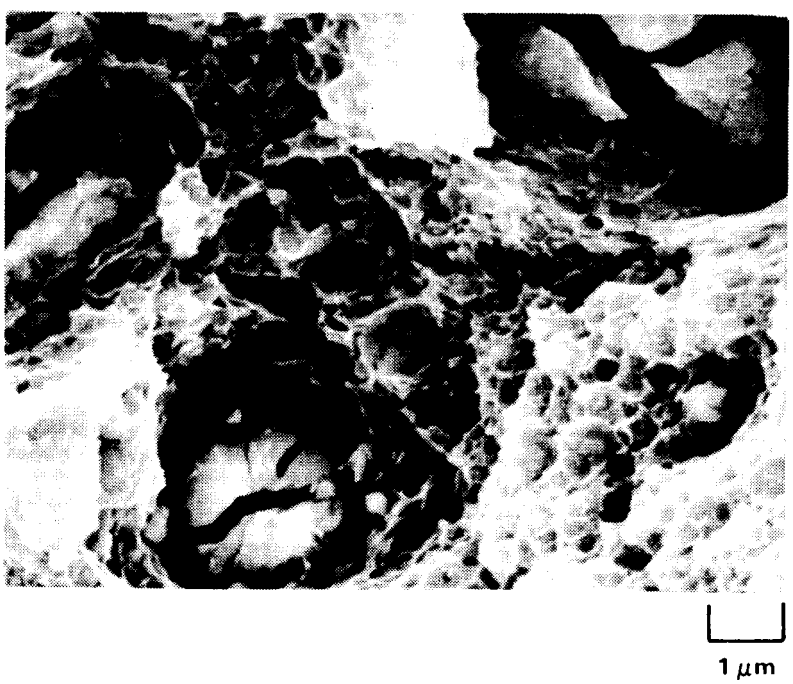

FIGURE 12. TENSILE FRACTURE SURFACE OF ALLOY 12 IN THE ARTIFICIALLY AGED CONDITION

perties of the Al-4Cu-1Mg-1.5Li and Al-4Cu-1Mg-1.5Fe-0.75Ce alloys made by the conventional consolidation of MA powder appears to be due to the changes in the sub-structure and dispersion strengthening. Also, mechanical alloying significantly increases the strength over that of similar alloys made from PA powder. The latter observation is discussed in more detail in a subsequent section.

5.4.3 Task III: Alloys Prepared by Containerless Vacuum Hot Pressing -

Al-4Cu-1Mg-1.5Li-0.2Zr Alloy Made from PA Powder - The tensile properties of the Al-4Cu-1Mg-1.5Li-0.2Zr alloy prepared by the CVHP of PA powder are presented in Table 20. In contrast with the alloys prepared by conventional consolidation, increasing the vacuum degassing temperature decreases the strength of these alloys, as seen by comparing the tensile properties of alloys 14 and 15. In contrast with alloys 1, 2, and 3 which are hot pressed at 675K (756°F) following vacuum degassing, alloys 13, 14, and 15 are hot pressed at the same temperature at which they are vacuum degassed. The only thermal exposure following the CVHP of the billets of alloys 13, 14, and 15 is at 644K (700°F) for three hours followed by the extrusion. Thus, while Al_3Zr precipitation occurs in alloys 1, 2, and 3 during hot pressing, it does not occur similarly in alloys 13, 14, and 15. Consequently, in contrast with the alloys prepared by conventional consolidation, the strength of the alloys prepared by CVHP decreases with increasing vacuum degassing temperature. However, the effect of billet diameter on the tensile properties is not clear. Except for the yield strength of alloy 13, the strength of the alloy in the AA condition is also lower than that of the corresponding alloy in the NA condition.

TABLE 20. LONGITUDINAL TENSILE PROPERTIES OF THE Al-4Cu-1Mg-1.5Li-0.2Zr ALLOY PREPARED BY THE CONTAINERLESS VACUUM HOT PRESSING OF PREALLOYED POWDER

ALLOY AND AGING CONDITION	BILLET DIAMETER		VACUUM DEGASSING TEMPERATURE		TIME	0.2% OFFSET YIELD STRENGTH		ULTIMATE TENSILE STRENGTH		ELONGATION
	mm	in.	K	°F	h	MPa	ksi	MPa	ksi	%
13 NA	114	4.5	750	891	6	434	63	531	77	3
14 NA	150	6.0	750	891	6	455	66	531	77	5
15 NA	150	6.0	790	963	6	434	63	496	72	5
13 AA	114	4.5	750	891	6	448	65	503	73	3
14 AA	150	6.0	750	891	6	427	62	490	71	4
15 AA	150	6.0	790	963	6	393	57	441	64	4
14 NA-T	150	6.0	750	891	6	365	53	414	60	2

T - Transverse

The tensile fracture surface of alloy 15 in the AA condition (Figure 13) shows a ductile fracture mode, but as with alloys 1, 2, and 3 the excess solute-rich phases result in low values of the ductility in these alloys. The notch tension properties of these alloys, presented in Table 21, are in agreement with the corresponding tension properties.

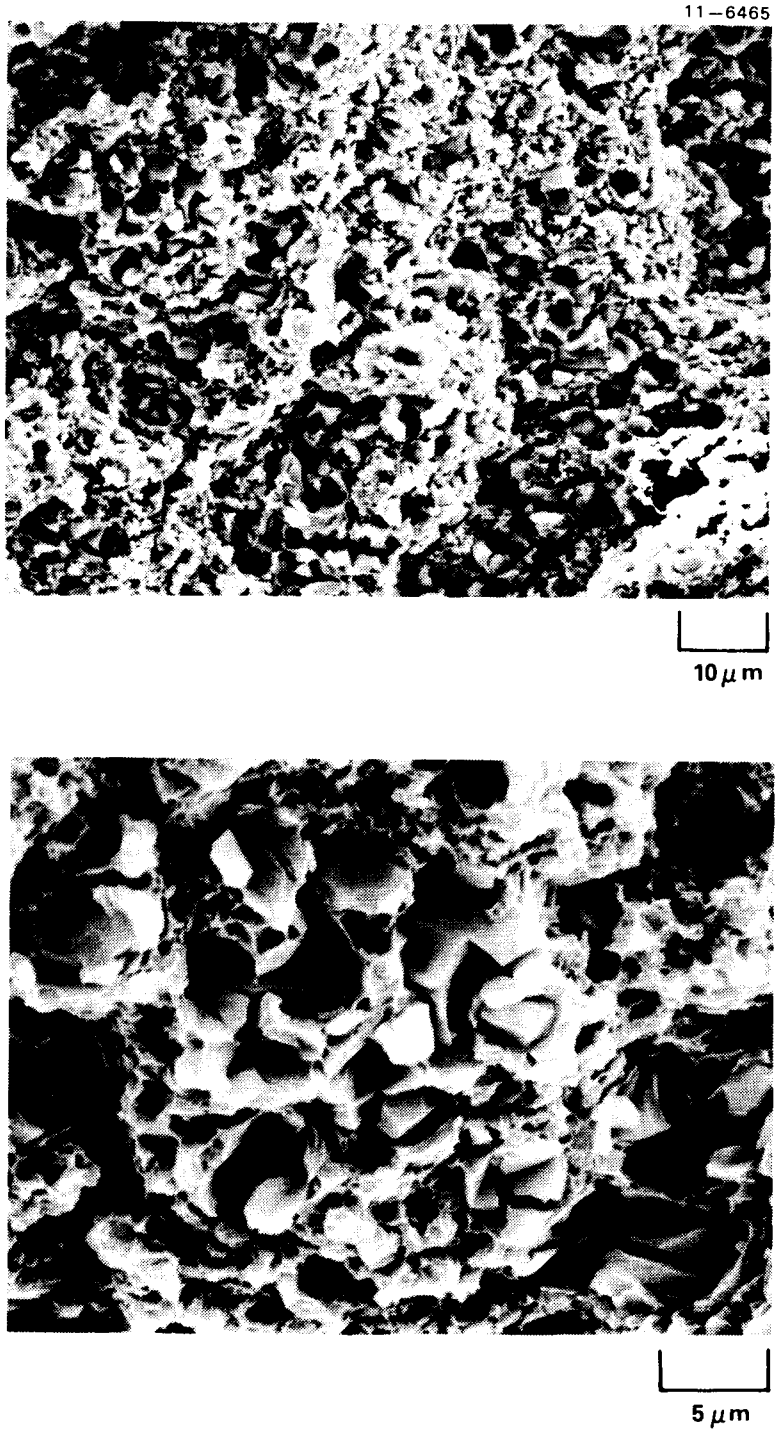

FIGURE 13. TENSILE FRACTURE SURFACE OF ALLOY 15 IN THE ARTIFICIALLY AGED CONDITION

TABLE 21. NOTCH TENSION PROPERTIES OF THE Al-4Cu-1Mg-1.5Li-0.2Zr ALLOY PREPARED BY THE CONTAINERLESS VACUUM HOT PRESSING OF PREALLOYED POWDER

ALLOY AND AGING TREATMENT	ORIENTATION	NTS		NYR	NSR	K_{IC}	
		MPa	ksi			$MPa(m)^{1/2}$	$ksi(in.)^{1/2}$
14 NA	L	324	47	0.71	0.61	16.6	15.1
15 NA	L	434	63	1.00	0.88	23.1	21.0
14 AA	L	207	30	0.48	0.42	10.6	9.6
15 AA	L	283	41	0.72	0.64	14.6	13.3
14 NA	T	200	29	0.55	0.48	--	9.3
14 AA	T	138	20	--	--	--	--

L - Longitudinal and T - Transverse

Al-4Cu-1Mg-1.5Li Alloy made from MA Powder - The tensile properties of the Al-4Cu-1Mg-1.5Li alloy prepared by the CVHP of MA powder are presented in Table 22. While the yield strength of the alloys pressed from billets of varying diameter are nearly identical, the tensile strength of the alloy extruded from the larger diameter billet is significantly lower. The reason for this reduction in the tensile strength is not clear. The strength of the alloy in the AA condition is also lower than that of the corresponding alloy in the NA condition. The very high strength and the low ductility result in poor notch tension properties (Table 23), although the tensile fracture surface of alloy 17 reveals very fine dimples and a ductile failure mode (Figure 14).

TABLE 22. LONGITUDINAL TENSILE PROPERTIES OF THE Al-4Cu-1Mg-1.5Li ALLOY PREPARED BY THE CONTAINERLESS VACUUM HOT PRESSING OF MECHANICALLY ALLOYED POWDER

ALLOY AND AGING CONDITION	BILLET DIAMETER		VACUUM DEGASSING TEMPERATURE		TIME	0.2% OFFSET YIELD STRENGTH		ULTIMATE TENSILE STRENGTH		ELONGATION
	mm	in.	K	°F	h	MPa	ksi	MPa	ksi	%
16 NA	114	4.5	750	891	6	634	92	710	103	3
17 NA	150	6.0	750	891	6	641	93	648	94	1
16 AA	114	4.5	750	891	6	524	76	641	93	2
17 AA	150	6.0	750	891	6	510	74	586	85	2
17 NA-T	150	6.0	750	891	6	565	82	579	84	1

T - Transverse

TABLE 23. NOTCH TENSION PROPERTIES OF THE Al-4Cu-1Mg-1.5Li ALLOY PREPARED BY THE CONTAINERLESS VACUUM HOT PRESSING OF MECHANICALLY ALLOYED POWDER

ALLOY AND AGING TREATMENT	ORIENTATION	NTS		NYR	NSR	K_{IC}	
		MPa	ksi			$MPa(m)^{1/2}$	$ksi(in.)^{1/2}$
17 NA	L	269	39	0.42	0.42	13.6	12.4
17 AA	L	228	33	0.45	0.39	11.6	10.5
17 NA	T	159	23	0.28	0.27	8.0	7.3
17 AA	T	172	25	--	--	--	--

L - Longitudinal and T - Transverse

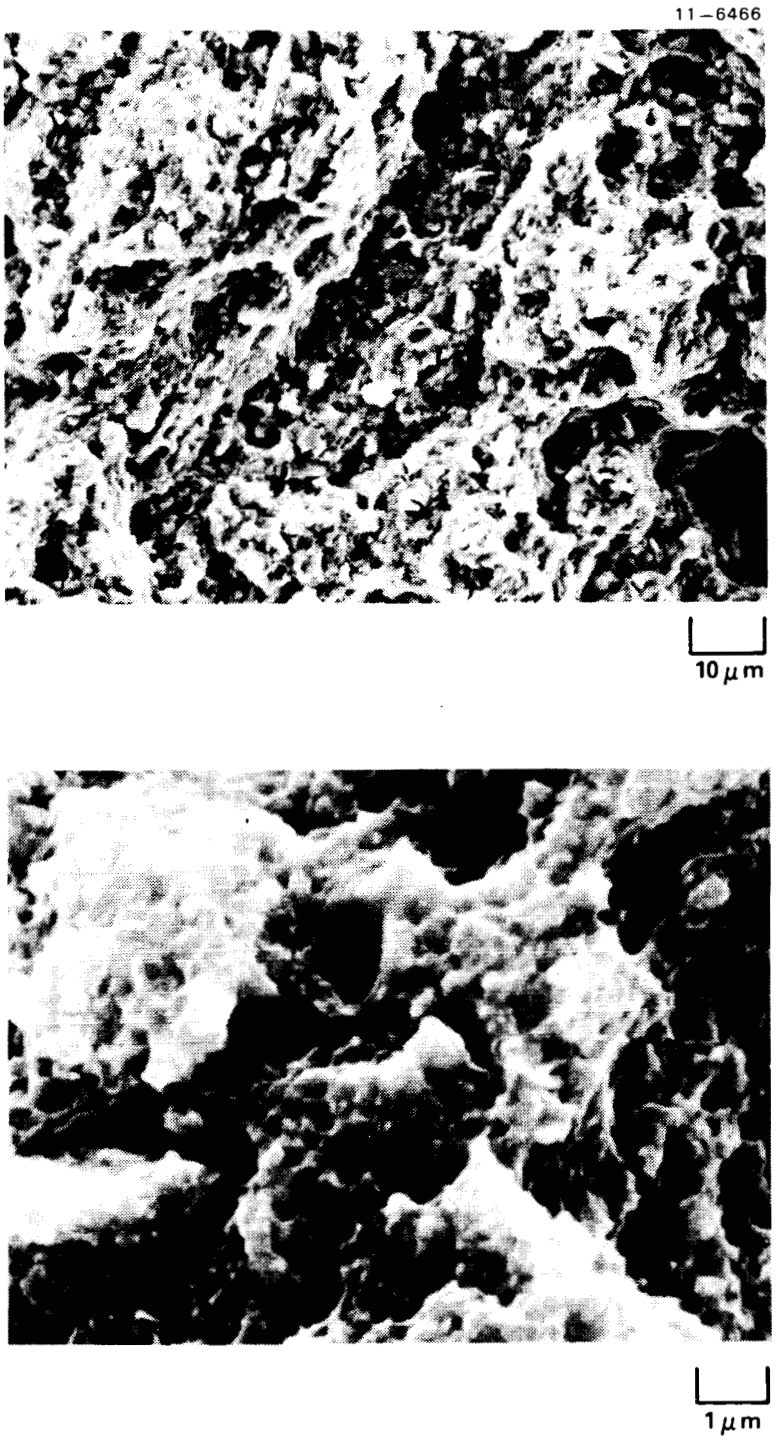

FIGURE 14. TENSILE FRACTURE SURFACE OF ALLOY 17 IN THE ARTIFICIALLY AGED CONDITION

Al-4Cu-1Mg-1.5Fe-0.75Ce Alloy made from MA Powder - The tensile properties of the Al-4Cu-1Mg-1.5Fe-0.75Ce prepared by the CVHP of MA powder are presented in Table 24. Unlike alloys 10, 11, and 12, alloys 18, 19, 20, and 21 are not hot pressed at 675K (756°F). Thus, additional dispersoid precipitation does not occur in the latter alloys subsequent to vacuum degassing. Consequently, the coarsening of the dispersoids with increasing vacuum degassing temperature causes a corresponding decrease of strength. Thus, the strength of alloys 18 and 20 is higher than that of alloys 19 and 21, respectively. Additionally, the alloys prepared by using PA Al-1.6Fe-0.8Ce powder are more homogeneous and contain a higher amount of the strengthening dispersoids. Thus, the strength of alloys 18 and 19 is higher than that of alloys 20 and 21, respectively. The strength of all of these alloys is also higher in the NA condition than in the AA condition. The absence of the coarse unalloyed particles in the alloys prepared from PA Al-1.6Fe-0.8Ce powder is evident from a comparison of the tensile fracture surfaces of alloys 19 and 21 (Figure 15). Alloys 18 and 19 also possess reasonable notch tension properties (Table 25).

TABLE 24. LONGITUDINAL TENSILE PROPERTIES OF THE Al-4Cu-1Mg-1.5Fe-0.75Ce ALLOY PREPARED BY THE CONTAINERLESS VACUUM HOT PRESSING OF MECHANICALLY ALLOYED POWDER

ALLOY AND AGING CONDITION	VACUUM DEGASSING TEMPERATURE		TIME	0.2% OFFSET YIELD STRENGTH		ULTIMATE TENSILE STRENGTH		ELONGATION
	K	°F	h	MPa	ksi	MPa	ksi	%
18 NA	750	891	6	483	70	545	79	5
19 NA	790	963	6	448	65	524	76	5
20 NA	750	891	6	441	64	510	74	5
21 NA	790	963	6	407	59	496	72	5
18 AA	750	891	6	455	66	503	73	4
19 AA	790	963	6	421	61	490	71	5
20 AA	750	891	6	400	58	476	69	5
21 AA	790	963	6	372	54	455	66	3
18 NA-T	750	891	6	476	69	517	75	2
19 NA-T	790	963	6	455	66	510	74	2

T - Transverse

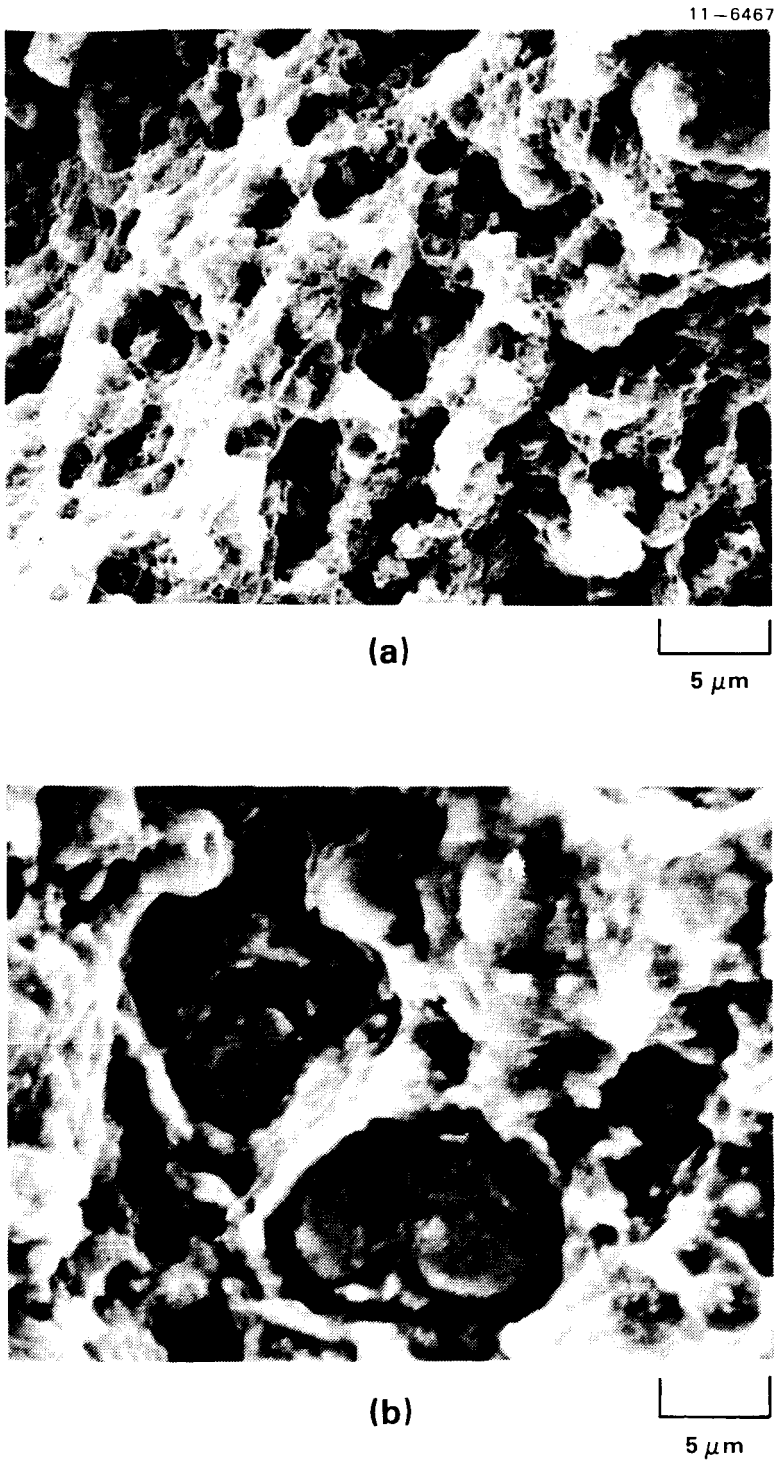

FIGURE 15. TENSILE FRACTURE SURFACE OF (a) ALLOY 19 AND (b) ALLOY 21 IN THE ARTIFICIALLY AGED CONDITION

TABLE 25. NOTCH TENSION PROPERTIES OF THE Al-4Cu-1Mg-1.5Fe-0.75Ce ALLOY PREPARED BY THE CONTAINERLESS VACUUM HOT PRESSING OF MECHANICALLY ALLOYED POWDER

ALLOY AND AGING TREATMENT	ORIENTATION	NTS		NYR	NSR	K_{IC}	
		MPa	ksi			$MPa(m)^{1/2}$	$ksi(in.)^{1/2}$
18 NA	L	483	70	1.00	0.89	25.7	23.4
19 NA	L	545	79	1.22	1.04	30.4	27.6
18 AA	L	407	59	0.89	0.81	21.6	19.6
19 AA	L	531	77	1.26	1.08	30.4	27.6
19 NA	T	448	65	0.98	0.88	24.2	22.0
19 AA	T	469	68	--	--	--	--

L - Longitudinal and T - Transverse

5.5 Influence of Alloying Approach on the Properties

The influence of the alloying approach (prealloying, mechanical alloying using prealloyed and elemental powder, and mechanical alloying using fully elemental powder) on the properties of the alloys is shown for various compositions and consolidation methods in Figures 16, 17, 18, and 19. In all cases, the dispersion strengthening due to carbides and oxides increases the strength of the alloy prepared from MA powder over that achieved in the corresponding alloy made from PA powder. However, the magnitude of this increase is influenced by the alloy composition, consolidation method, and heat treatment.

In the Li-containing alloys prepared by conventional consolidation processing, the increase in the strength due to mechanical alloying is offset by the coarsening of the dispersoids at the higher vacuum degassing temperature. Additionally, as discussed earlier, the strength of the alloys made from the PA powder increases with increasing vacuum degassing temperature due to the decreasing sub-grain size. Thus, as shown in Figure 16, the incremental strengthening due to mechanical alloying decreases with increasing vacuum degassing temperature and/or time. The strengthening due to mechanical alloying is not accompanied by a significant loss of toughness, and for the alloy vacuum degassed at 790K (963°F) for 6 hours results in an increased value of K_{IC}. Since the Li-containing alloy prepared by the CVHP of MA powder was not vacuum degassed at 790K (963°F), a similar comparison as made for the alloys prepared by conventional consolidation processing is not possible.

In the Fe- and Ce-containing alloys prepared by conventional consolidation processing, the increase in the strength due to mechanical alloying increases with increasing vacuum degassing temperature (compare alloys 5 and 6

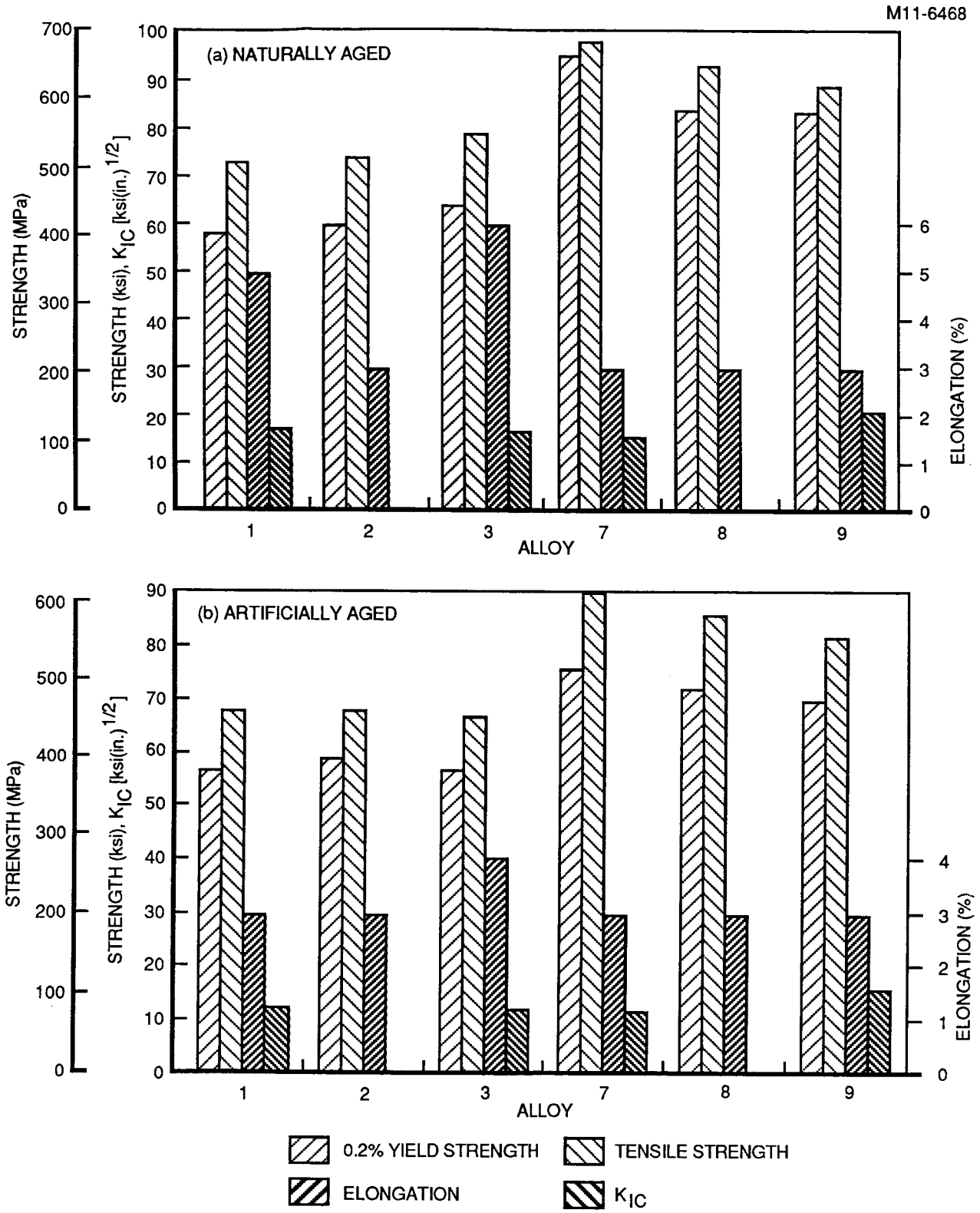

FIGURE 16. INFLUENCE OF ALLOYING APPROACH ON THE PROPERTIES OF Li - CONTAINING ALLOYS PREPARED BY CONVENTIONAL CONSOLIDATION

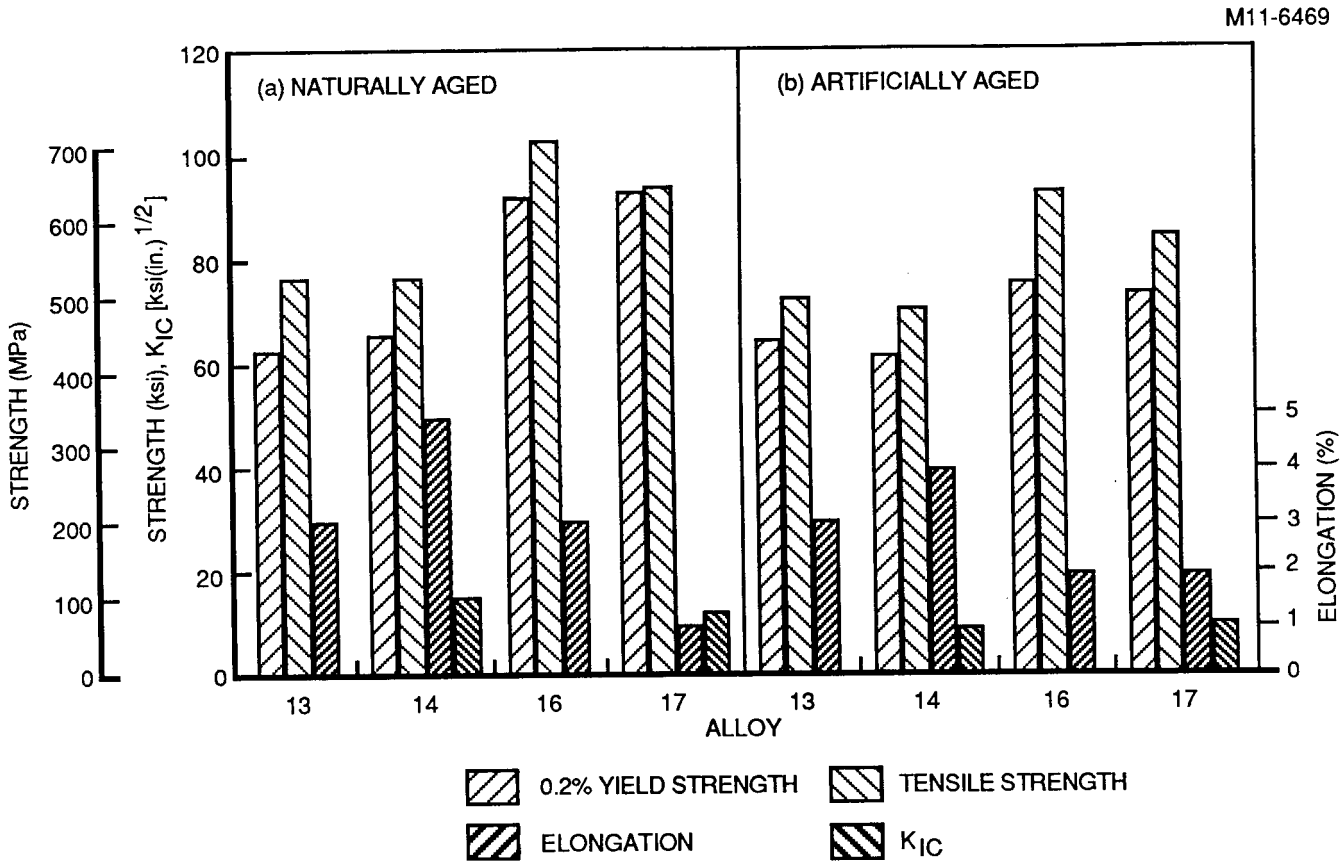

FIGURE 17. INFLUENCE OF ALLOYING APPROACH ON THE PROPERTIES OF Li - CONTAINING ALLOYS PREPARED BY CONTAINERLESS VACUUM HOT PRESSING

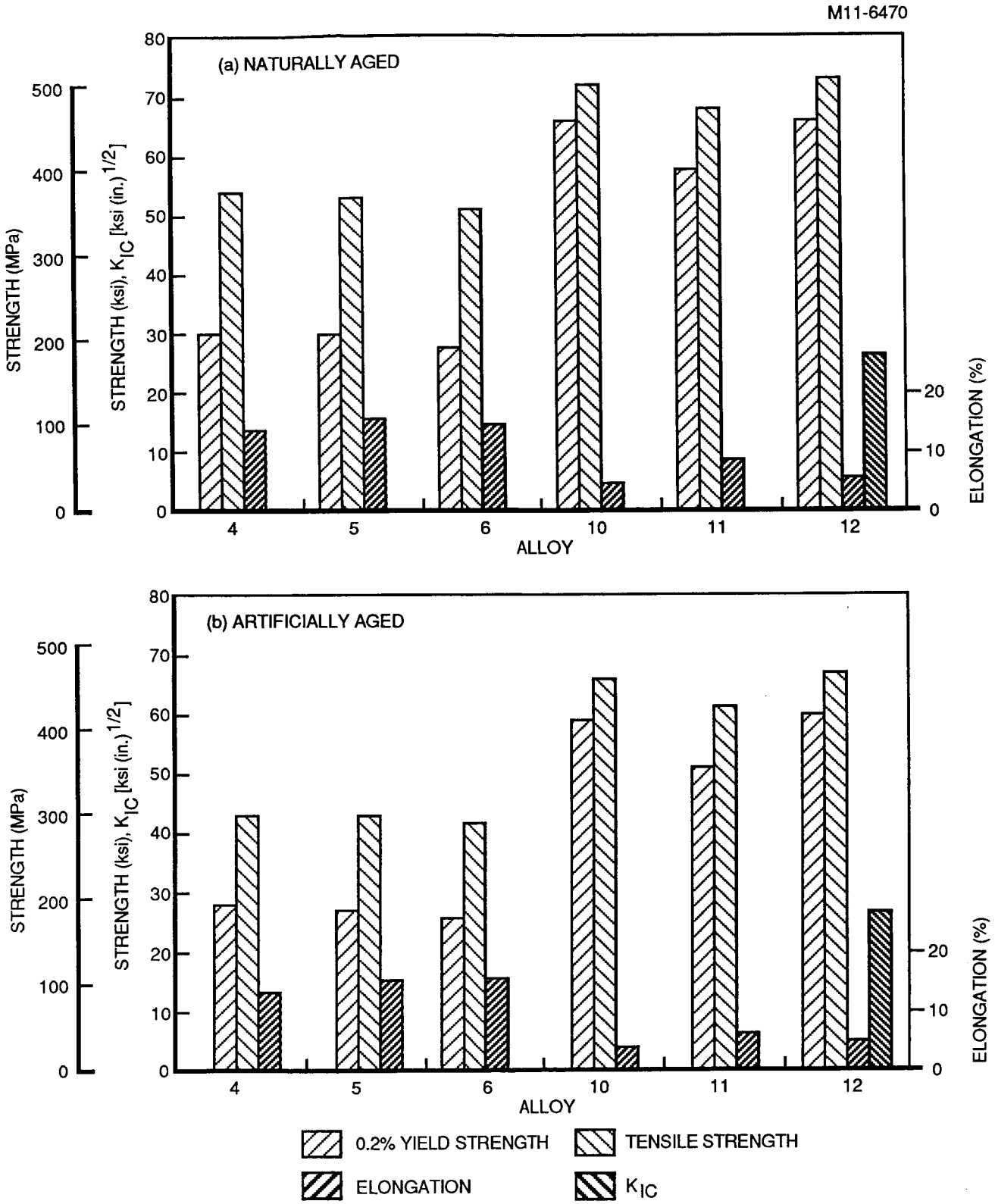

FIGURE 18. INFLUENCE OF ALLOYING APPROACH ON THE PROPERTIES OF Fe - AND Ce - CONTAINING ALLOYS PREPARED BY CONVENTIONAL CONSOLIDATION

M11-6471

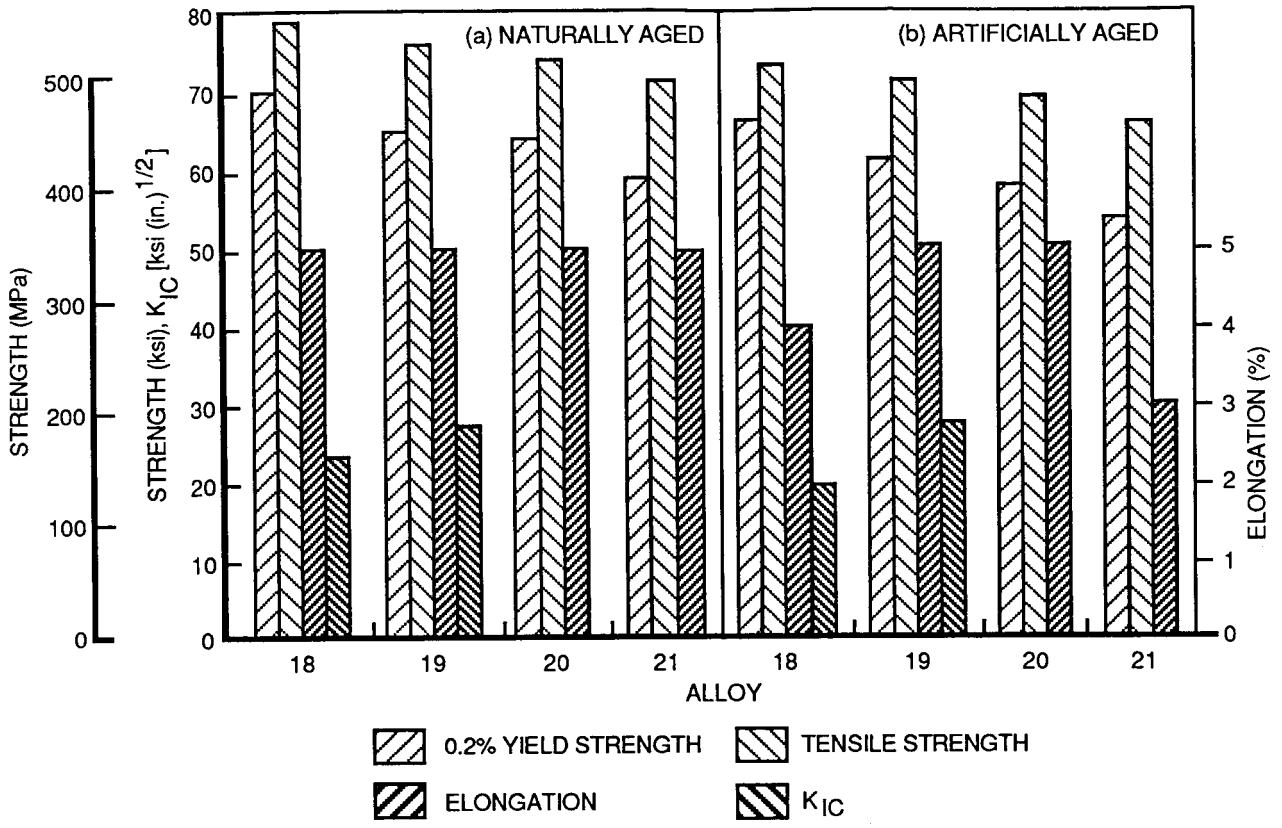

FIGURE 19. INFLUENCE OF ALLOYING APPROACH ON THE PROPERTIES OF Fe - AND Ce - CONTAINING ALLOYS PREPARED BY CONTAINERLESS VACUUM HOT PRESSING

with alloys 11 and 12), as shown in Figure 18. The reason for this increase can again be traced to the influence of the vacuum degassing temperature on the properties of the alloys made from the PA or the MA powder. For the Fe- and Ce-containing alloys prepared by the CVHP of MA powder, use of PA powder for the alloying of Fe and Ce results in a more homogeneous alloy with a consequent increase of strength over that of the alloy made from fully elemental powder (Figure 19).

5.6 Influence of Consolidation Processing Method on the Properties

The influence of the consolidation processing method on the properties of the alloys is shown in Figures 20, 21, and 22. The data, available for alloys with similar compositions, alloying approach, and vacuum degassing parameters indicates that consolidation by CVHP is beneficial for the Li-containing alloys prepared from the PA powder (Figure 20), increases the tensile strength of the Li-containing alloy prepared from the MA powder (Figure 21), and reduces the yield strength of Fe- and Ce-containing alloys prepared from the MA powder (Figure 22). However, these data are very limited, and preclude a general assessment of the influence of varying the consolidation processing method on the mechanical properties.

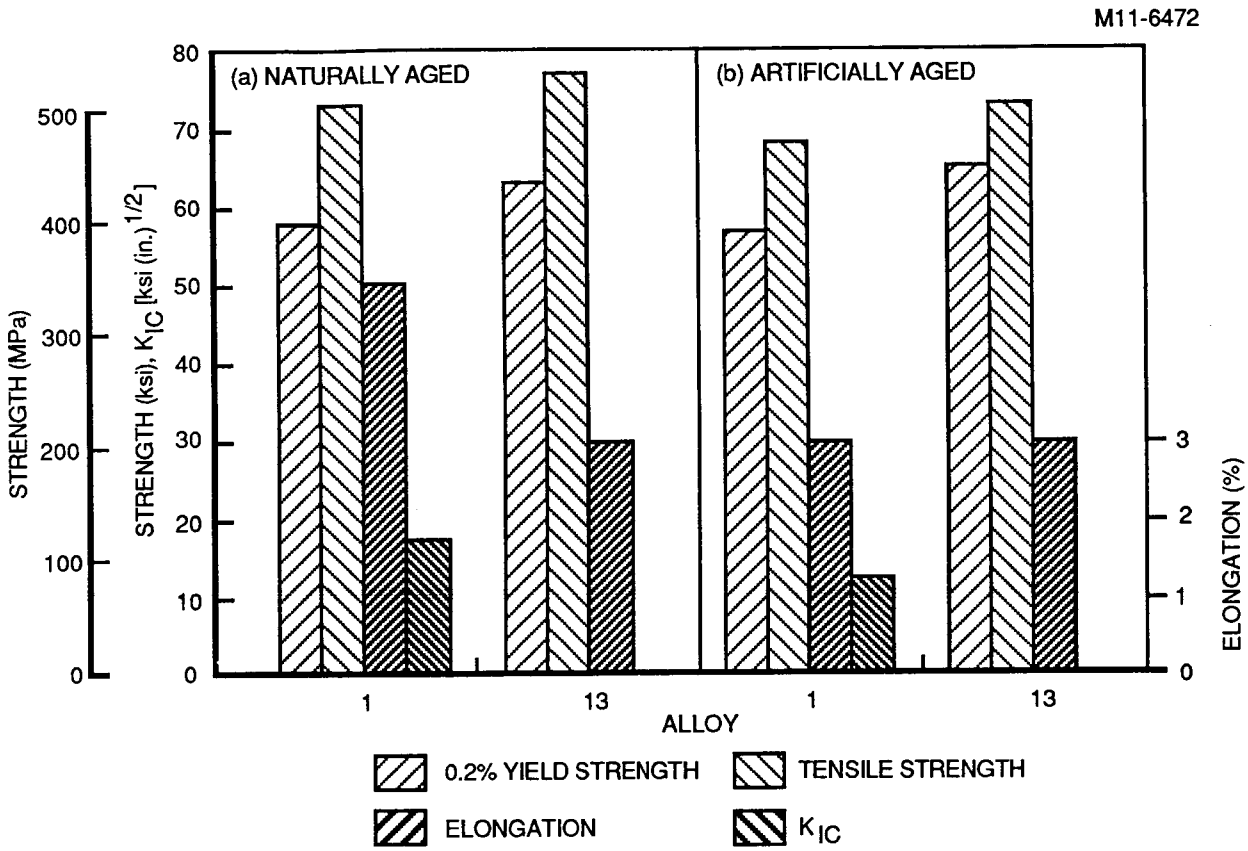

FIGURE 20. INFLUENCE OF CONSOLIDATION PROCESSING METHOD ON THE PROPERTIES OF Li - CONTAINING ALLOYS PREPARED FROM PREALLOYED POWDER

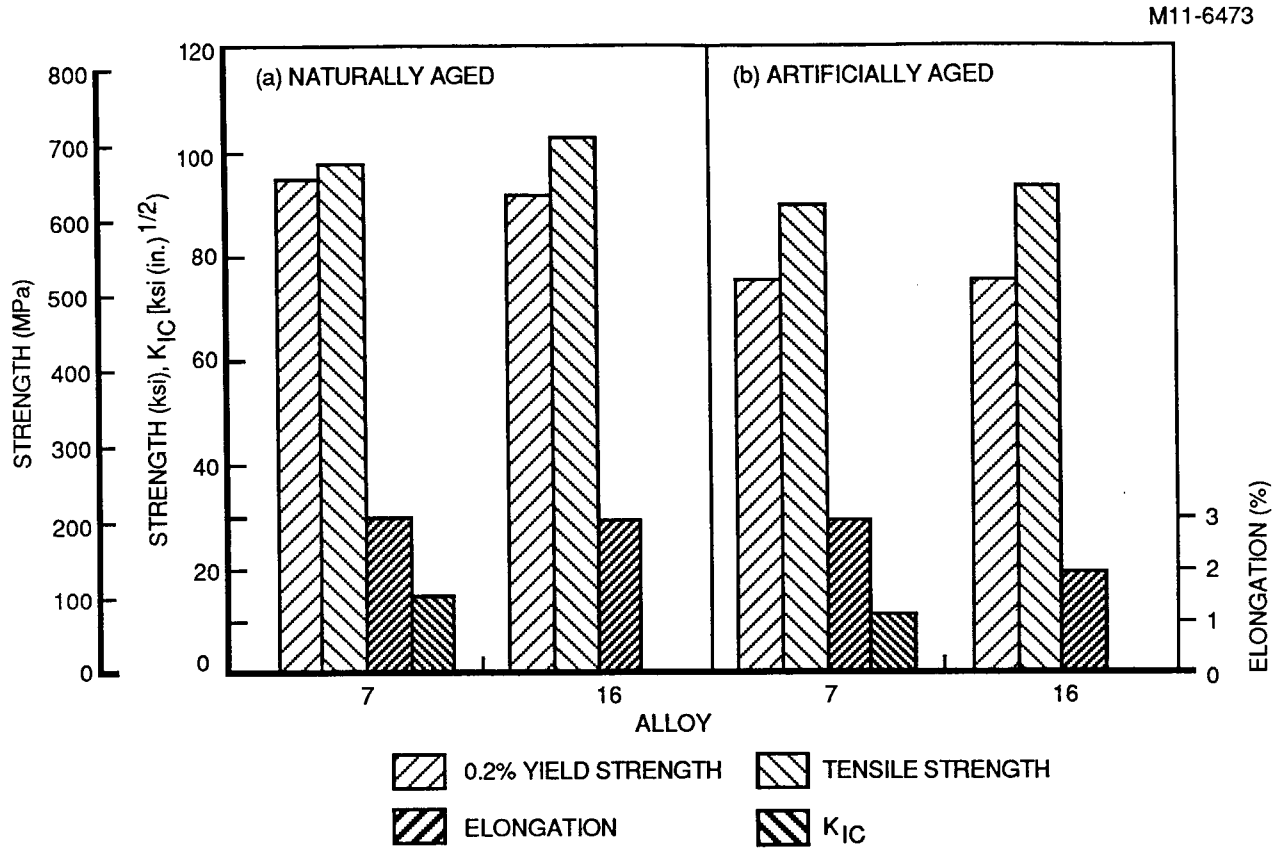

FIGURE 21. INFLUENCE OF CONSOLIDATION PROCESSING METHOD ON THE PROPERTIES OF Li -CONTAINING ALLOYS PREPARED FROM MECHANICALLY ALLOYED POWDER

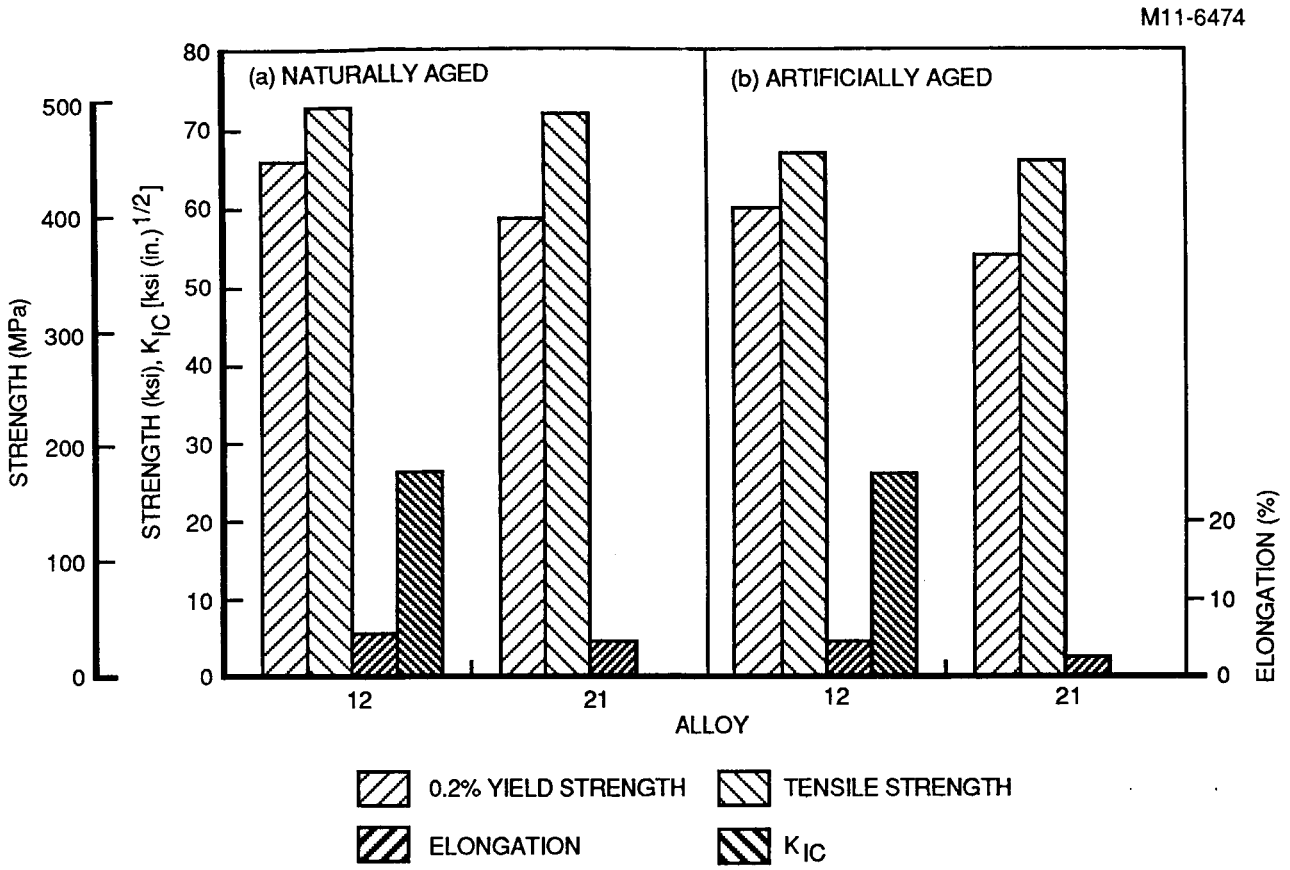

FIGURE 22. INFLUENCE OF CONSOLIDATION PROCESSING METHOD ON THE PROPERTIES OF Fe - AND Ce - CONTAINING ALLOYS PREPARED FROM MECHANICALLY ALLOYED POWDER

5.7 Influence of Orientation on the Properties

The influence of orientation on the tensile properties of the alloys is shown in Figure 23. The transverse tensile properties of the Li-containing alloys are significantly lower than the properties in the longitudinal orientation. The properties of the Fe- and Ce-containing alloys are only slightly affected. As observed in a recent study (17), these results indicate deficiencies in the consolidation processing of the Li-containing alloys. The transverse properties are strongly dependent on the distribution of prior-particle surface oxide. Insufficient densification during the hot pressing of the degassed billet could result in reduced disintegration and a less uniform distribution of the oxide particles during extrusion with deleterious effects on the properties in the transverse direction. The oxide layer in Li-containing alloys can be expected to be thicker and more adherent than in the Fe- and Ce-containing alloys. Thus, the effect is more pronounced in the Li-containing alloys, thereby explaining the observed difference between the two types of alloys in the dependence of the tensile properties on the orientation.

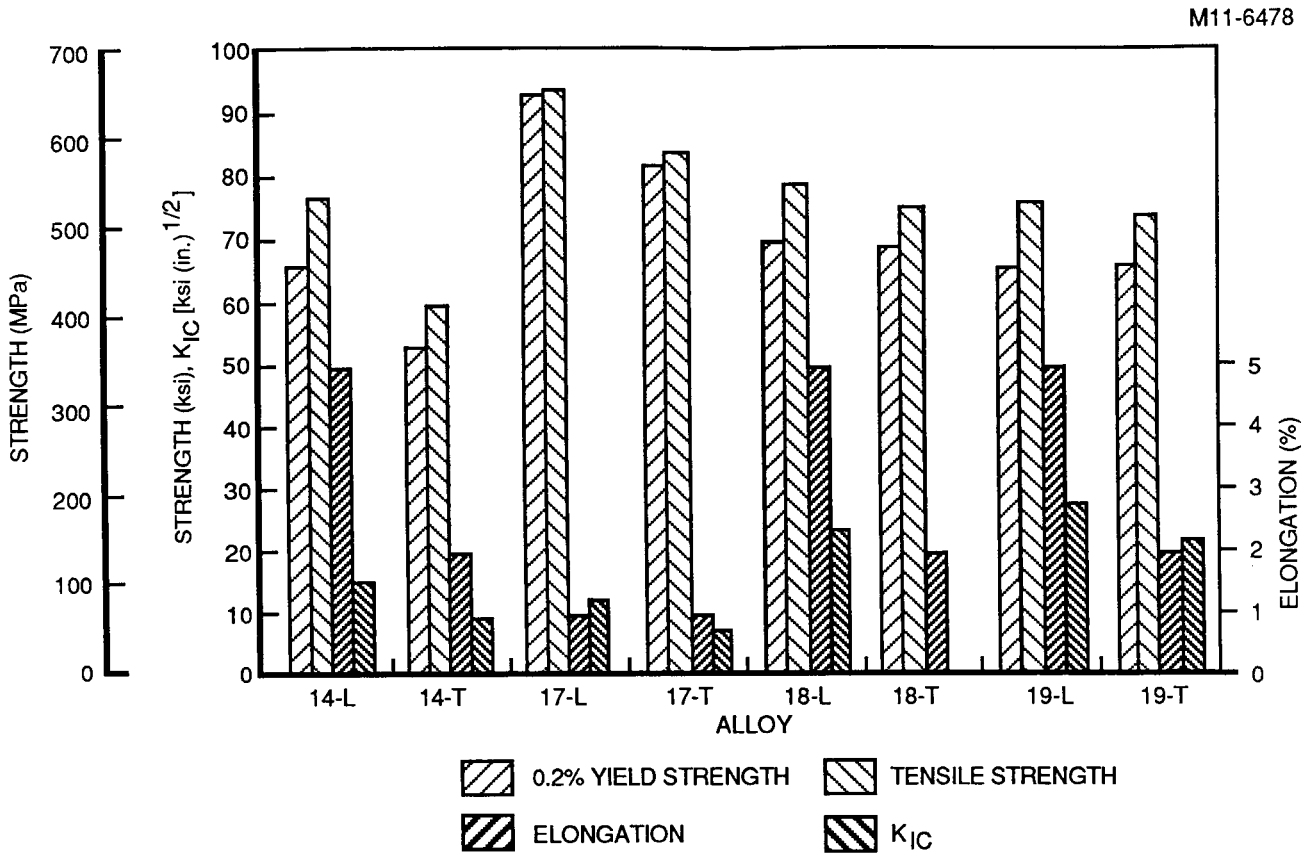

FIGURE 23. INFLUENCE OF ORIENTATION ON THE PROPERTIES OF THE ALLOYS. ALL ALLOYS NATURALLY AGED (L: LONGITUDINAL, T: TRANSVERSE)

The influence of orientation on the NTS is shown in Figure 24. Except for alloy 7 in the NA condition, the NTS of all of the alloys in the transverse orientation is lower, by varying amounts, than in the longitudinal orientation.

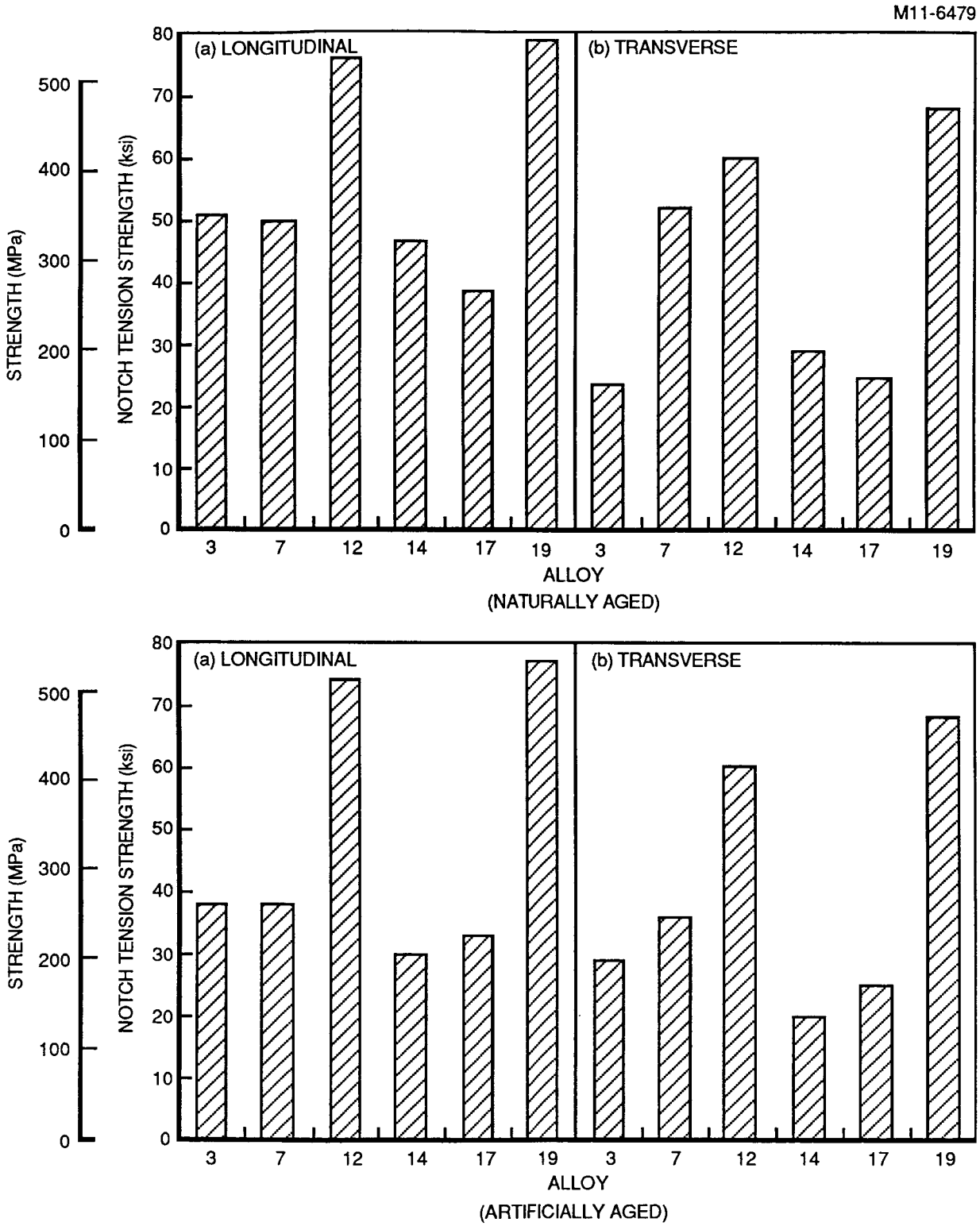

FIGURE 24. INFLUENCE OF ORIENTATION ON THE NOTCH TENSION STRENGTH

6. CONCLUSIONS

1. The influence of vacuum degassing parameters on the properties of powder-processed aluminum alloys is affected by the alloy composition, and the alloying, consolidation, and post-consolidation processing approach.

2. Vacuum degassing lowers the hydrogen content of powder-processed aluminum alloys, and its efficiency generally increases with increasing temperature.

3. The hydrogen contents of powder-processed aluminum alloys, Li-Containing alloys, and the alloys fabricated by containerless vacuum hot pressing are higher than those of ingot-processed alloys, non-Li alloys, and the alloys fabricated by conventional consolidation, respectively.

4. The range over which the vacuum degassing parameters were varied in the present study was not sufficiently large to cause significant changes in the degassing efficiency. The observed changes in the properties of the alloys that were vacuum degassed under varying conditions resulted from the varying contributions to strengthening by the sub-structure and the dispersoids.

5. Strengthening by the fine sub-grains, fine grains, and the dispersoids individually or in combination is more effective in the alloys containing shearable precipitates such as GP zones. Thus, the strength of all of the alloys is higher in the naturally aged condition than in the artificially aged condition.

6. Mechanical alloying results in a significant increase of the strength over that of alloys of similar compositions prepared from prealloyed powder. The extent of this increase is determined by the influence of the vacuum degassing parameters on the sub-structural and dispersion strengthening.

7. The homogeneity of mechanically alloyed materials is improved by the use of prealloyed powder for the alloying of elements such as Fe and Ce. The strength of the alloys prepared by the mechanical alloying of prealloyed powder is also higher than those of the alloys prepared by the mechanical alloying of elemental powder.

8. The mechanical properties of the alloys in the transverse orientation are lower than in the longitudinal orientation. This effect is more pronounced in the Li-containing alloys.

9. Among all of the alloys that were prepared for this study, the Fe- and Ce-containing alloys prepared from mechanically alloyed powder possess better combinations of strength, ductility, and toughness.

7. REFERENCES

1. J. W. Simon, Direct Processing of Aluminum Powder Metallurgy Alloys, Report No. AFWAL-TR-84-4144 on Air Force Contract No. F33615-82-C-5132 (December 1984).

2. J. M. Fitzpatrick, R. E. Lewis, and D. D. Crooks, Direct Processing of Aluminum Powder Metallurgy Alloys, Report No. AFWAL-TR-84-4176 on Air Force Contract No. F33615-82-C-5023 (April 1985).

3. J. R. Pickens and E. A. Starke, Jr., The Effect of Rapid Solidification on the Microstructures and Properties of Aluminum Powder Metallurgy Alloys, in Rapid Solidification Processing: Principles and Technologies, III, R. Mehrabian, ed. (National Bureau of Standards, Gaithersburg, MD, 1982), p. 150.

4. T. E. Tietz and I. G. Palmer, Advanced P/M Aluminum Alloys, in Advances in Powder Technology, G.Y.Chin, ed. (American Society for Metals, Metals Park, OH, 1982), p. 189.

5. D. J. Chellman, Development of Powder Metallurgy 2XXX Series Al Alloy Plate and Sheet Materials for High Temperature Aircraft Structural Applications, NASA Contractor Report 172521 on Contract No. NAS1-16048 (April 1985).

6. R. E. Sanders, Jr. and G. J. Hildeman, Elevated Temperature Aluminum Alloy Development, Report No. AFWAL-TR-81-4076 on Air Force Contract No. F33615-77-C-5086 (June 1981).

7. R. Ray, Advanced Powder Metallurgy Aluminum Alloys via Rapid Solidification Technology, NASA Contractor Report 172343 on Contract No. NAS1-17578 (May 1984).

8. C. M. Adam, R. G. Bourdeau, and J. W. Broch, Application of Rapidly Solidified Alloys, Report No. AFWAL-TR-81-4188 on Air Force Contract No. F33615-76-C-5136 (February 1982).

9. D. J. Skinner, R. L. Bye, D. Raybould, and A. M. Brown, Dispersion Strengthened Al-Fe-V-Si Alloys, Scripta Metallurgica 20, 867 (1986).

10. J. R. Pickens, Aluminum-Powder Metallurgy Technology for High-Strength Applications, Journal of Materials Science 16, 1437 (1981).

11. Y. W. Kim, W. M. Griffith, and F. H. Froes, Surface Oxides in P/M Aluminum Alloys, Journal of metals 37, 27 (1985).

12. J. S. Benjamin and R. D. Schelleng, Dispersion Strengthened Aluminum-4 Pct Magnesium Alloy Made by Mechanical Alloying, Metallurgical Transactions 12A, 1827 (1980).

13. S. J. Donachie, High Strength, P/M Aluminum Mill Products, Phase I. Low Cost Billet Manufacturing, Report No. AFWAL-TR-81-4090 on Air Force Contract No. F33615-79-C-5160 (November 1981).

14. E. A. Starke, Jr., T. H. Sanders, Jr., and I. G. Palmer, New Approaches to Alloy development in the Al-Li System, Journal of Metals 33, 24 (1981).

15. E. Klar and J. W. Fesko, Gas and Water Atomization, in Metals Handbook (Ninth Edition), Volume 7 - Powder Metallurgy (American Society for Metals, Metals Park, OH, 1984), p. 25.

16. H. Matyja, B. C. Giessen, and N. J. Grant, Effect of Cooling Rate on the Dendrite Spacing in Splat Cooled Aluminum Alloys, Journal of the Institute of Metals 96, 30 (1968).

17. P. J. Meschter, R. J. Lederich, J. E. O'Neal, and P. S. Pao, Study on Effects of Flake Chemistry and Morphology on the Properties of Al-Cu-Mg-X-X-X Powder Metallurgy Advanced Aluminum Alloys, NASA Contractor Report 177946 on Contract NAS1-17107 (November 1985).

18. H. K. Hardy and J. M. Silcock, The Phase Sections at 500°C and 350°C of Aluminum-Rich Aluminum-Lithium-Copper Alloys, Journal of the Institute of Metals 84, 423 (1955-56).

19. R. F. Singer, W. C. Oliver, and W. D. Nix, Identification of Dispersoid Phases Created in Aluminum During Mechanical Alloying, Metallurgical Transactions 11A, 1895 (1980).

20. J. M. Silcock, The Structural Aging Characteristics of Aluminum-Copper-Lithium Alloys, Journal of the Institute of Metals 88, 357 (1959-60).

21. B. Noble, I. R. McLaughlin, and G. Thompson, Solute Atom Clustering Processes in Aluminum-Copper-Lithium Alloys, Acta Metallurgica 18, 339 (1970).

22. B. M. Watts, M. J. Stowell, B. L. Baikie, and D. G. E. Owen, Superplasticity in Al-Cu-Zr Alloys, Part I: Material Preparation and Properties (p. 189) and Part II: Microstructural Study (p. 198), Metal Science 10 (1976).

23. J. D. Embury, Strengthening by Dislocation Substructures, in Strengthening Mechanisms in Crystals, A. Kelley and R. B. Nicholson, eds. (Applied Science Publishers, London, 1971), p. 342.

24. Rapid Inexpensive Tests for Determining Fracture Toughness, Report of the Committee on Rapid Inexpensive Tests for Determining Fracture Toughness, National Materials Advisory Board (National Academy of Sciences, Washington, D.C., 1976), p. 62.

25. J. W. Bohlen and S. W. Ping, Development of High Strength Fatigue Crack Growth Resistant Aluminum Alloys By Rapid Solidification Technology, Final Technical Report on Navy Contract N60921-82-C-0043 (1983).

8. APPENDIX

Under authority granted by the NASA Contracting Officer to furnish samples of alloys prepared under the present contract for additional evaluation, such samples were used by the contractor for an ongoing independent analytical investigation of powder-processed aluminum alloys. This investigation included powder surface characterization and transmission electron microscopy. The latter study was conducted by Mr. Robert Wheeler, graduate student, and Professor Hamish L. Fraser of the Department of Mining and Metallurgical Engineering, University of Illinois - Champaign. Highlights of the results of these studies are summarized in the following paragraphs for general information.

Thermogravimetric analysis (TGA) of prealloyed Al-4Cu-1Mg-1.5Li-0.2Zr powder revealed a continuous loss of weight with increasing temperature up to 623K (662°F), followed by an increase of weight above this temperature. Mass spectrometric analysis of the constituents that are liberated on heating the powder revealed the presence of only water. X-ray photoelectron spectroscopy of this powder also revealed the presence of only oxide on the surface. Because of the very weak signals from the powder surface, infrared spectroscopy could not be used successfully for characterizing the surface. The above results suggest the absence of chemically bound water on the powder surface thereby obviating the need for vacuum degassing above the highest post-consolidation processing temperature.

The weight loss between 323K (122°F) and 623K (662°F) for the Al-4Cu-1Mg-1.5Li-0.2Zr powder was 0.76 pct. (Figure A1), between 328K (131°F) and 708K (815°F) for the Al-4Cu-1Mg-1.5Fe-0.75Ce powder was 0.27 pct. (Figure A2), and between 328K (131°F) and 828K (1031°F) for the Al-1.6Fe-0.8Ce powder was 0.12 pct (Figure A3). The absolute weight loss values for the Fe- and Ce-containing alloys were about three orders of magnitude lower than that reported for air-atomized 7091 alloy.

The fine sub-grain structure resulting from the refinement due to the Al_3Zr dispersoids in the alloys made from prealloyed Al-4Cu-1Mg-1.5Li-0.2Zr powder are shown for alloy 3 in Figure A4. The fine sub-grains and the Fe- and Ce-containing dispersoids in the alloys made from prealloyed Al-4Cu-1Mg-1.5Fe-0.75Ce powder are shown for alloy 6 in Figure A5. The transmission electron micrograph of alloy 9 (Figure A6) reveals the very fine recrystallized grains typical of mechanically alloyed materials. The transmission electron micrograph of the hot pressed billet of alloy 15 (Figure A7) shows the prior-particle surface oxide film in a bright field and dark field pair, and that of the extrusion of the same alloy (Figure A8) shows the development of sub-grains following hot working.

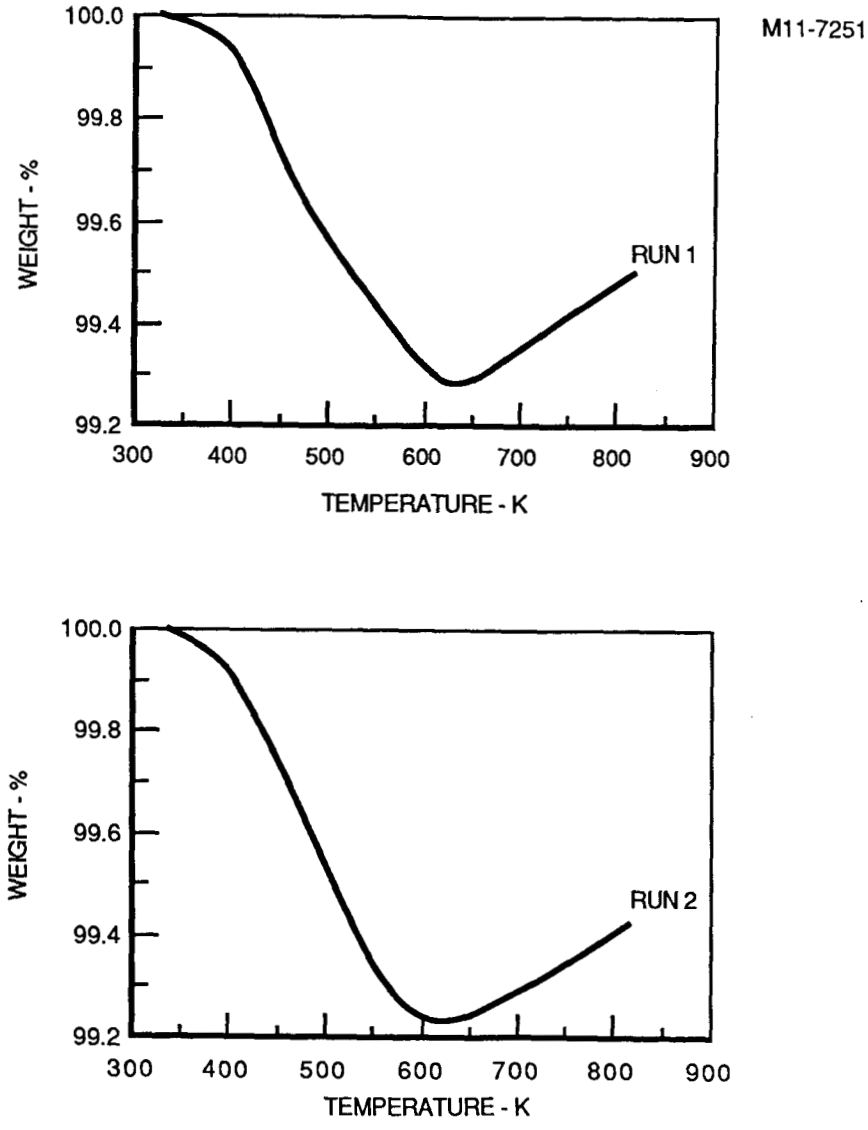

FIGURE A1. THERMOGRAVIMETRIC ANALYSIS SCANS FROM PREALLOYED Al - 4 Cu - 1Mg - 1.5Li - 0.2 Zr POWDER

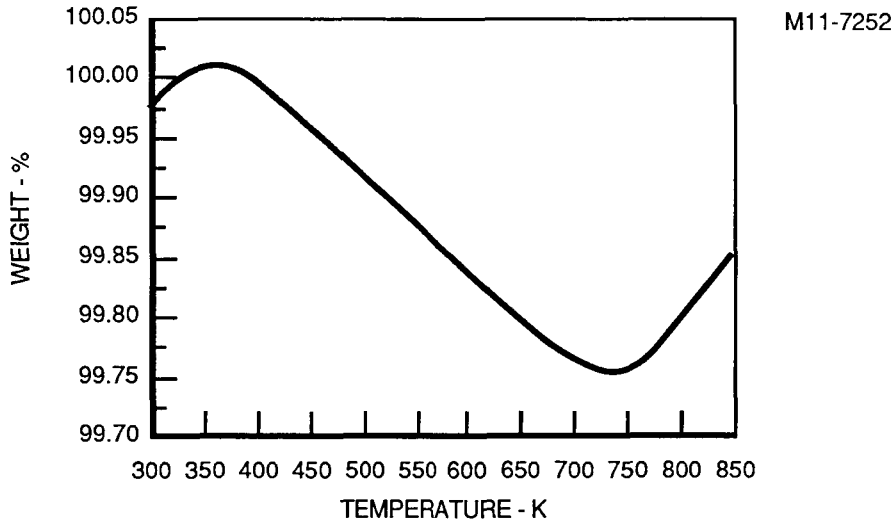

FIGURE A2. THERMOGRAVIMETRIC ANALYSIS SCAN FROM PREALLOYED Al - 4Cu - 1Mg - 1.5Fe - 0.75 Ce POWDER

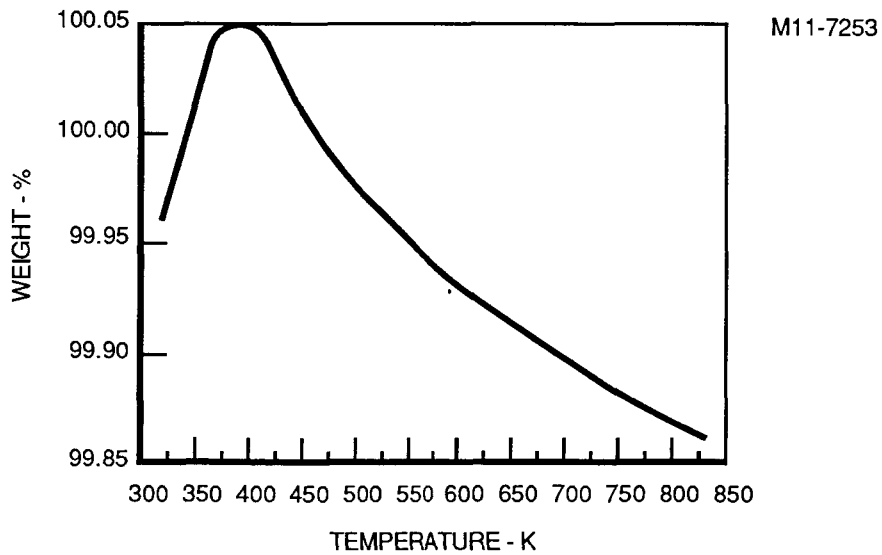

FIGURE A3. THERMOGRAVIMETRIC ANALYSIS SCAN FROM PREALLOYED Al - 1.6 Fe - 0.8 Ce POWDER

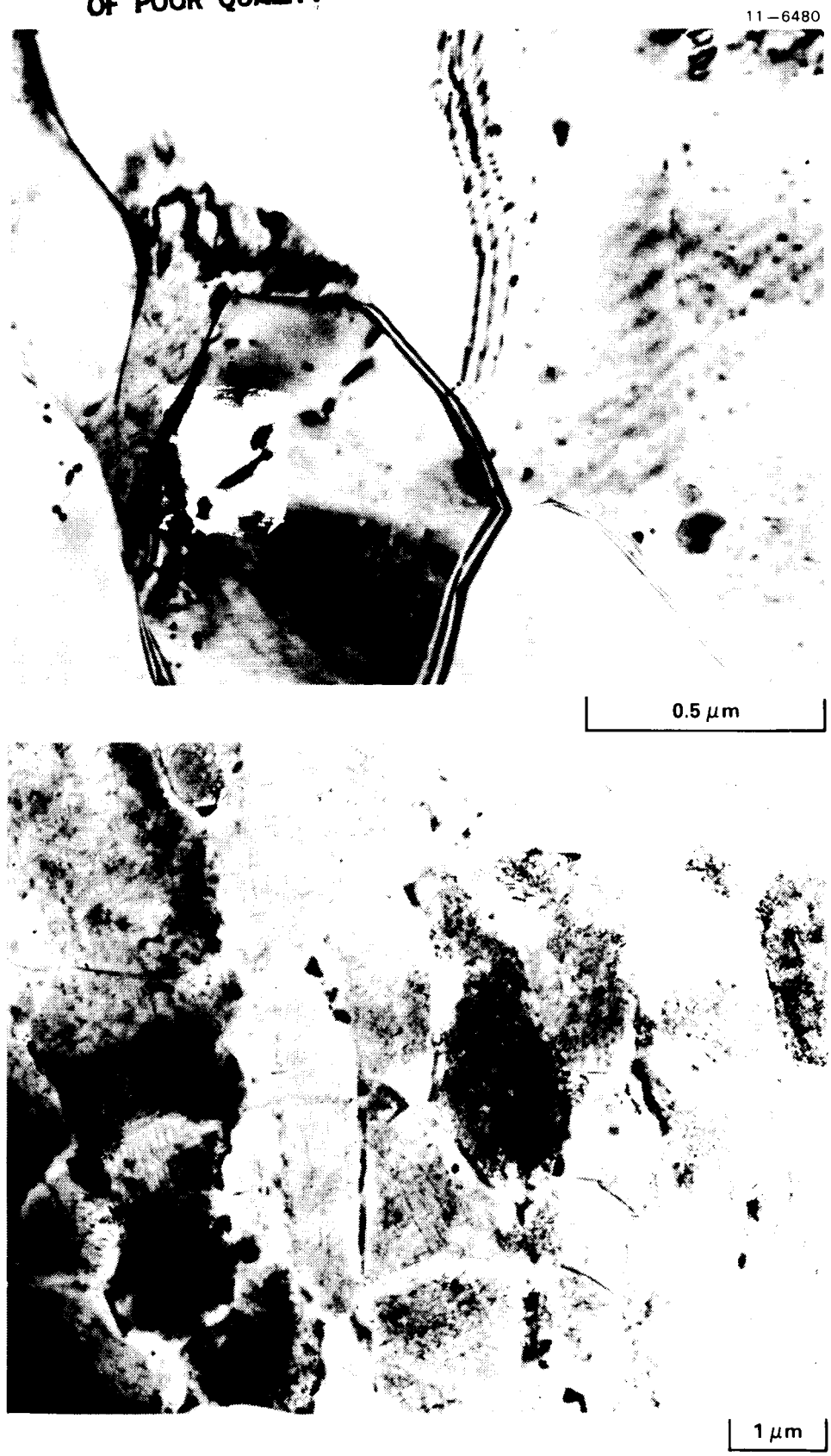

FIGURE A4. TRANSMISSION ELECTRON MICROGRAPH OF ALLOY 3 IN THE ARTIFICIALLY AGED CONDITION

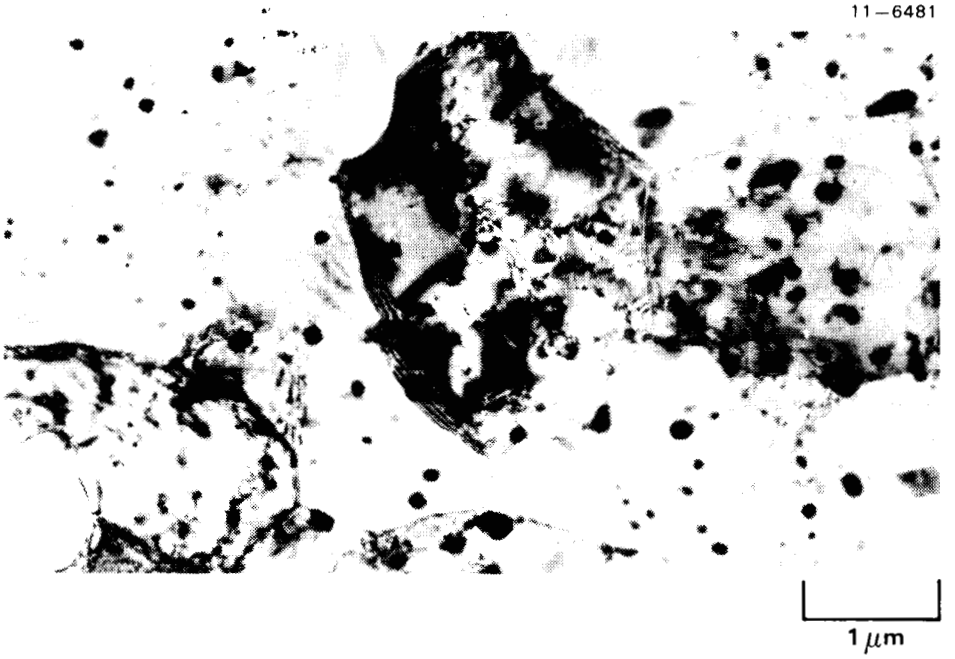

FIGURE A5. TRANSMISSION ELECTRON MICROGRAPH OF ALLOY 6 IN THE EXTRUDED CONDITION

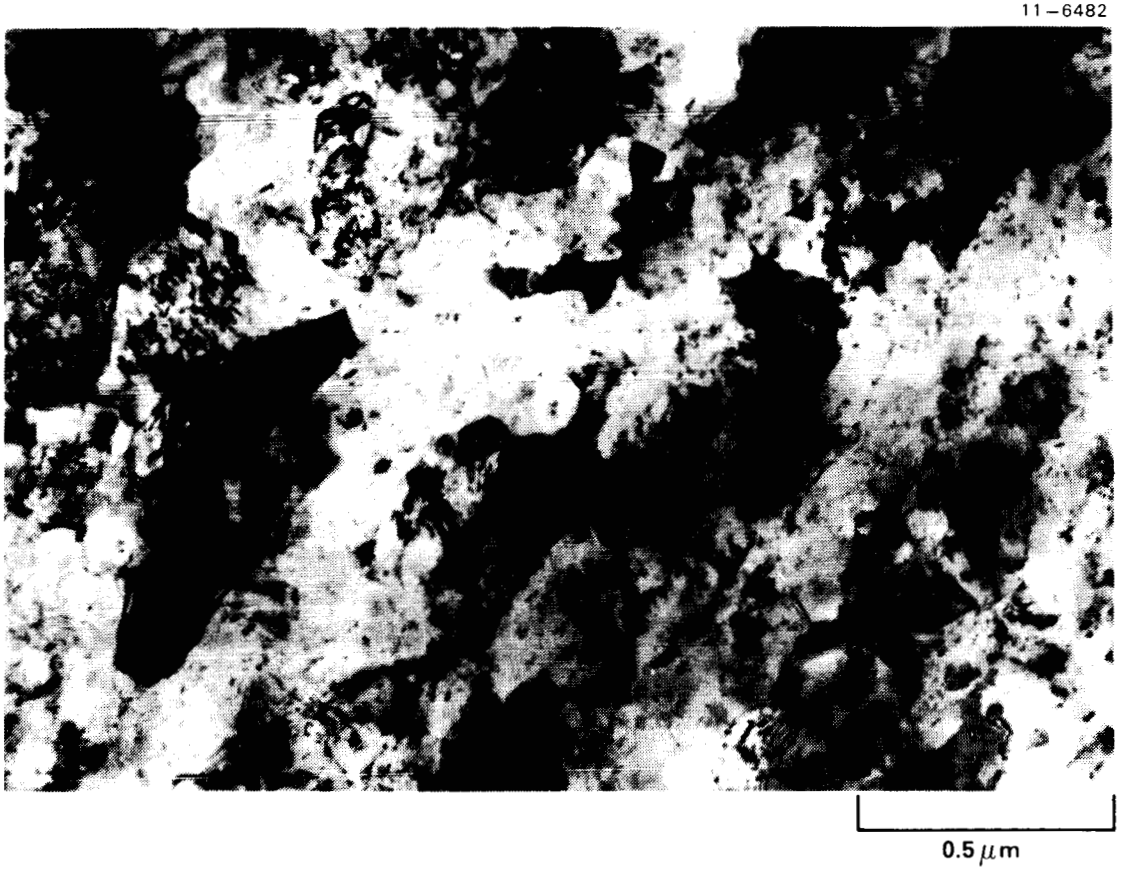

FIGURE A6. TRANSMISSION ELECTRON MICROGRAPH OF ALLOY 9 IN THE SOLUTION HEAT TREATED CONDITION

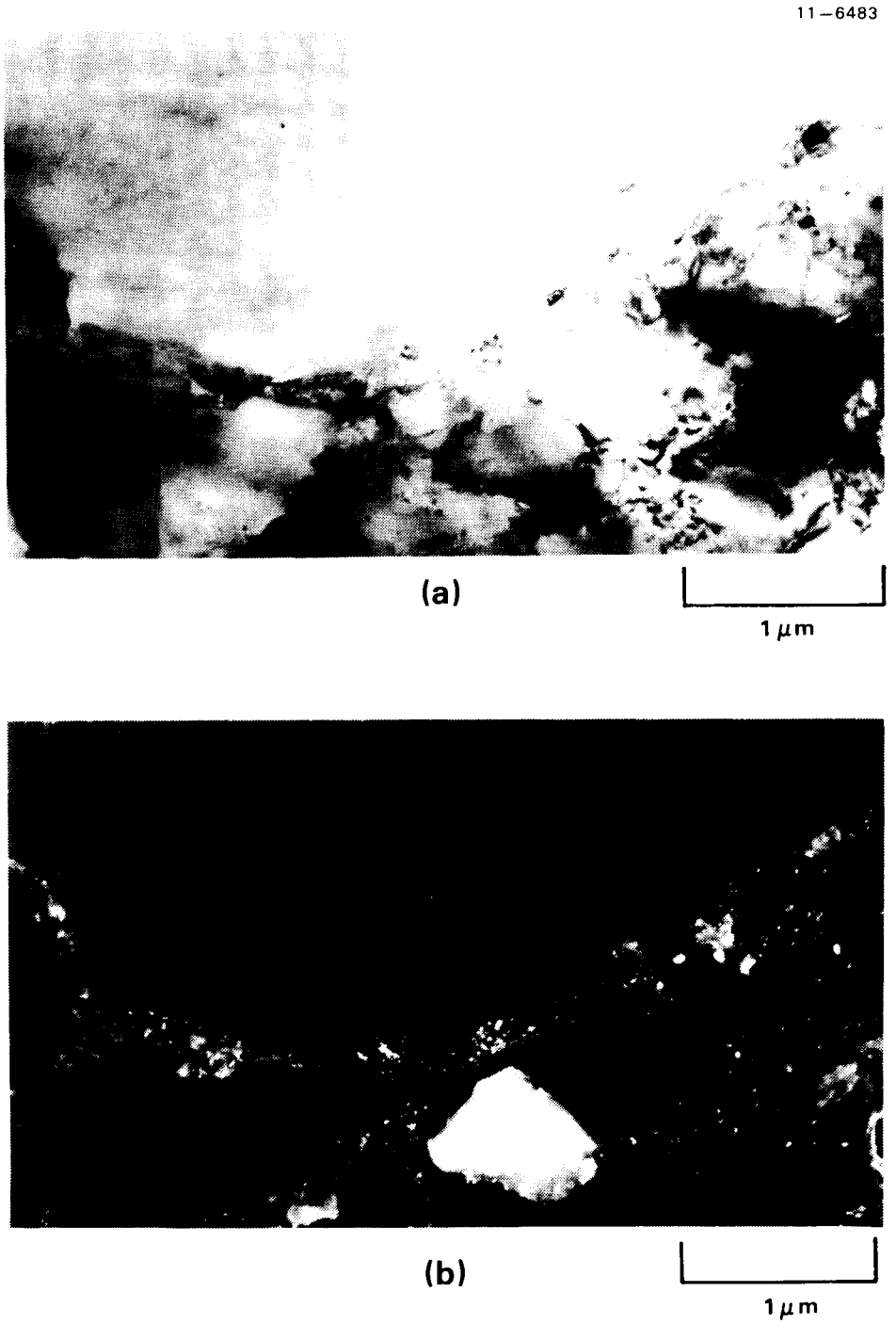

FIGURE A7. TRANSMISSION ELECTRON MICROGRAPH OF ALLOY 15 FOLLOWING CONTAINERLESS VACUUM HOT PRESSING. (a) BRIGHT FIELD AND (b) DARK FIELD

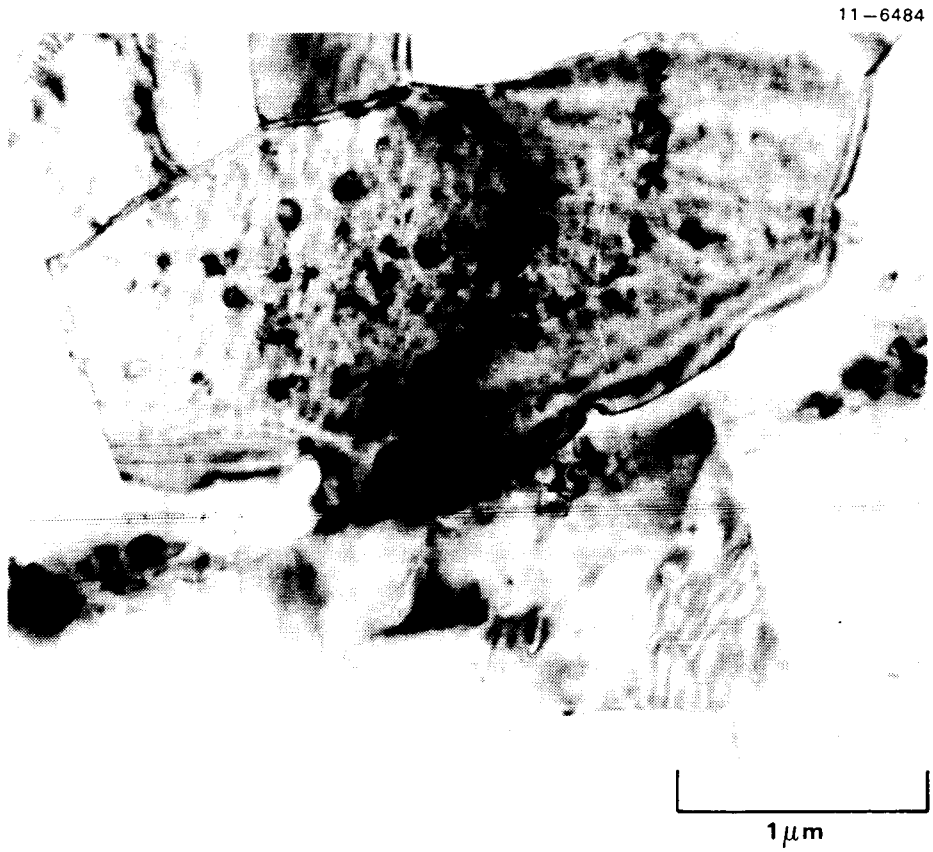

FIGURE A8. TRANSMISSION ELECTRON MICROGRAPH OF ALLOY 15 IN THE EXTRUDED CONDITION

Standard Bibliographic Page

1. Report No.	2. Government Accession No.	3. Recipient's Catalog No.
NASA CR-178227		

4. Title and Subtitle	5. Report Date
CONSOLIDATION PROCESSING PARAMETERS AND ALTERNATIVE PROCESSING METHODS FOR POWDER METALLURGY Al-Cu-Mg-X-X ALLOYS	February 1987
	6. Performing Organization Code

7. Author(s)	8. Performing Organization Report No.
K. K. Sankaran	

9. Performing Organization Name and Address	10. Work Unit No.
McDonnell Douglas Astronautics Company-St.Louis Division P. O. Box 516 St. Louis, Missouri 63166	11. Contract or Grant No. NAS1-16967

12. Sponsoring Agency Name and Address	13. Type of Report and Period Covered
National Aeronautics and Space Administration Washington, DC 20546	Contractor Report
	14. Sponsoring Agency Code 505-63-01-02

15. Supplementary Notes

Langley Technical Monitor: Dennis L. Dicus
Final Report

16. Abstract

A study was conducted to determine the effects of varying the vacuum degassing parameters on the microstructure and properties of Al-4Cu-1Mg-X-X (X-X = 1.5Li-0.2Zr or 1.5Fe-0.75Ce) alloys processed from either prealloyed (PA) or mechanically alloyed (MA) powder, and consolidated by either using sealed aluminum containers or containerless vacuum hot pressing. The consolidated billets were hot extruded for evaluating the microstructure and properties. The MA Li-containing alloy did not include Zr, and the MA Fe- and Ce-containing alloy was made from both elemental and partially prealloyed powder. The alloys were vacuum degassed both above and below the solution heat treatment temperature. While vacuum degassing lowered the hydrogen content of these alloys, the range over which the vacuum degassing parameters were varied was not large enough to cause significant changes in degassing efficiency, and the observed variations in the mechanical properties of the heat treated alloys were attributed to varying contributions to strengthening by the sub-structure and the dispersoids. Mechanical alloying increased the strength over that of alloys of similar composition made from PA powder. The inferior properties in the transverse orientation, especially in the Li-containing alloys, suggested deficiencies in degassing. Among all of the alloys processed for this study, the Fe- and Ce-containing alloys made from MA powder possessed better combinations of strength and toughness.

17. Key Words (Suggested by Authors(s))	18. Distribution Statement
Powder-Processed Aluminum Alloys Rapid Solidification Mechanical Alloying Powder Vacuum Degassing Al-Cu-Mg Alloys	Unclassified - Unlimited Subject Category 26

19. Security Classif.(of this report)	20. Security Classif.(of this page)	21. No. of Pages	22. Price
Unclassified	Unclassified	80	

For sale by the National Technical Information Service, Springfield, Virginia 22161